Truths universally acknowledged?
Some thoughts on CR folklore

Andy Strong
MPE Garching

The Origin of Galactic Cosmic Rays
APC Paris Dec 7-9 2016

It is a truth universally acknowledged ...

It is a truth universally acknowledged, that
a single man in possession of a good fortune,
must be in want of a wife.

(Jane Austen, *Pride and Prejudice*)

Talk at Cosmic Rays beyond the Standard Model, San Vito di Cadore, Sept 2016

11 things which are taken as given but are not and deserve further investigation

1 The Pion Bump has been detected in SNR by Fermi-LAT
2 CR are extragalactic only >10^{15} eV or so
3 CR cannot come from the Galactic Centre only
4 The CR gradient in the Galaxy can be determined accurately
5 The spectrum of CR in the Galaxy has the same shape as the local spectrum
6 Reacceleration is a viable explanation of the B/C peak
7 Secondary production in sources is negligible
8 60Fe tells about CR age, delay
9 Positron/pbar ratio agrees with standard model
10 Diffuse Galactic emission is mainly interstellar not unresolved sources
11 CR are not important for galaxy evolution

3 Common notions: folklore?

1 The Pion Bump has been detected in SNR by Fermi-LAT

2 Diffusive Reacceleration is a viable explanation of the B/C peak

3 CR are extragalactic only $>10^{15}$ eV or so

The origin of Cosmic-Rays from SNRs: confirmations and challenges after the first direct proof.

M.Cardillo[a,*], M.Tavani[b,c,d], A.Giuliani[e]

[a] *INAF-Osservatorio Astrofisico di Arcetri, Largo E.Fermi 5, 50125, Florence (Italy)*
[b] *INAF/IAPS, I-00133 Roma, Italy*
[c] *Dip. di Fisica, Univ. Tor Vergata, I-00133 Roma, Italy*
[d] *CIFS-Torino, I-10133 Torino, Italy*
[e] *INAF/IASF-Milano, I-20133 Milano, Italy*

Abstract

Until now, providing an experimental unambiguous proof of Cosmic Ray (CR) origin has been elusive. The SuperNova Remnant (SNR) study showed an increasingly complex scenario with a continuous elaboration of theoretical models. The middle-aged supernova remnant (SNR) W44 has recently attracted attention because of its relevance regarding the origin of Galactic cosmic-rays. The gamma-ray missions AGILE and Fermi have established, for the first time for a SNR, the spectral continuum below 200 MeV which can be attributed to neutral pion emission. Our work is focused on a global re-assessment of all available data and models of particle acceleration in W44 and our analysis strengthens previous studies and observations of the W44 complex environment, providing new information for a more detailed modeling. However, having determined the hadronic nature of the gamma-ray emission on firm ground, a number of theoretical challenges remains to be addressed in the context of CR acceleration in SNRs.

Nuc Phys B 256, 65 (2014), arXiv:1410.4063

SNRs : several with claimed 'pion-peak'

But beware, this is at $m(\pi^o)/2$ = 67.5 MeV, so Fermi hardly covers it.

NB multiplying by E^2 is good but shifts the peak to higher energies, do not see the 'bump'

May be instead an indication for break in proton spectrum.

Sample spectrum: W44, Cardillo etal 2014. Model proton spectrum has break at 20 GeV.

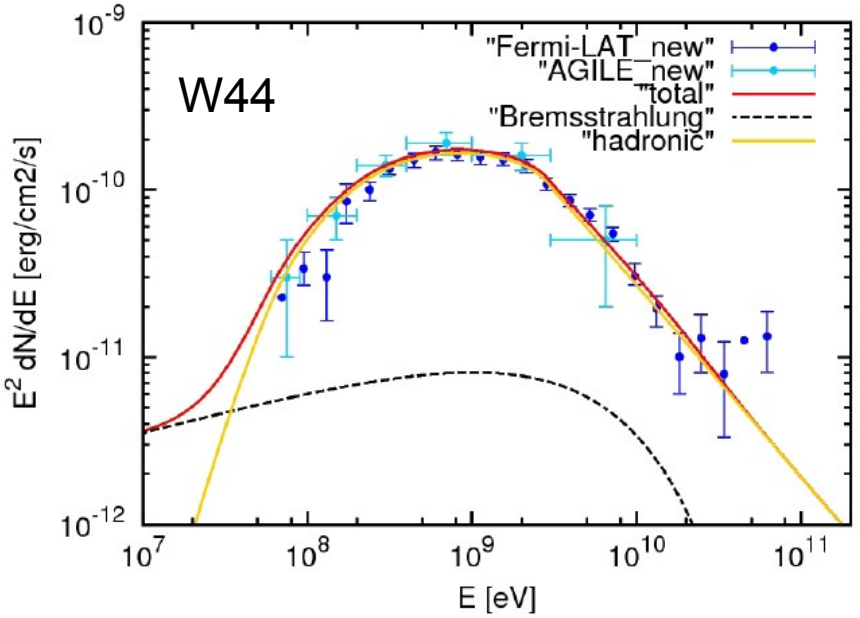

NASA SP-249

COSMIC GAMMA RAYS

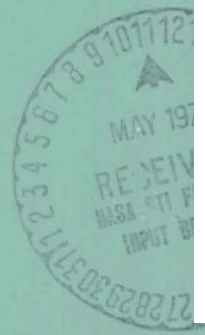

NATIONAL AERONAUTICS AND SPACE ADMINISTRATION

NASA SP-249

COSMIC GAMMA RAYS

FLOYD WILLIAM STECKER

Goddard Space Flight Center

We have thus proved an important kinematic property regarding the energy range of secondary γ-rays that are the product of two-body decays; viz, (1–225)

> The geometric mean of the energy range of secondary γ-rays which are produced in all two-body decays is equal to the energy of the γ-rays in the rest system of the decaying primary μ and is independent of the energy of the primary particle.

these γ-rays, ium energies.

spectrum. We therefore deduce a second important kinematic property, which holds for two-body decays that produce γ-rays isotropically in the rest system of the decaying primary; viz,

> The energy spectra of γ-rays produced isotropically in the rest system of the decaying primary will be symmetric on a logarithmic plot with respect to $E_\gamma = \mu$ and will peak at $E_\gamma = \mu$.

Isotropic decay in CM

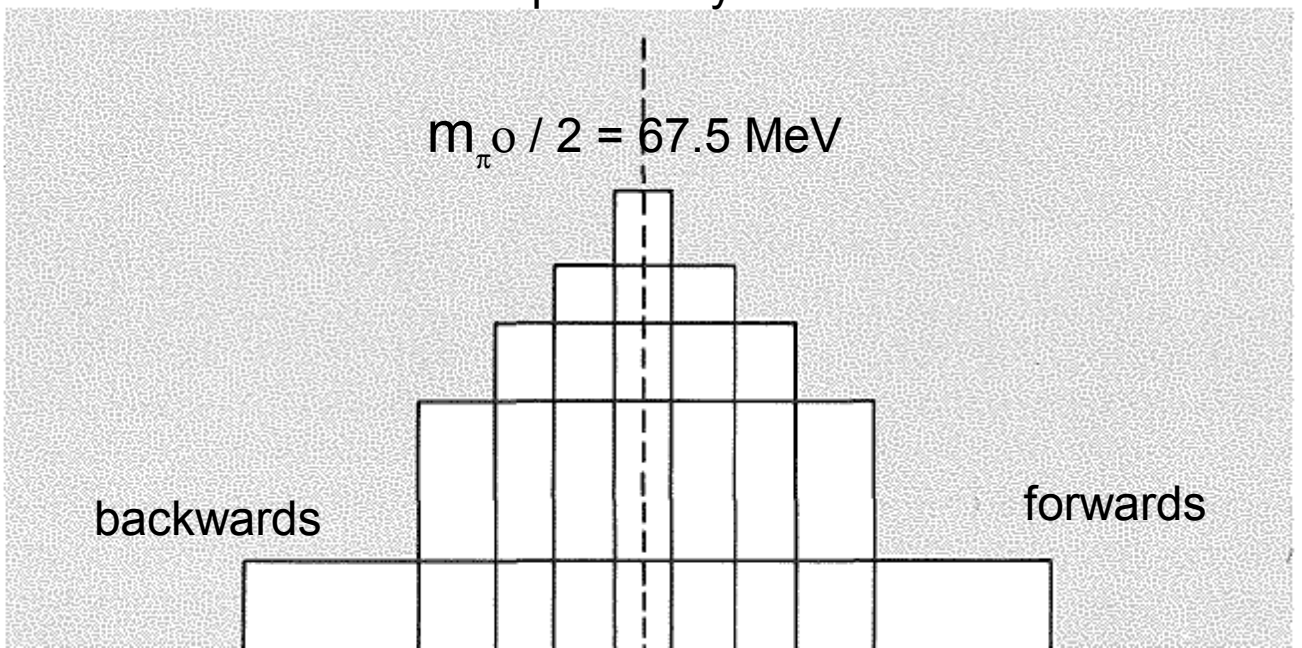

This result, combined with equations (5–26) and (5–27), yields the conclusion that ϵ increases monotonically with δ. Since $F[\epsilon]$ is a monotonically decreasing functional of ϵ, it follows that $F[\delta]$ is a monotonically decreasing functional of δ. Thus, $F[\delta]$ is a maximum at $\delta = 0$ and decreases more and more with increasing δ. It follows that $F(E_\gamma)$ is a maximum at $\ln E_\gamma = \nu$; i.e., at $E_\gamma = \frac{1}{2} m_\pi$ and that this is, in fact, the only maximum. Note that these results were reached by less rigorous arguments in our general discussion in section 1–6.

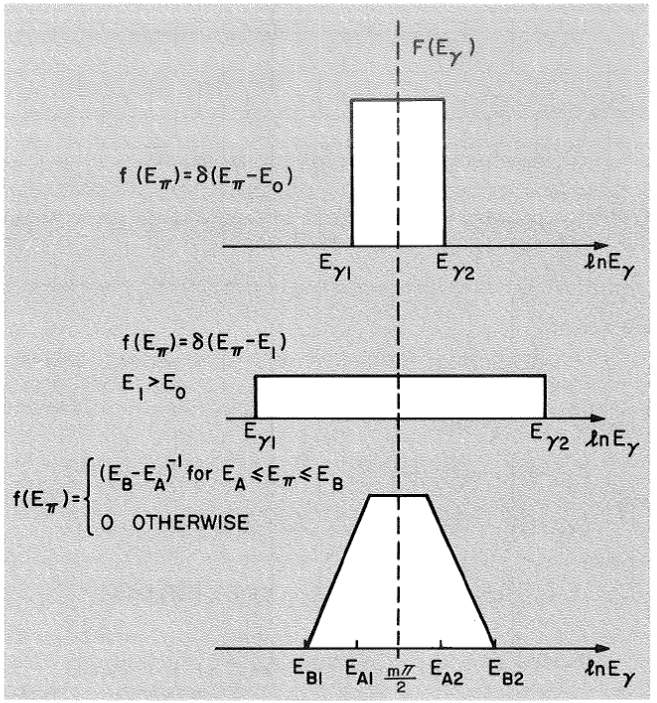

FIGURE 5–3.—Some ideal γ-ray spectra resulting from the decay of some ideal spectra of neutral pions.

SNRs : several with claimed 'pion-peak'

But beware, this is at $m(\pi^o)/2$ = 67.5 MeV, so Fermi hardly covers it.

NB multiplying by E^2 is good but shifts the peak to higher energies, do not see the 'bump'

May be instead an indication for break in proton spectrum.

Sample spectrum: W44, Cardillo et al 2014. .

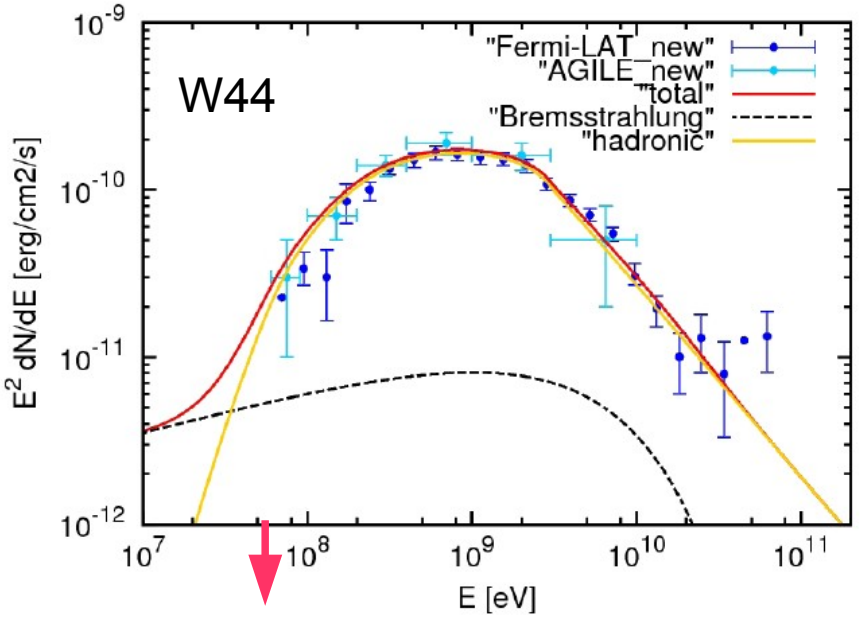

$m_{\pi o} / 2$ = 67.5 MeV

SNRs : several with claimed 'pion-peak'

But beware, this is at $m(\pi^o)/2$ = 67.5 MeV, so Fermi hardly covers it.

NB multiplying by E^2 is good but shifts the peak to higher energies, do not see the 'bump'

May be instead an indication for break in proton spectrum.

Need Fermi extension to lower energies, coming with Pass 8.

Sample spectrum: W44, Cardillo etal 2014. Model proton spectrum has break at 20 GeV.

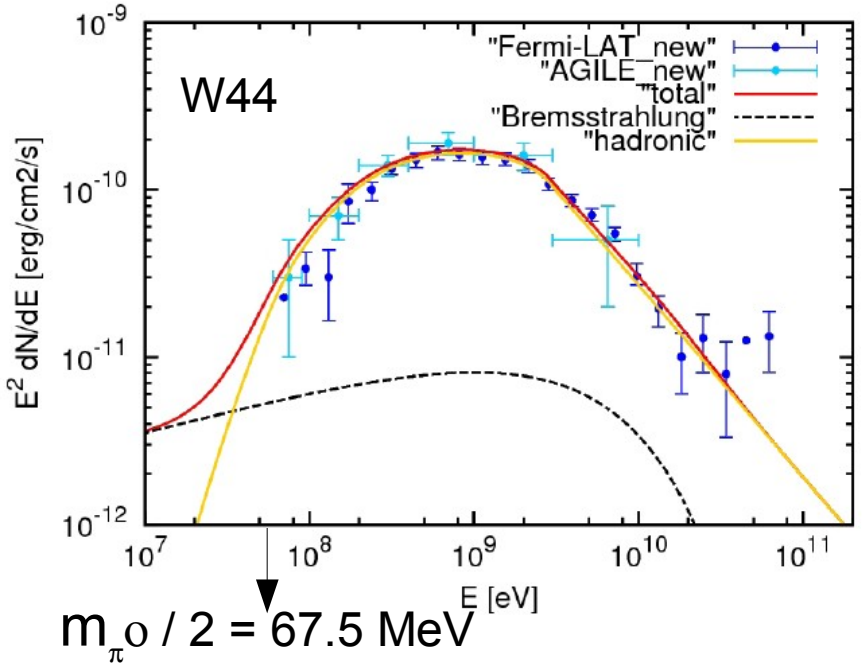

Spectrum X E^2

Shifts the peak
to higher energy
but Fermi cannot
see a peak which is
below it's range!

Sample spectrum: W44, Cardillo etal 2014. Model proton spectrum has break at 20 GeV.

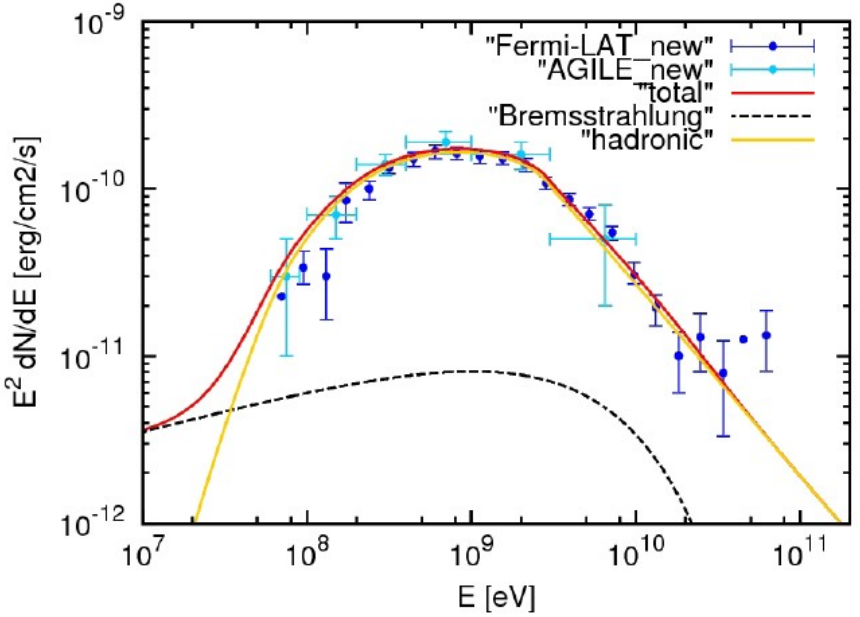

Spectrum X E^2

Shifts the peak
to higher energy
but Fermi cannot
see a peak which is
below it's range!

Spectrum times E^2

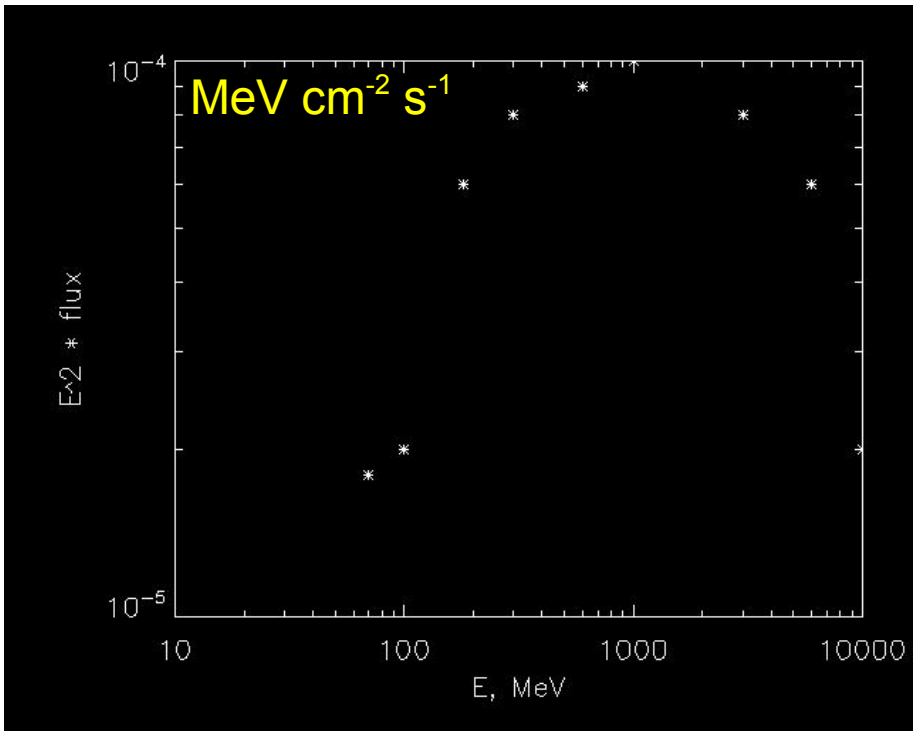

Sample spectrum: W44, Cardillo etal 2014. Model proton spectrum has break at 20 GeV.

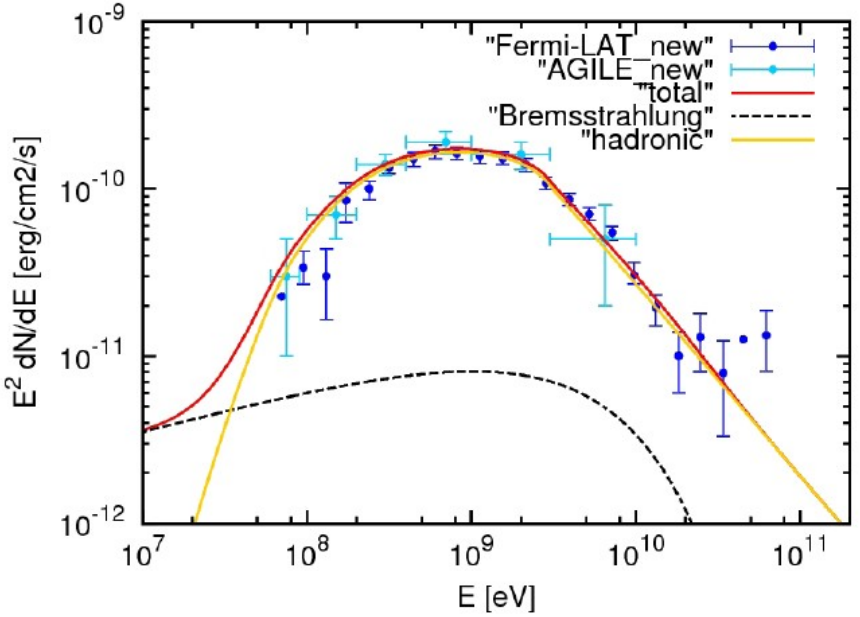

Spectrum X E^2

Shifts the peak
to higher energy
but Fermi cannot
see a peak which is
below it's range!

Spectrum times E^2

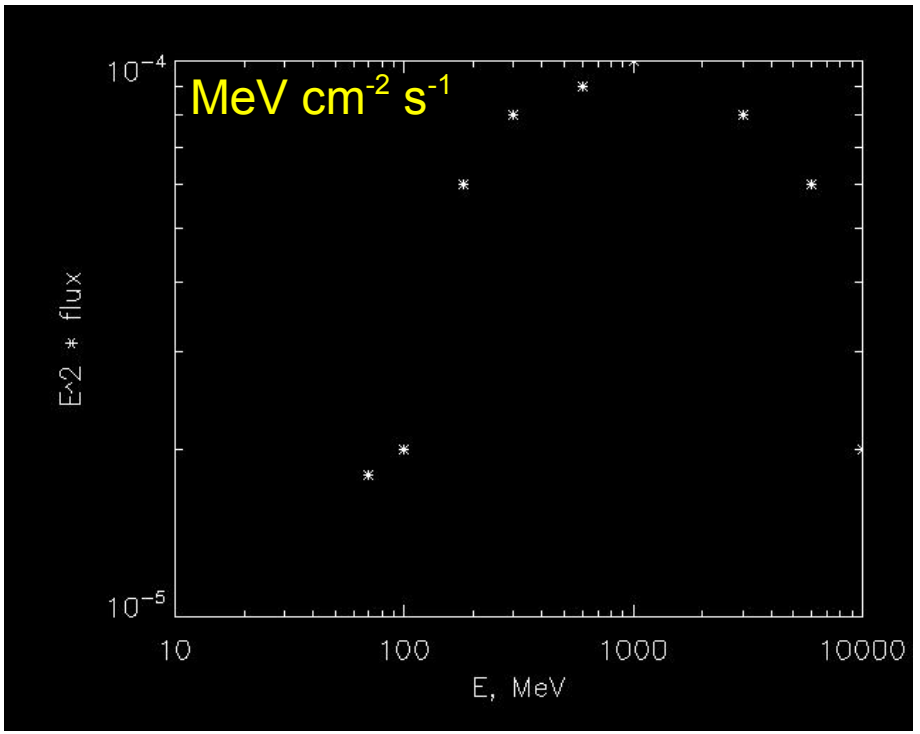

Spectrum without E^2

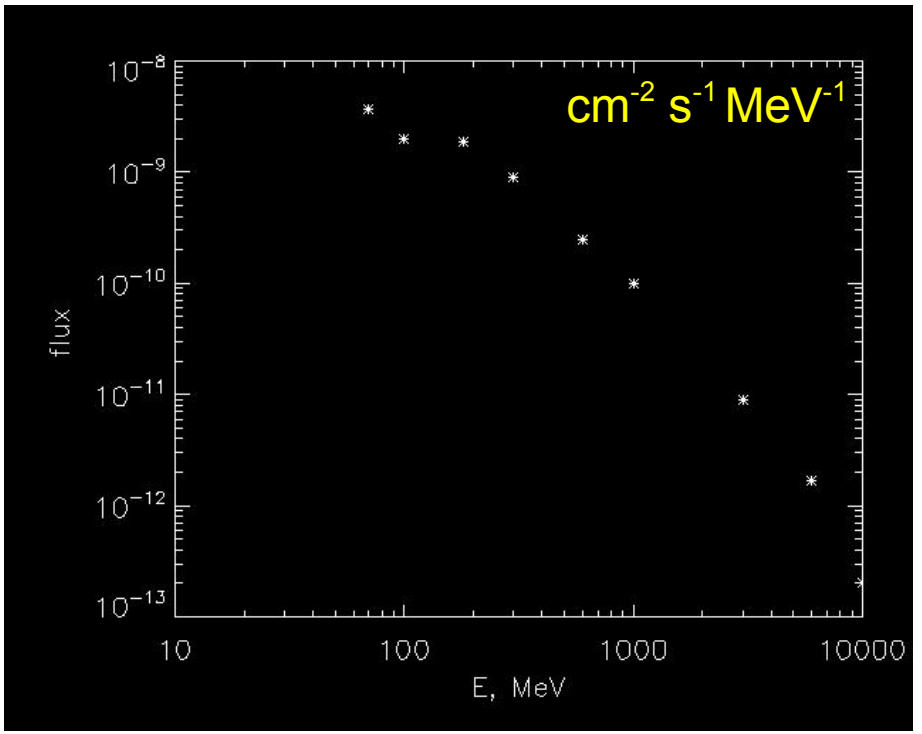

Sample spectrum: W44, Cardillo etal 2014. Model proton spectrum has break at 20 GeV.

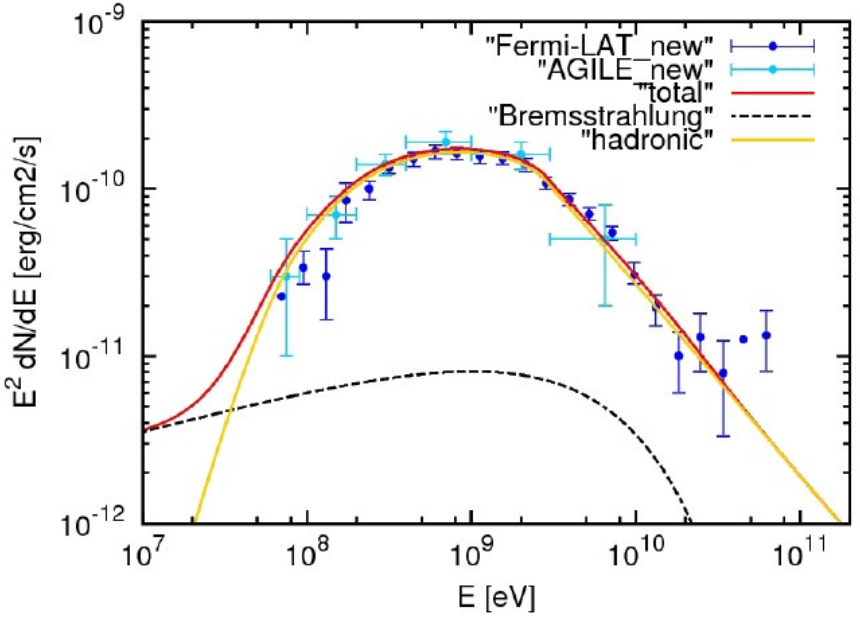

Spectrum X E^2

Shifts the peak to higher energy but Fermi cannot see a peak which is below it's range!

Spectrum times E^2

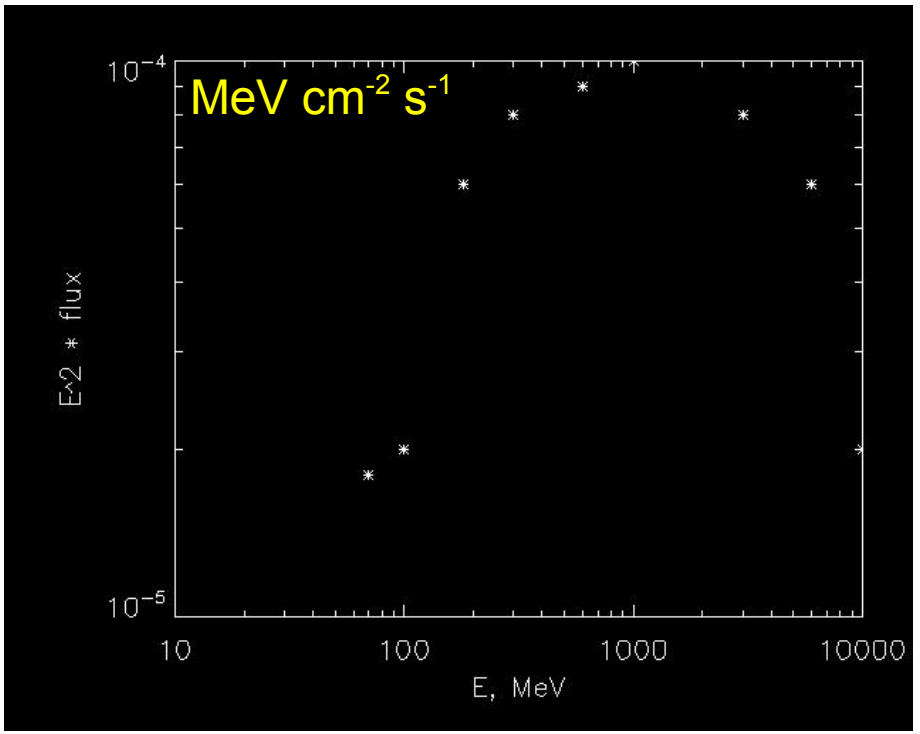

Spectrum without E^2

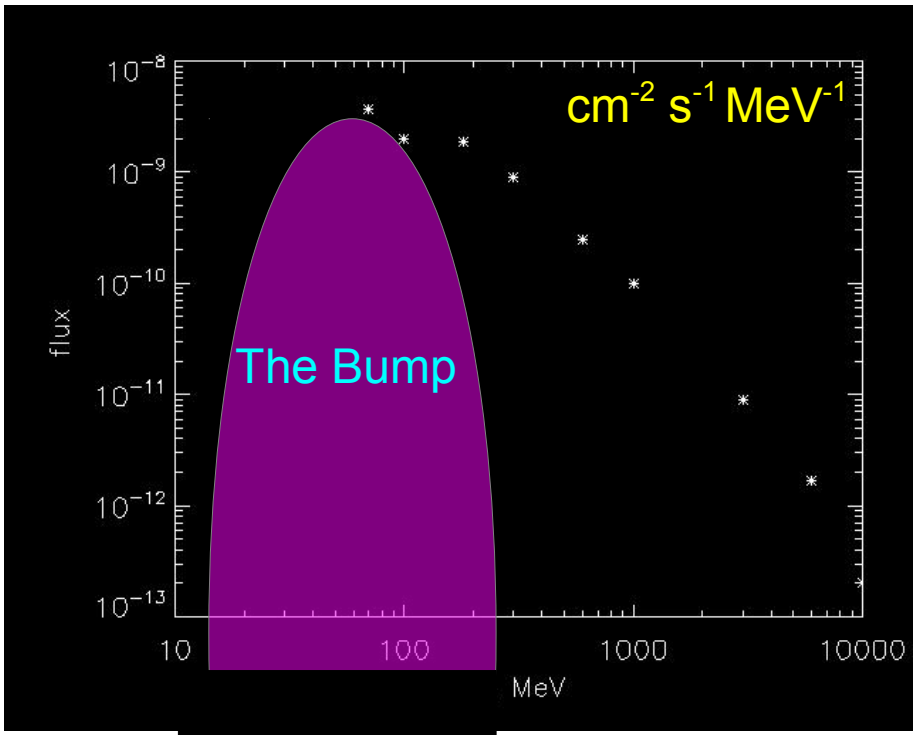

The supernova remnant W44: a case of Cosmic-Ray reacceleration.

M. Cardillo[1], E. Amato[1], and P. Blasi[1,2]

[1] INAF/Osservatorio Astrofisico di Arcetri, Largo E. Fermi, 5 - 50125 Firenze, Italy
e-mail:martina@arcetri.astro.it
[2] Gran Sasso Science Institute (INFN), viale F. Crispi 7, 67100 L' Aquila, Italy.

Received / Accepted

ABSTRACT

Supernova remnants (SNRs) are thought to be the primary sources of Galactic Cosmic Rays (CRs). In the last few years, the wealth of γ-ray data collected by GeV and TeV instruments has provided important information about particle energisation in these astrophysical sources, allowing us to make progress in assessing their role as CR accelerators. In particular, the spectrum of the γ-ray emission detected by AGILE and Fermi-LAT from the two middle aged Supernova Remnants (SNRs) W44 and IC443, has been proposed as a proof of CR acceleration in SNRs. Here we discuss the possibility that the radio and γ-ray spectra from W44 may be explained in terms of re-acceleration and compression of Galactic CRs. The recent measurement of the interstellar CR flux by Voyager I has been instrumental for our work, in that the result of the reprocessing of CRs by the shock in W44 depends on the CR spectrum at energies that are precluded to terrestrial measurement due to solar modulation. We introduce both CR protons and helium nuclei in our calculations, and secondary electrons produced *in situ* are compared with the flux of Galactic CR electrons reprocessed by the slow shock of this SNR. We find that the multi-wavelength spectrum of W44 can be explained by reaccelerated particles with no need of imposing any break on their distribution, but just a high energy cut-off at the maximum energy the accelerator can provide. We also find that a model including both re-acceleration and a very small fraction of freshly accelerated particles may be more satisfactory on physical grounds.

ArXiv:1604.02321 July 2016

The supernova remnant W44: a case of Cosmic-Ray reacceleration.

M. Cardillo[1], E. Amato[1], and P. Blasi[1, 2]

arXiv: 1604.02321

teractions with ambient matter. Indeed the γ-ray spectrum of W44 showed the pion bump that can be unequivocally linked to CR hadronic interactions, as later confirmed by the Fermi-LAT

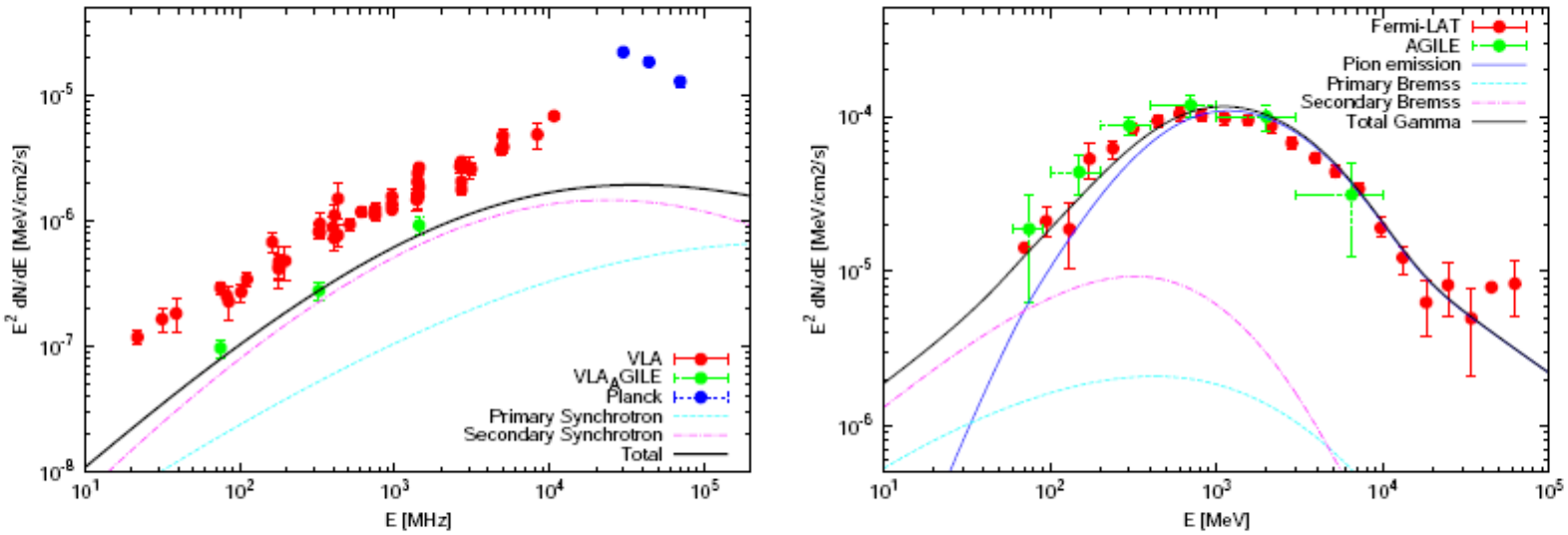

Fig. 3. Left:VLA (red) and Planck (blue) radio data from the whole remnant (Castelletti et al. 2007; Planck collaboration 2014) and VLA radio data from the high-energy emitting region (green), plotted together with primary (cyan dashed line), secondary (magenta dot-dashed line) and total (black line) synchrotron radio emission obtained in our best fit reacceleration model. **Right**: AGILE (green) and Fermi-LAT (red) γ-ray points (Cardillo et al. 2014; Ackermann et al. 2013) plotted with γ-ray emission from pion decay (blue dotted line), emission due to bremsstrahlung of primary (cyan dashed line) and secondary (magenta dot-dashed line) electrons, and total emission (black line).

The supernova remnant W44: a case of Cosmic-Ray reacceleration.

M. Cardillo[1], E. Amato[1], and P. Blasi[1, 2]

arXiv: 1604.02321

'bump' is result of break in proton spectrum

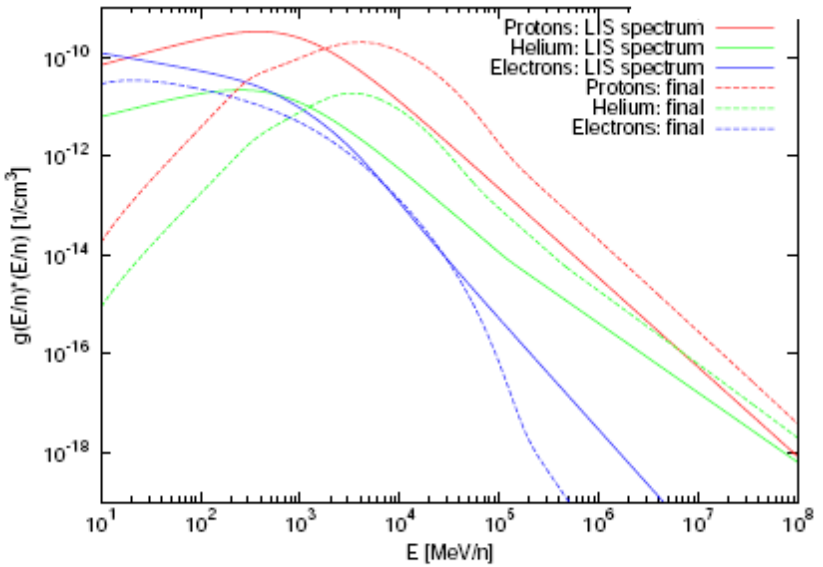

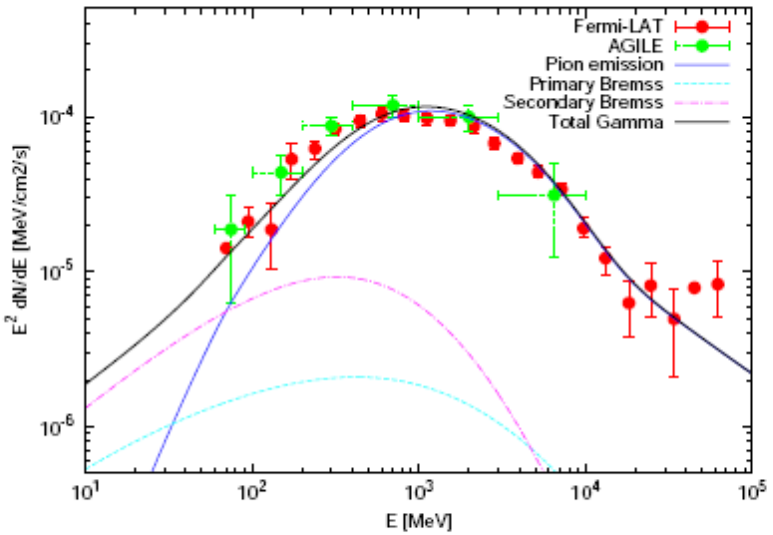

Fig. 2. Spectra of protons, He nuclei and electrons in the local ISM (solid lines) and after shock reacceleration and compression in the crushed cloud (dashed lines). The change of slope at ~ 10 GeV is associated with the acceleration cutoff. Particles at higher energy are simply compressed in the cloud. Ionisation energy losses affect the spectral slopes at lower energies, synchrotron losses steepen the electron spectrum at higher energies, whereas Bremsstrahlung and pp losses mainly affect the normalization.

…mnant (Castelletti et al. 2007; Planck collaboration 2014) and VLA radio primary (cyan dashed line), secondary (magenta dot-dashed line) and total …leration model. **Right**: AGILE (green) and Fermi-LAT (red) γ-ray points …on from pion decay (blue dotted line), emission due to bremsstrahlung of …ectrons, and total emission (black line).

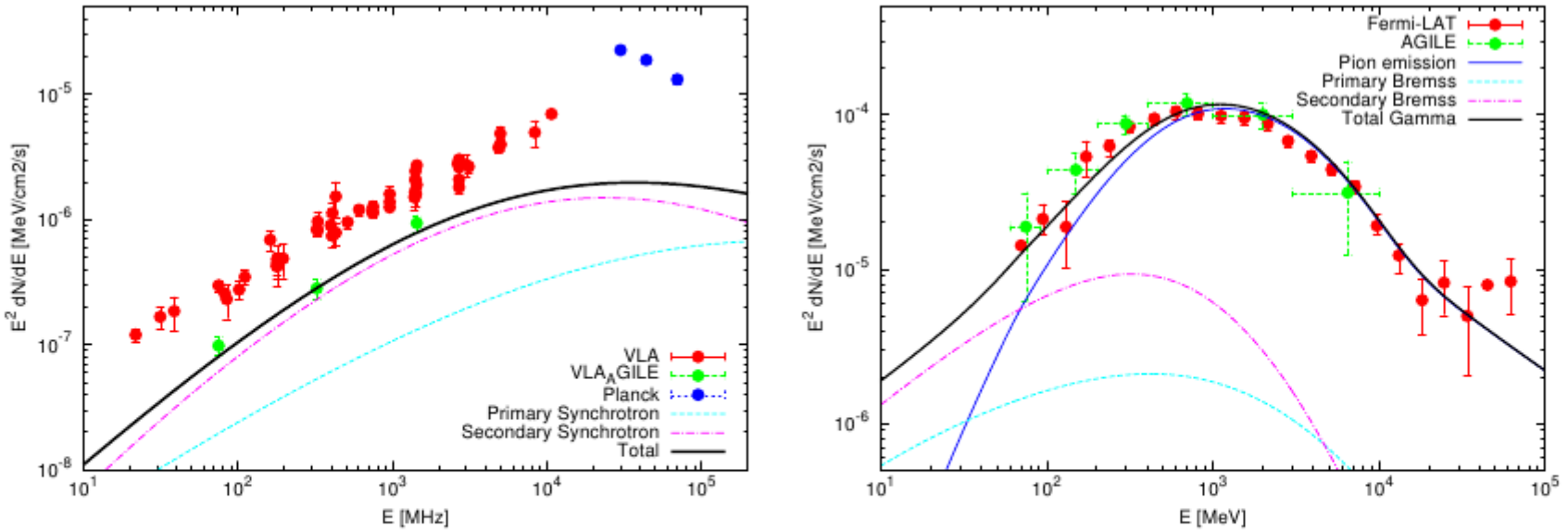

Fig. 3. Left:VLA (red) and Planck (blue) radio data from the whole remnant (Castelletti et al. 2007; Planck collaboration 2014) and VLA radio data from the high-energy emitting region (green), plotted together with primary (cyan dashed line), secondary (magenta dot-dashed line) and total (black line) synchrotron radio emission obtained in our best fit reacceleration model. **Right**: AGILE (green) and Fermi-LAT (red) γ-ray points (Cardillo et al. 2014; Ackermann et al. 2013) plotted with γ-ray emission from pion decay (blue dotted line), emission due to bremsstrahlung of primary (cyan dashed line) and secondary (magenta dot-dashed line) electrons, and total emission (black line).

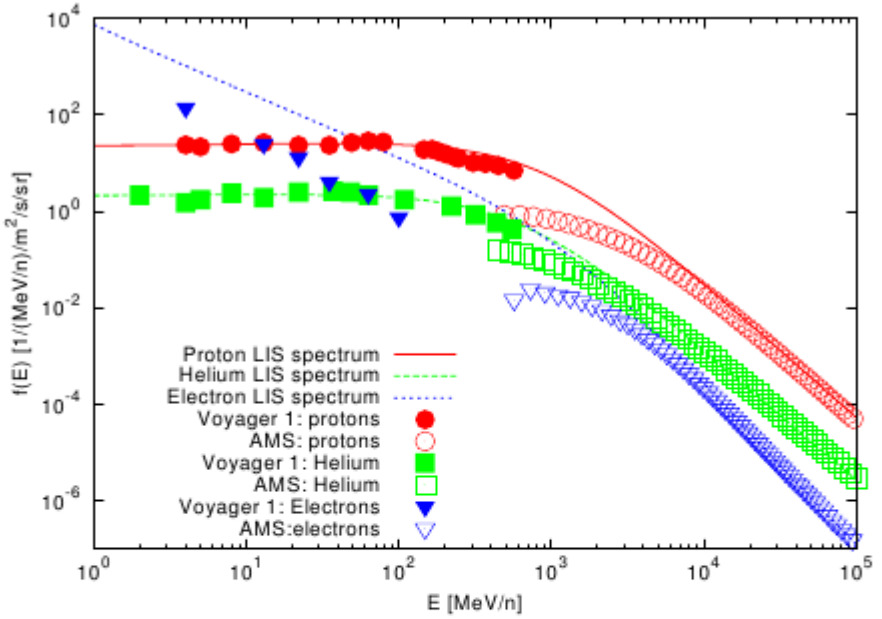

Fig. 1. Protons (red), Helium (green) and electrons (blue) spectra. Cir-

Cardillo etal 2016

W49B
Fermi + H.E.S.S.
arXiv: 1609.00900
2 Sept 2016
A&A in press

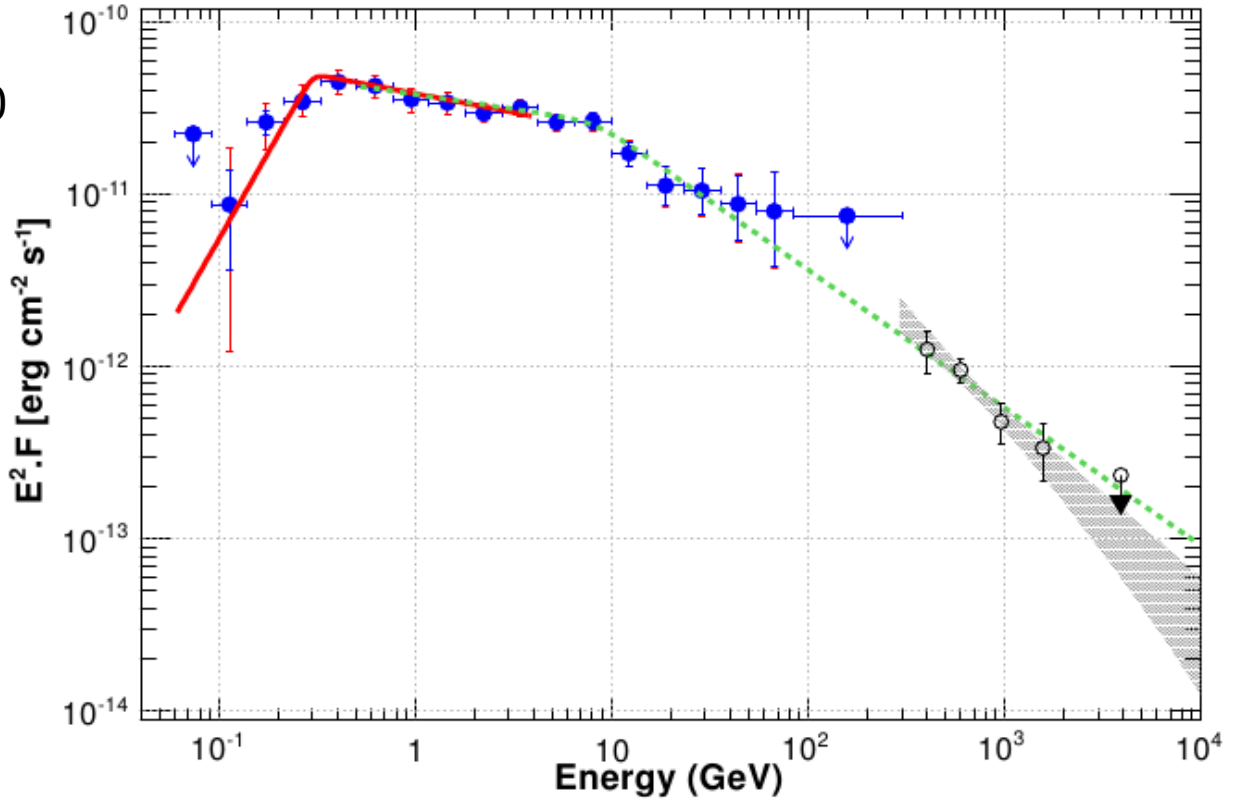

Fig. 3. *Fermi*-LAT and H.E.S.S. spectrum of W49B. The red line shows the best fit of a smoothly broken power-law derived between 60 MeV and 4 GeV and the blue data points indicate the fluxes measured in each energy bin with the *Fermi*-LAT. The statistical errors are shown in blue, while the red lines take into account both the statistical and systematic errors as discussed in Sect. 2.2.2. The gray band shows the 68% confidence level (CL) uncertainty of the best-fit power-law model with H.E.S.S. The open black circles are the spectral points computed from the forward-folding fit with their statistical errors shown in black. For both instruments, a 95% CL upper limit is computed when the statistical significance is lower than 2σ. The dotted green line shows the best smoothly broken power-law model obtained from the joint fit of the *Fermi*-LAT and H.E.S.S. data between 500 MeV and 10 TeV, as described in Sect. 2.3.

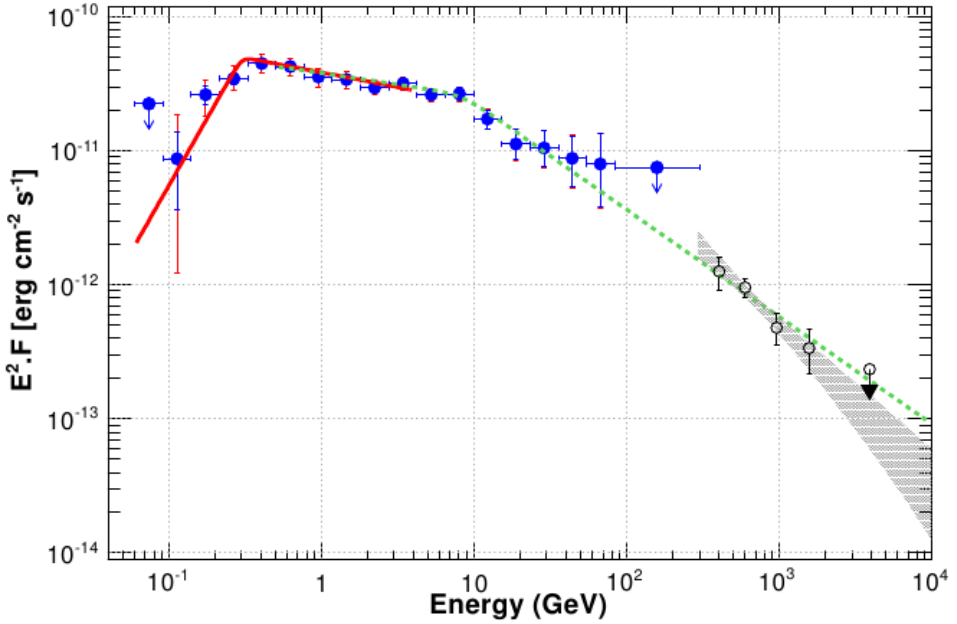
10^{-10}
10^{-11}
10^{-12}
10^{-13}
10^{-14}
$E^2.F$ [erg cm^{-2} s^{-1}]
10^{-1}
1
10
10^{2}
10^{3}
10^{4}
Energy (GeV)

W49B

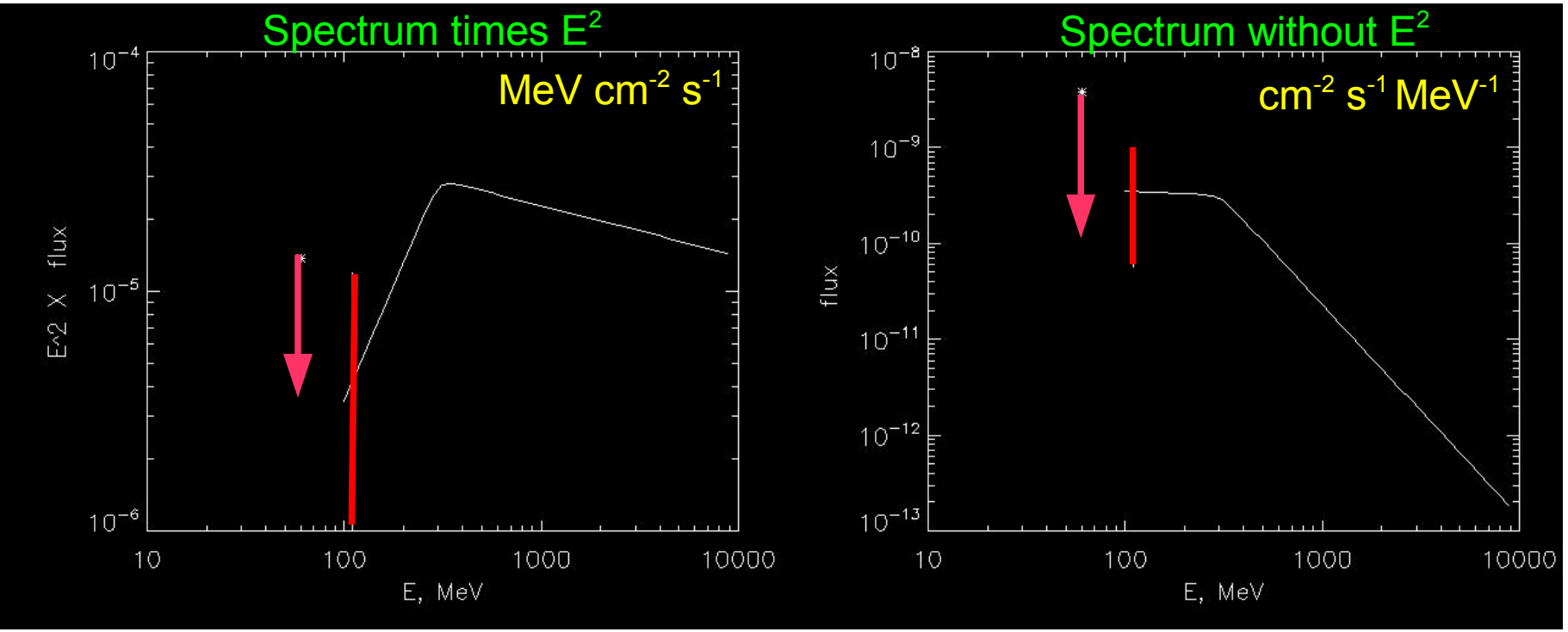
Spectrum times E^2
MeV cm^{-2} s^{-1}
10^{-4}
10^{-5}
10^{-6}
E^2 X flux
10
100
1000
10000
E, MeV
Spectrum without E^2
cm^{-2} s^{-1} MeV^{-1}
10^{-8}
10^{-9}
10^{-10}
10^{-11}
10^{-12}
10^{-13}
flux
10
100
1000
10000
E, MeV

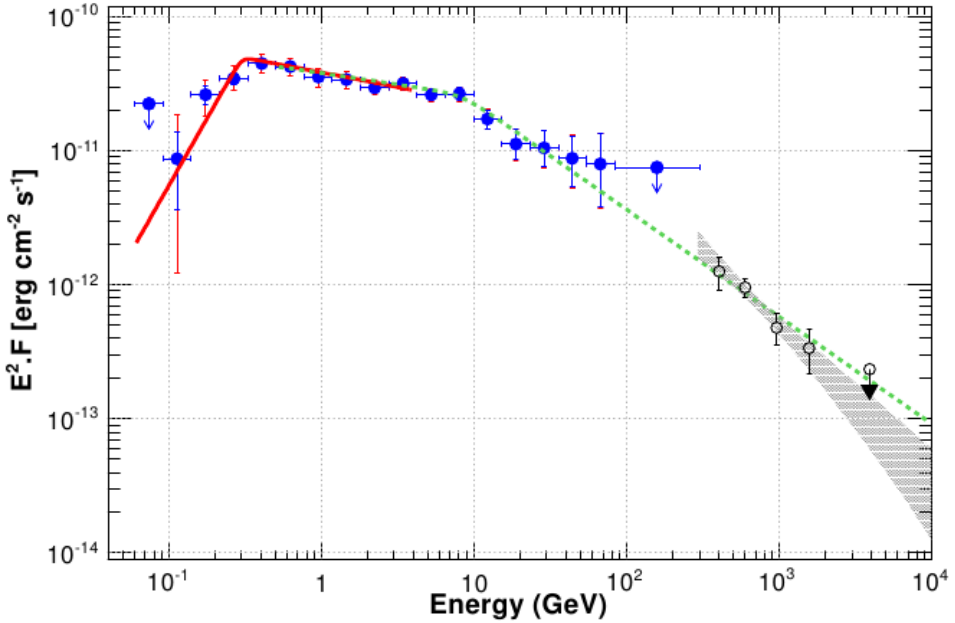
10^{-10}
10^{-11}
10^{-12}
10^{-13}
10^{-14}
$E^2.F$ [erg cm^{-2} s^{-1}]
10^{-1}
1
10
10^{2}
10^{3}
10^{4}
Energy (GeV)

W49B

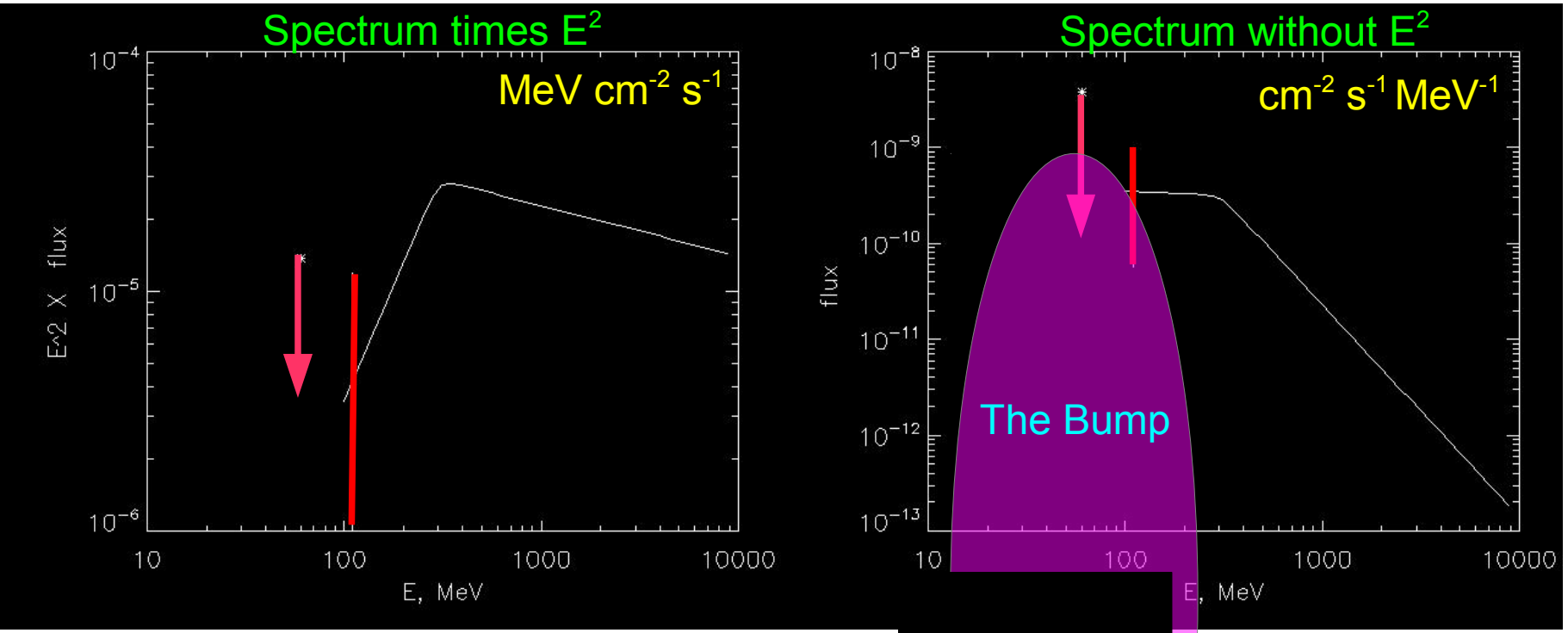
Spectrum times E^2
MeV cm^{-2} s^{-1}
10^{-4}
10^{-5}
10^{-6}
E^2 X flux
10
100
1000
10000
E, MeV
Spectrum without E^2
cm^{-2} s^{-1} MeV^{-1}
10^{-8}
10^{-9}
10^{-10}
10^{-11}
10^{-12}
10^{-13}
flux
The Bump
10
100
1000
10000
E, MeV

W49B
Fermi + H.E.S.S.
arXiv: 1609.00900
2 Sept 2016
A&A in press

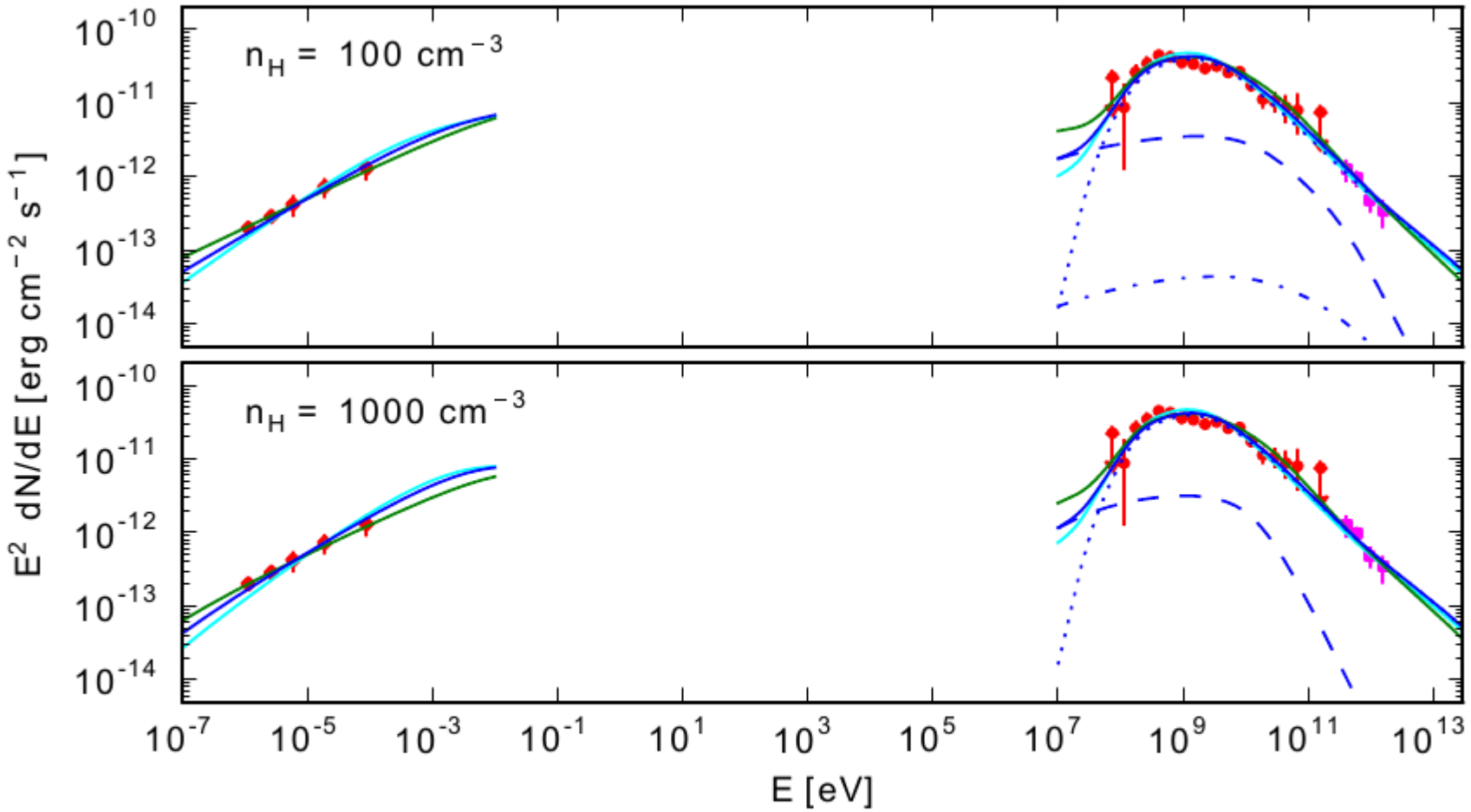

Fig. 5. SEDs of W49B with model curves for the hadronic-dominant scenario. The upper and the lower panels show (a1–3) and (a4–6) respectively (see Table 2). The red diamonds, red circles, and magenta squares represent observed data in the radio (Moffett & Reynolds 1994), LAT, and H.E.S.S. bands respectively. The radio emission is explained by the synchrotron radiation from the relativistic electrons. The γ-ray emission can be decomposed into π^0-decay (dotted line), bremsstrahlung (dashed line), and IC scattering (dot-dashed line). The solid line represents the total flux of the components. The cases (a1)/(a4), (a2)/(a5), and (a3)/(a6) are represented by cyan, blue, and green lines respectively in the upper/lower panel. The decomposed emissions are shown for the cases (a2) and (a5) in the upper and the lower panels respectively.

Draft version January 26, 2016
Preprint typeset using LaTeX style emulateapj v. 5/2/11

DEEP MORPHOLOGICAL AND SPECTRAL STUDY OF THE SNR RCW 86 WITH *FERMI*-LAT

M. Ajello[2], L. Baldini[3,4], G. Barbiellini[5,6], D. Bastieri[7,8], R. Bellazzini[9], E. Bissaldi[10], E. D. Bloom[4], R. Bonino[11,12], E. Bottacini[4], T. J. Brandt[13], J. Bregeon[14], P. Bruel[15], R. Buehler[16], G. A. Caliandro[4,17], R. A. Cameron[4], M. Caragiulo[18,10,1], E. Cavazzuti[19], E. Charles[4], A. Chekhtman[20], S. Ciprini[19,21], J. Cohen-Tanugi[14], B. Condon[22,1], F. Costanza[10], S. Cutini[19,23,21], F. D'Ammando[24,25], F. de Palma[10,26], R. Desiante[27,11], N. Di Lalla[9], M. Di Mauro[4], L. Di Venere[18,10], P. S. Drell[4], G. Dubner[28], D. Dumora[22], L. Duvidovich[28], C. Favuzzi[18,10], W. B. Focke[4], P. Fusco[18,10], F. Gargano[10], D. Gasparrini[19,21], E. Giacani[28], N. Giglietto[18,10], T. Glanzman[4], D. A. Green[29], I. A. Grenier[30], S. Guiriec[13,31], E. Hays[13], J.W. Hewitt[32], A. B. Hill[33,4], D. Horan[15], T. Jogler[4], G. Jóhannesson[34], I. Jung-Richardt[35], S. Kensei[36], M. Kuss[9], S. Larsson[37,38], L. Latronico[11], M. Lemoine-Goumard[22,1], J. Li[39], L. Li[37,38], F. Longo[5,6], F. Loparco[18,10], M. N. Lovellette[40], P. Lubrano[21], J. Magill[41], S. Maldera[11], A. Manfreda[9], M. Mayer[16], M. N. Mazziotta[10], J. E. McEnery[13,41], P. F. Michelson[4], W. Mitthumsiri[42], T. Mizuno[43], M. E. Monzani[4], A. Morselli[44], I. V. Moskalenko[4], M. Negro[11,12], E. Nuss[14], M. Orienti[24], E. Orlando[4], J. F. Ormes[45], D. Paneque[46,4], J. S. Perkins[13], M. Pesce-Rollins[9,4], F. Piron[14], G. Pivato[9], T. A. Porter[4], S. Rainò[18,10], R. Rando[7,8], M. Razzano[9,47], A. Reimer[48,4], O. Reimer[48,4], T. Reposeur[22], J. Schmid[30], A. Schulz[16], C. Sgrò[9], D. Simone[10], E. J. Siskind[49], F. Spada[9], G. Spandre[9], P. Spinelli[18,10], J. B. Thayer[4], L. Tibaldo[50], D. F. Torres[39,51], G. Tosti[21,52], E. Troja[13,41], Y. Uchiyama[53], G. Vianello[4], J. Vink[54], K. S. Wood[40], M. Yassine[14]

Draft version January 26, 2016

ABSTRACT

RCW 86 is a young supernova remnant (SNR) showing a shell-type structure at several wavelengths and is thought to be an efficient cosmic-ray (CR) accelerator. Earlier *Fermi* Large Area Telescope results reported the detection of γ-ray emission coincident with the position of RCW 86 but its origin (leptonic or hadronic) remained unclear due to the poor statistics. Thanks to 6.5 years of data acquired by the *Fermi*-LAT and the new event reconstruction Pass 8, we report the significant detection of spatially extended emission coming from RCW 86. The spectrum is described by a power-law function with a very hard photon index ($\Gamma = 1.42 \pm 0.1_{\rm stat} \pm 0.06_{\rm syst}$) in the 0.1–500 GeV range and an energy flux above 100 MeV of $(2.91 \pm 0.8_{\rm stat} \pm 0.12_{\rm syst}) \times 10^{-11}$ erg cm^{-2} s^{-1}. Gathering all the available multiwavelength (MWL) data, we perform a broadband modeling of the nonthermal emission of RCW 86 to constrain parameters of the nearby medium and bring new hints about the origin of the γ-ray emission. For the whole SNR, the modeling favors a leptonic scenario in the framework of a two-zone model with an average magnetic field of 10.2 ± 0.7 μG and a limit on the maximum energy injected into protons of 2×10^{49} erg for a density of 1 cm^{-3}. In addition, parameter values are derived for the North-East (NE) and South-West (SW) regions of RCW 86, providing the first indication of a higher magnetic field in the SW region.

RCW 86

7.2. *Modeling of the whole SNR*

Here we present the results of two leptonic scenario models. Since a pure hadronic scenario requires unlikely parameter values such as a very hard spectral index for protons (as it was already suggested in Lemoine-Goumard et al. 2012) and a high magnetic field ($B > 100$ μG), we did not consider this case. The presence of a high magnetic field is not excluded in very thin regions, near the shock, but it is very unlikely to have such high values for the whole remnant. Moreover, a spectral index softer than 1.7 is excluded with more than 3σ, as described in Section 3.2. The hadronic model re-

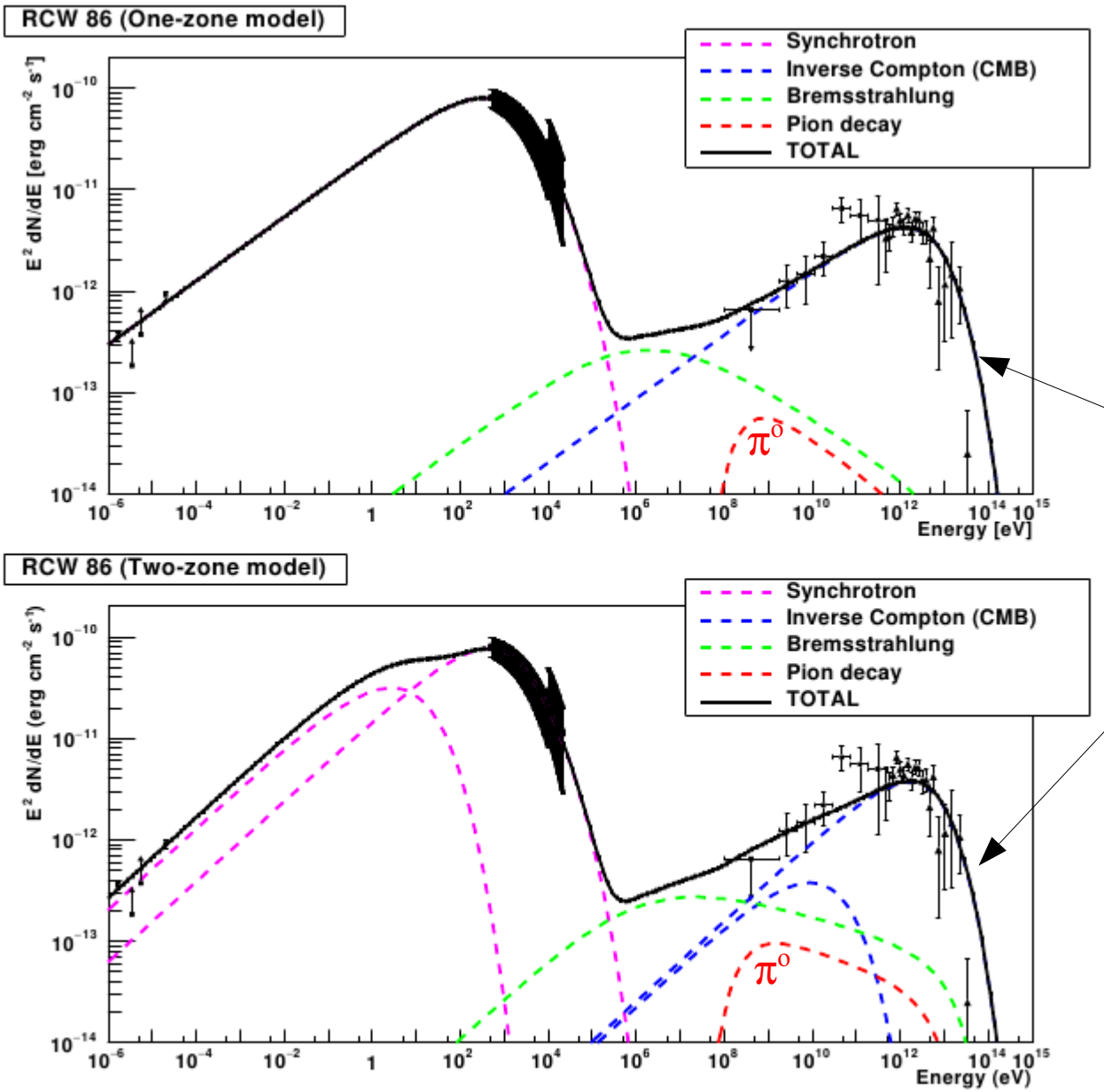

Inverse Compton dominates

FIG. 9.— Spectral Energy Distribution of RCW 86 with the best-fit leptonic one-zone (top) and two-zone (bottom) models. The radio points are from Molonglo at 408 MHz and Parkes at 5 GHz (Caswell et al. 1975; Lemoine-Goumard et al. 2012) and lower limits from MOST at 843 MHz and ATCA at 1.43 GHz (Whiteoak & Green 1996; Dickel et al. 2001). X-ray spectra from ASCA and RXTE are from Lemoine-Goumard et al. (2012). The *Fermi*-LAT spectral points and upper limits (95% C.L.) derived in Section 3.2 and the H.E.S.S. data points in the VHE γ-ray domain from Abramowski et al. (2015) are also shown.

Moral:

Fit to hadronic models but don't call it the Pion Bump or even Pion Rise!

Need multiwavelength models to show hadronic origin, and this is of course done.

Diffusive Reacceleration

Luke Drury and AWS, A&A 2016, in press, arXiv:1608.04227

Diffusion is on *moving* scatterers → momentum gain & loss.

Diffusion in momentum: $D_{pp} \sim v_A^2 / 9D_{xx}$

Popular explanation of GeV peak in B/C
Allows Kolmogorov D(p) index 1/3, helps with anisotropy at high energies

But then large fraction of energy in GeV CR comes from reacceleration not SNR!

Analytical and GALPROP estimates agree.
Is that physically plausible?

BAYESIAN ANALYSIS OF COSMIC-RAY PROPAGATION: EVIDENCE AGAINST HOMOGENEOUS DIFFUSION

G. JÓHANNESSON[1], R. RUIZ DE AUSTRI[2], A.C. VINCENT[3], I. V. MOSKALENKO[4,5], E. ORLANDO[4,5], T. A. PORTER[4], A. W. STRONG[6], R. TROTTA[7,8], F. FEROZ, P. GRAFF[9], AND M.P. HOBSON[10]

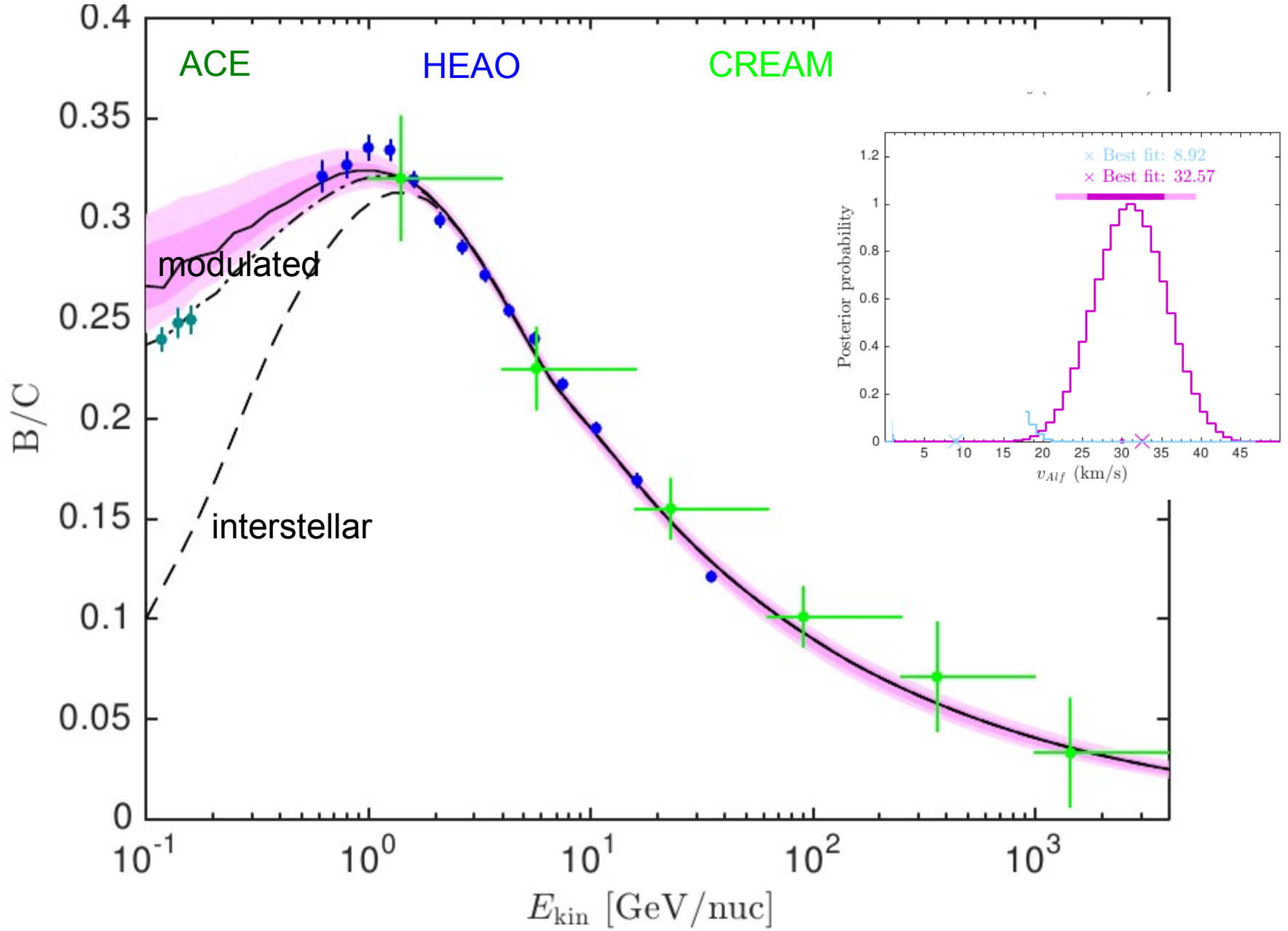

Diffusive Reacceleration

NB B/C break already produced by energy losses
Energy losses are tricky, ~Z^2 so C losses 36X proton losses
Modulation is uncertain anyway
Main evidence for peak is from ACE @ 100 MeV.

How far should we trust all this?

Astronomy & Astrophysics manuscript no. QERP
October 11, 2016

Power requirements for cosmic ray propagation models involving diffusive reacceleration; estimates and implications for the damping of interstellar turbulence.

Luke O'C. Drury[1] and Andrew W. Strong[2]

[1] Dublin Institute for Advanced Studies, School of Cosmic Physics, 31 Fitzwilliam Place, Dublin 2, Ireland
[2] MPI für Extraterrestrische Physik, Postfach 1312, 85741 Garching, Germany

ABSTRACT

We make quantitative estimates of the power supplied to the Galactic cosmic ray population by second-order Fermi acceleration in the interstellar medium, or as it is usually termed in cosmic ray propagation studies, diffusive reacceleration. Using recent results on the local interstellar spectrum from the Voyager missions we show that for parameter values, in particular the Alfvén speed, typically used in propagation codes such as GALPROP to fit the B/C ratio, the power contributed by diffusive reacceleration is significant and can be of order 50% of the total Galactic cosmic ray power. The implications for the damping of interstellar turbulence are briefly considered.

Spatial diffusion Momentum diffusion

$$\frac{\partial f}{\partial t} = Q + \nabla\left(D_{xx}\nabla f\right) + \frac{1}{4\pi p^2}\frac{\partial}{\partial p}\left(4\pi p^2 D_{pp}\frac{\partial f}{\partial p}\right) + ...$$

$$D_{xx}D_{pp} = p^2 V_A^2 \frac{1}{\delta(4-\delta)(4-\delta^2)} \geq \frac{1}{9}p^2 V_A^2$$

$$D_{pp} = \vartheta p^2 V_A^2 \frac{1}{D_{xx}}.$$

$$D_{xx} = D_0\left(\frac{v}{c}\right)\left(\frac{p}{mc}\right)^{\delta}$$

For a Kolmogorov spectrum with $\delta = 1/3$ we have $\vartheta = 81/385 \approx 0.21$ and the largest it can be is for $\delta = 1$ where we have $\vartheta = 1/9 \approx 0.11$; the results of Strong & Moskalenko (1998) can be obtained by setting

$$\vartheta = \frac{4}{3\delta(4-\delta^2)(4-\delta)w}. \qquad (17)$$

Simple derivation of diffusive reacceleration

Diffusive Reacceleration

If diffusion occurs in the ISM and particles gain or lose momentum on moving scatterers then some diffusion in momentum is inevitable.

Thornbury & Drury MNRAS 442 3010 (2014)
Simple derivation of diffusion coefficient in momentum D_{pp}

$D_{xx} \sim (1/3)\, \lambda^2/\tau = (1/3)\, \lambda\, v = (1/3)\, v^2\, \tau$ $\quad$ λ=mean-free-path $\quad$ τ = time between scatterings

At each scattering the particle undergoes momentum change

$\Delta p \sim V_A / v$ $\quad$ (taking V_A as typical of speed of scatterers)

$D_{pp} \sim (1/3)\, (\Delta p)^2/\tau = (1/3)\, p^2\, V_A^{\,2} / (v^2\, \tau)$

Hence

$$\mathbf{D_{xx} D_{pp} \sim (1/9)\, p^2 V_A^{\,2}}$$

More precise calculations: depends on turbulence spectral index δ, factor is

$1 / [\delta(4-\delta)(4-\delta^2)]$ $\quad$ ($= 1/9$ for $\delta = 1$, $\quad$ 0.2 for Kolmogorov $\delta = 1/3$)

Term in propagation equation

$$\mathbf{\partial \psi / \partial t} = \partial/\partial p\, [p^{\,2} D_{pp}\, \partial/\partial p\, (\psi / p^{\,2})]$$

The local reacceleration power density (energy per unit time and per unit volume) is shown in Thornbury & Drury (2014), assuming very reasonable regularity conditions on the particle distribution function, to be given by the integral over the particle spectrum,

$$P_R = \int_0^\infty 4\pi p^2 f \frac{1}{p^2} \frac{\partial}{\partial p} \left(p^2 D_{pp} v \right) dp \tag{18}$$

$$P_R = \int_0^\infty 4\pi p^2 f \left(\frac{\vartheta V_A^2 p v}{D_{xx}} \right) \left[4 + \frac{\partial \ln(v/D_{xx})}{\partial \ln p} \right] dp. \tag{19}$$

If we parametrise the spatial diffusion in the usual fashion as

$$D_{xx} = D_0 \left(\frac{v}{c} \right) \left(\frac{p}{mc} \right)^\delta \tag{20}$$

where m is the particle mass and c the speed of light this can be written in the useful and rather transparent form

$$P_R = \vartheta(4 - \delta) \frac{V_A^2}{D_0} mc^2 \int 4\pi p^2 f \left(\frac{p}{mc} \right)^{1-\delta} dp \tag{21}$$

Reacceleration power

$$P_R = \vartheta(4-\delta)\frac{V_A^2}{D_0}mc^2 \int 4\pi p^2 f \left(\frac{p}{mc}\right)^{1-\delta} dp \qquad (21)$$

which gives the local reacceleration power density in terms of a simple integral over the spectrum. The formula is interesting in that the term V_A^2/D is a rate, mc^2 is just the particle rest mass energy, and the integral is essentially just the total number density of cosmic ray particles biased by a power-law factor with exponent $1-\delta$. Thus the energy transfer is more or less as if all particles were acquiring their own rest mass energy on a time scale of D/V_A^2. Integrating this over the entire Galaxy then gives the total power transferred to the cosmic ray population from Alfvénic turbulence.

$D \sim 3\ 10^{28}$ cm^2 s^{-1}

$V_A \sim 30$ km s^{-1}

Time-scale to gain GeV ~ 10^8 years ~ CR residence time in Galaxy

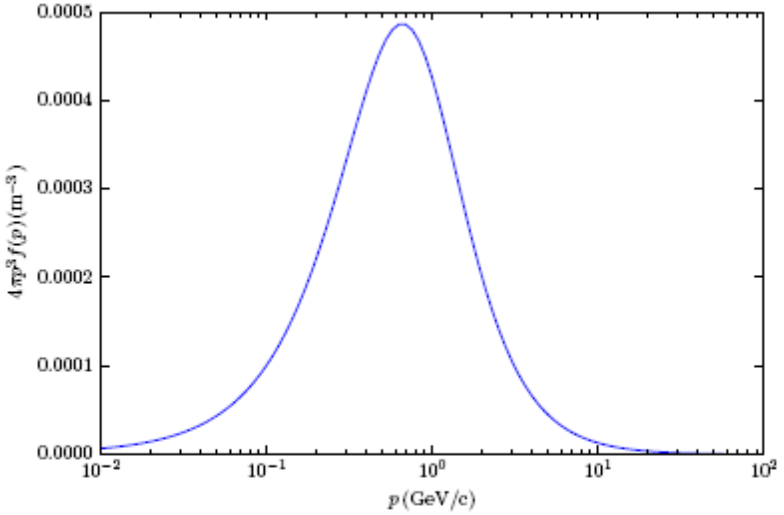

Fig. 1. The local interstellar proton number spectrum from Vos & Potgieter (2015)

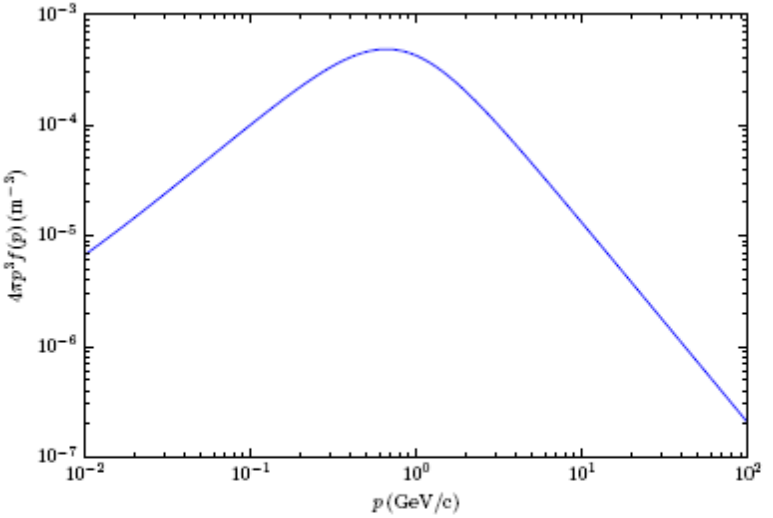

Fig. 2. The local interstellar proton number spectrum from Vos & Potgieter (2015) in a more conventional log log representation showing the power-law tails

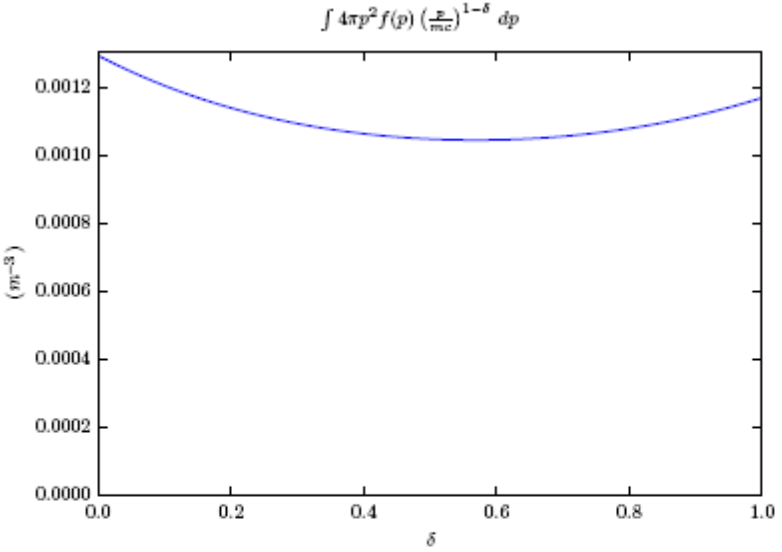

Fig. 3. The integral of $(p/mc)^{1-\delta}$ weighted by the local interstellar proton number spectrum from Vos & Potgieter (2015) as a function of δ - note that the dimensions are m^{-3}. The value for $\delta = 1$ is just the cosmic ray number density.

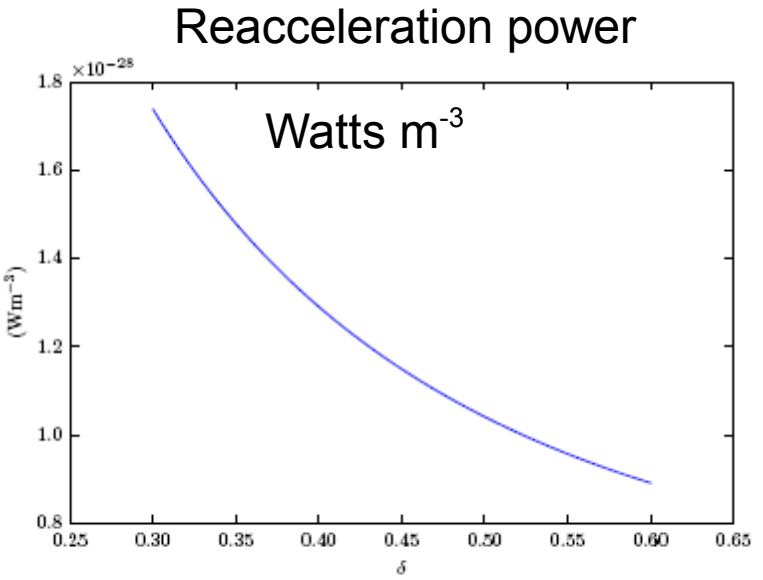

Fig. 4. The local reacceleration power density from Eq. 21, the Vos and Potgieter local interstellar spectrum, $V_A = 30\,\mathrm{km\,s^{-1}}$ and $D_0 = 10^{28}\mathrm{cm^2 s^{-1}}$

We can now evaluate the integral in Eq. 21 over the local interstellar spectrum as parametrized by Vos and Potgieter. The result is shown in Fig 3 and shows a very weak dependence on δ. In Fig. 4 we show the corresponding power density from Eq. 21 using

$$\vartheta = \frac{4}{3\delta(4-\delta^2)(4-\delta)}, \tag{25}$$

and canonical values

$$V_A = 30\,\mathrm{km\,s^{-1}} \qquad D_0 = 10^{28}\,\mathrm{cm^2 s^{-1}}. \tag{26}$$

We only plot the physically relevant range $0.3 < \delta < 0.6$ where we see that the power density is

$$P_R \approx 1.3 \pm 0.4 \times 10^{-28}\,\mathrm{W\,m^{-3}} = \underline{1.3 \pm 0.4 \times 10^{-27}\,\mathrm{erg\,cm^{-3}}} \tag{27}$$

if we now naively take the effective volume for the Galaxy to be $4 \times 10^{61}\,\mathrm{m^3}$ then the total power input from diffusive reacceleration can be estimated as $5 \times 10^{33}\,\mathrm{W} = \underline{5 \times 10^{40}\,\mathrm{erg\,s^{-1}}}$. This should be compared with the canonical estimate of the total cosmic ray Galactic luminosity of order $10^{34}\,\mathrm{W}$ or $\underline{10^{41}\,\mathrm{erg\,s^{-1}}}$ (see discussion in Drury (2014) where it is noted that there is probably half a decade of systematic uncertainty in this estimate either way). Thus we have the, at first sight rather remarkable, result that diffusive reacceleration may be contributing as much as 50% of the total cosmic ray luminosity of the Galaxy!

2.2. Estimates using GALPROP

As a cross-check on the above we now use the numerical CR-propagation package GALPROP[1], using parameters which reproduce B/C with reacceleration, and then with the same parameters but without the reacceleration term, so that the difference in energy content is due to the reacceleration process[2] The total CR proton energy content of the Galaxy is computed by integration over momentum and volume.

We base the calculation on the model z04LMS, which has reacceleration and a CR halo height of 4 kpc and $V_A = 30$ km s^{-1} Strong et al. (2010). This model has typical parameter values which reproduce B/C in reacceleration models (see also Trotta et al. (2011); Jóhannesson et al. (2016)).

The CR proton energy content of the Galaxy is $(8.1,\ 6.4) \times 10^{55}$erg with and without reacceleration respectively. Hence 1.7×10^{55} erg results from reacceleration, or ≈20% of of the total; stated another way, the original energy injected by sources is boosted by ≈25%.

The luminosity of the Galaxy can be estimated from the total energy content using a value for the residence time of CR in the Galaxy. The total proton luminosity for our reacceleration model[3] is 8×10^{40} erg s^{-1} Strong et al. (2010), so the effective CR residence time is $\approx 3 \times 10^7$ yr. Hence the proton luminosity is $8.0,\ 6.3 \times 10^{40}$ erg s^{-1} with and without reacceleration respectively. This is consistent with the analytical estimates in Section 2.1. Note that the relative values quoted above are independent of the assumed residence time.

GALPROP

Protons without and with reacceleration, v_A = 30 km s^{-1}

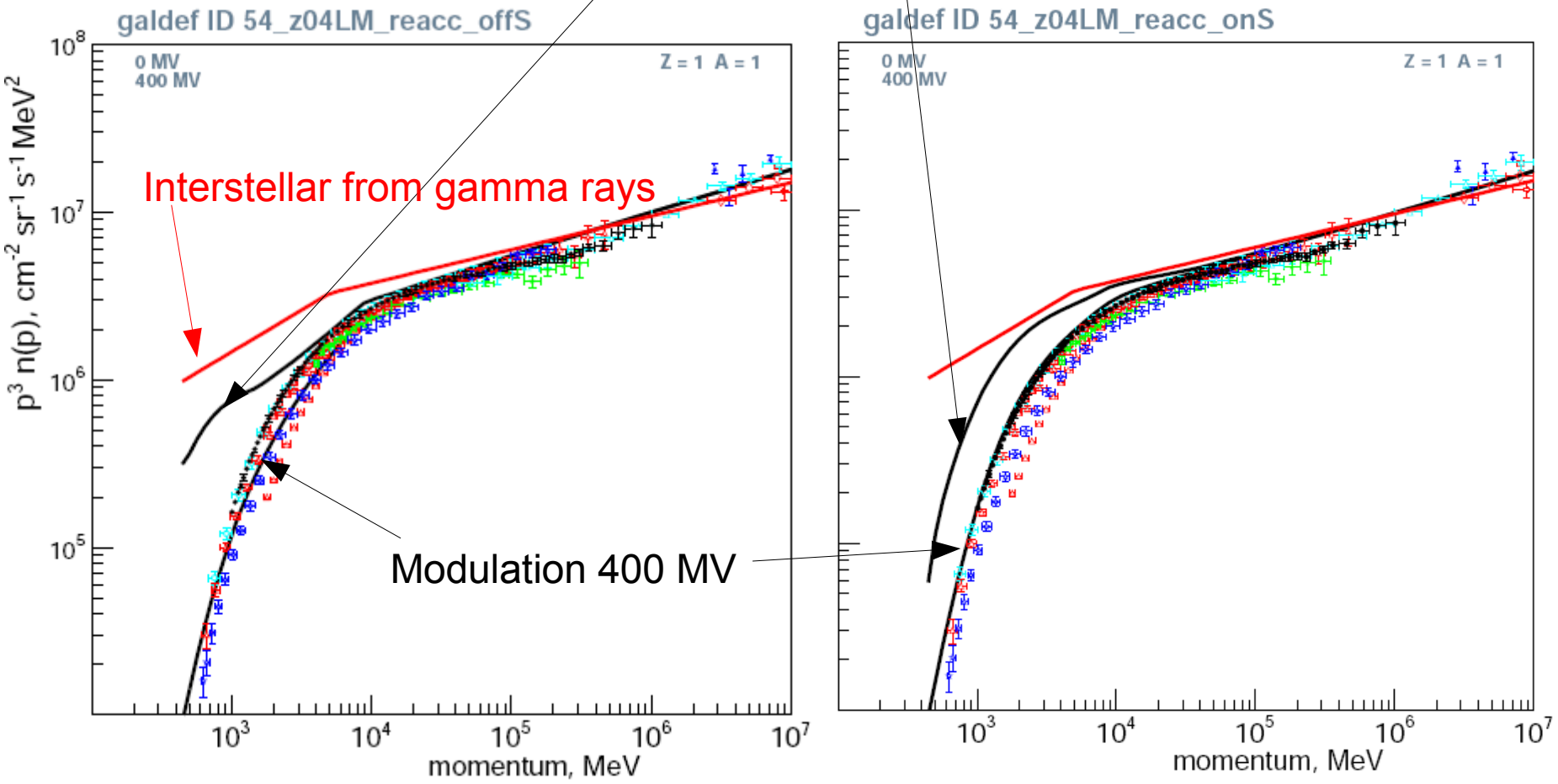

GALPROP

Protons without and with reacceleration, v_A = 30 km s^{-1}

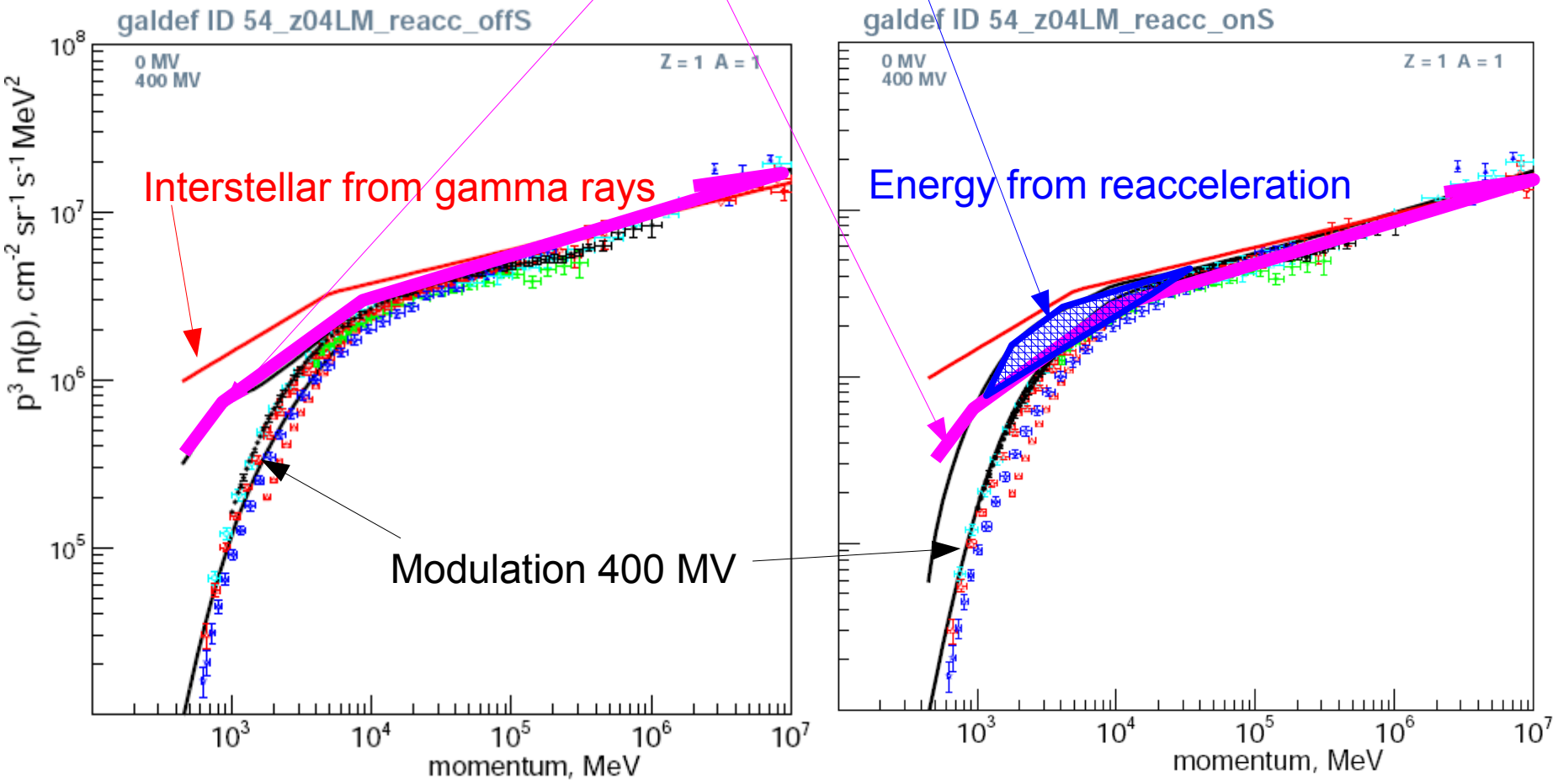

Our estimates of the reacceleration power are necessarily approximate, but suffice to demonstrate that, for parameters chosen to reproduce B/C and commonly used in propagation calculations, the energy input via reacceleration is of order a quarter to half the total energy input. SNRs are then not "*the* sources of CR" in such models, at least not in the conventional sense! In retrospect this is perhaps not as surprising as it first seems. If the bulk of the energy resides in mildly relativistic and subrelativistic particles, and if the spectrum in this region is to be significantly modified by reacceleration, then the energy input must be significant.

An interesting consequence is that the cosmic rays in such models must also damp interstellar turbulence and it is interesting to ask whether this is physically plausible and significant. Energetically it is not impossible. The main energy input into interstellar turbulence is generally taken to be the mechanical energy from expanding SNR shells and there is thus enough power input, but at quite large scales (Elmegreen & Scalo 2004; Scalo & Elmegreen 2004). The turbulence is normally assumed to be dissipated by non-linear cascading to high wave-number modes and the question is whether the cosmic rays can extract enough energy from the cascade at the scales which scatter mildly relativistic particles before thermal dissipation takes over. This is far from obvious, but if it is the case then the cosmic rays may define the inner scale of the interstellar turbulence. SNRs would then remain the ultimate engine driving cosmic ray acceleration, but through two channels; a direct one involving shock acceleration, and an indirect one mediated by interstellar turbulence.

Meanwhile it is essential to consider alternative explanations of the peak in the energy-dependence B/C, in particular convection gives a fairly natural mechanism (e.g. Korsmeier & Cuoco 2016) and there is evidence for a Galactic wind (e.g. Everett et al. 2012). The main message of this work is that behind the reacceleration term in the propagation codes there is a significant impact on the total energy budget of both the cosmic rays and the interstellar turbulence. It is not a free parameter than one can tune at will without physical consequences.

Note that the velocity term in D_{xx} and energy losses both already cause a reduction in B/C at low energies.

So reaccleration or convection just boost these already-present effects.

Sample convection + diffusion model
(no reacceleration)
No break in D_{xx}
Wind-speed = 100 km s^{-1}

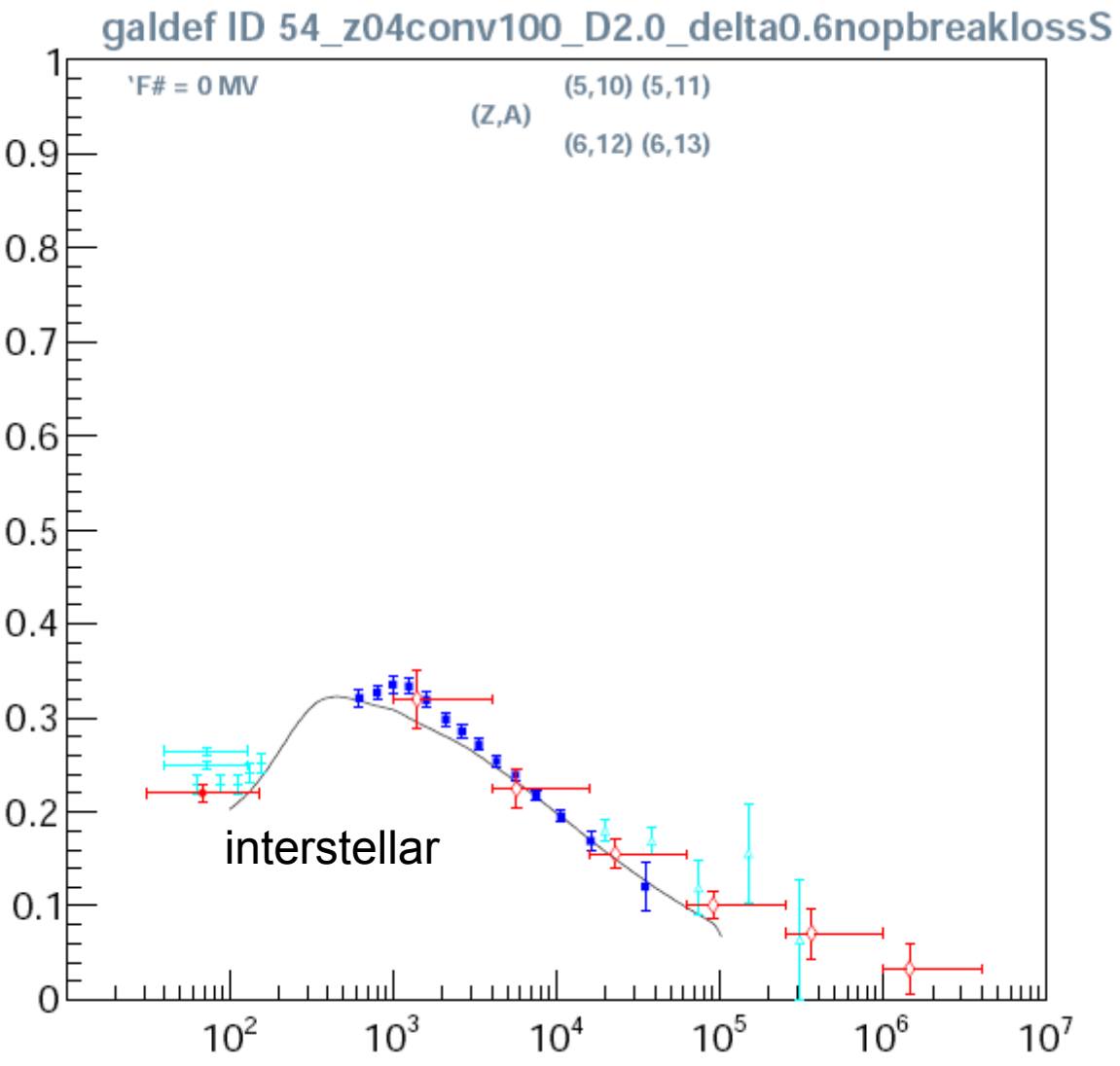

THE ASTROPHYSICAL JOURNAL, 174:253–291, 1972 June 1

1972

EXTRAGALACTIC COSMIC RAYS

K. BRECHER AND G. R. BURBIDGE
Department of Physics, University of California, San Diego
Received 1971 September 27; revised 1971 December 28

ABSTRACT

A detailed analysis is given of the possibility that a large part of the primary cosmic-ray flux is of extragalactic origin. Following the introduction, § II contains a critical discussion of problems en-

Thus the limits of the background γ-ray flux only rule out extragalactic cosmic-ray schemes in cosmological models in which mass at a number density of 10^{-5} cm^{-3} exists in the form of diffuse gas in contact with the cosmic rays, or in models in which it is supposed that there was rapid evolution of sources in the past. There is certainly no evidence that gas at a density 10^{-5} cm^{-3} is present (Burbidge 1971), and the evidence for rapid

THE ASTROPHYSICAL JOURNAL, 174:253–291, 1972 June 1

1972

EXTRAGALACTIC COSMIC RAYS

K. BRECHER AND G. R. BURBIDGE
Department of Physics, University of California, San Diego
Received 1971 September 27; revised 1971 December 28

ABSTRACT

A detailed analysis is given of the possibility that a large part of the primary cosmic-ray flux is of extragalactic origin. Following the introduction, § II contains a critical discussion of problems en-

Both gamma-ray and cosmological information have improved! 44 years on ...

Thus the limits of the background γ-ray flux only rule out extragalactic cosmic-ray schemes in cosmological models in which mass at a number density of 10^{-5} cm^{-3} exists in the form of diffuse gas in contact with the cosmic rays, or in models in which it is supposed that there was rapid evolution of sources in the past. There is certainly no evidence that gas at a density 10^{-5} cm^{-3} is present (Burbidge 1971), and the evidence for rapid

Nature 241 109 (1973)

Consequences of a Universal Cosmic-ray Theory for γ-ray Astronomy

THE problem of the origin of cosmic rays is well known; but in spite of considerable advances in knowledge concerning energetic extra-terrestrial objects in recent years, no satisfactory solution has appeared. It is not clear, even, whether the important sources are within the Galaxy or outside it[1,2].

Here we consider the possibility of reviving a theory due to Hillas[3] in which the observed shape of the primary spectrum up to about 3×10^{19} eV is explained in terms of an evolving sources model with constant spectral index at production, and interactions with the microwave background radiation. Such a model can explain the sharp change of slope at 3×10^{15} eV inferred from measurements of the sizes of extensive air

A. W. STRONG
A. W. WOLFENDALE

Physics Department,
University of Durham

J. WDOWCZYK

Institute of Nuclear Physics,
Lodz, Poland

Receive

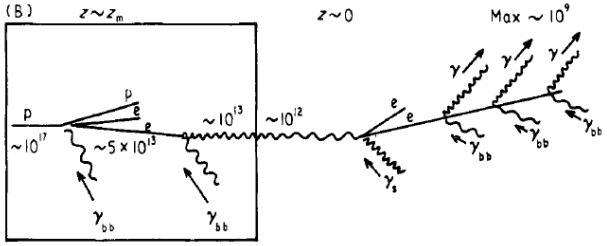

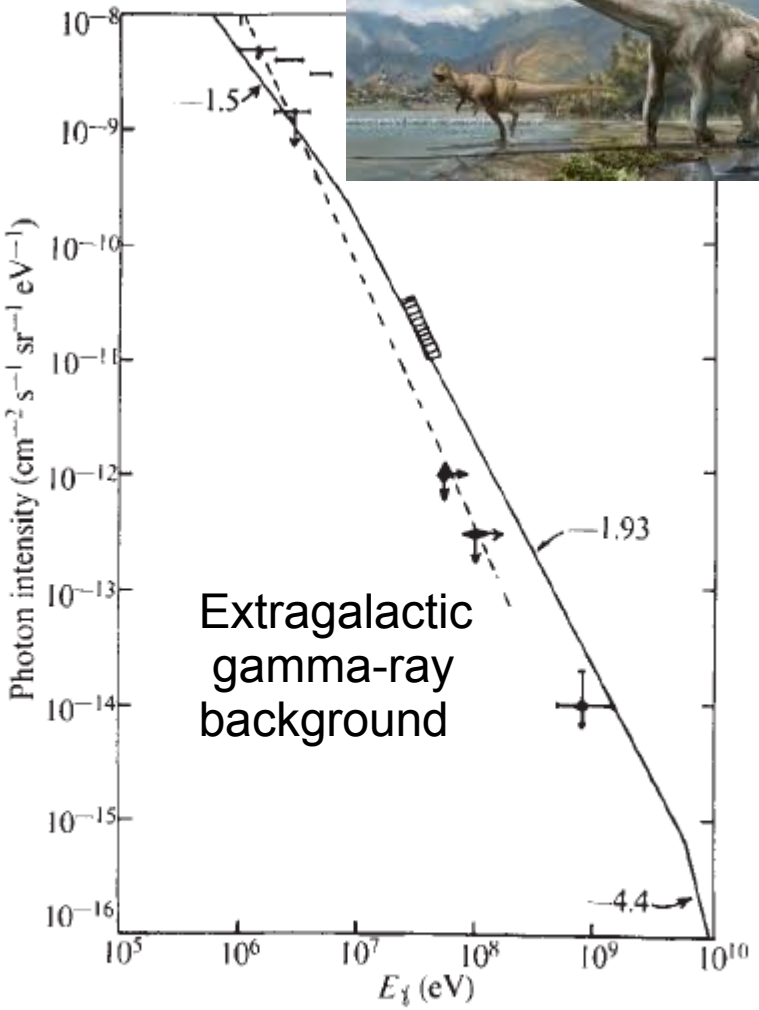

Fig. 1 The expected γ-ray spectrum (solid line). ◆, Ref. 9 (OSO-3); ◆, ref. 8 (COSMOS-208); ✸, ref. 8 (PROTON-2); ⊢⊣, ref. 10 (COSMOS-163); ⊢⊣ ref. 11 (ERS-18); - - - - -, ref. 10 ($E^{-2.4}$ fit to experimental data); ▥, ref. 12 (balloon experiment).

Universal EGCR, zmax=15, protons > 10^{15} eV, EM cascades, source evolution
Produces CR spectral break, energy -> gamma rays, provides the normalization!

The gamma-ray background: a consequence of metagalactic cosmic ray origin?

J. Phys. A, 7, 120 (1974)

A W Strong, J Wdowczyk† and A W Wolfendale

Physics Department, University of Durham, South Road, Durham City, UK

EGCR

injected

converted to gamma rays

propagated

Extragalactic gamma-ray background

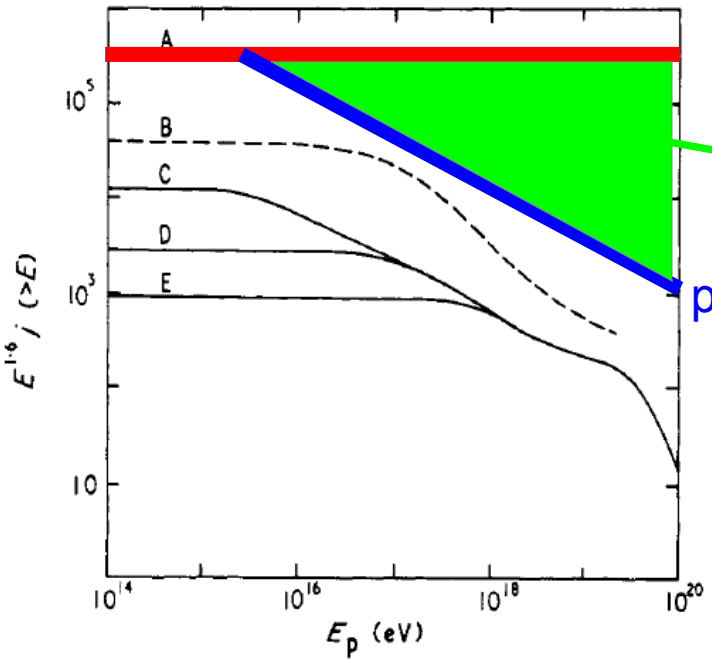

Figure 1. Primary spectra on Hillas' theory for various parameters, compared with (normalized) experimental summary. Curve A, experimental; B, $z_D = 10$; C, $z_m =$ D, $z_m = 3$ and E, $z_m = 1$. Power law evolution: $\beta = 4{\cdot}5$, exponential evolution: ... $(1+z_D)z(1+z)^{-1}$.

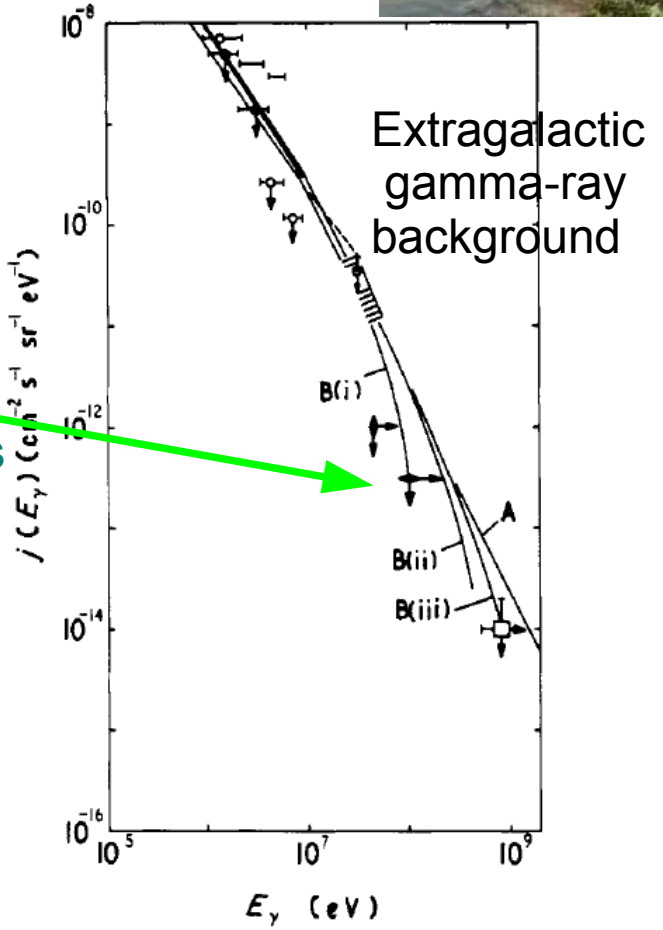

Figure 3. Gamma-ray spectrum expected from Hillas' model

Universal EGCR, zmax=15, protons > 10^{15} eV, EM cascades, source evolution
Produces CR spectral break, energy -> gamma rays, provides the normalization!

The gamma-ray background: a consequence of metagalactic cosmic ray origin?

J. Phys. A, 7, 120 (1974)

A W Strong, J Wdowczyk† and A W Wolfendale

Physics Department, University of Durham, South Road, Durham City, UK

EGCR

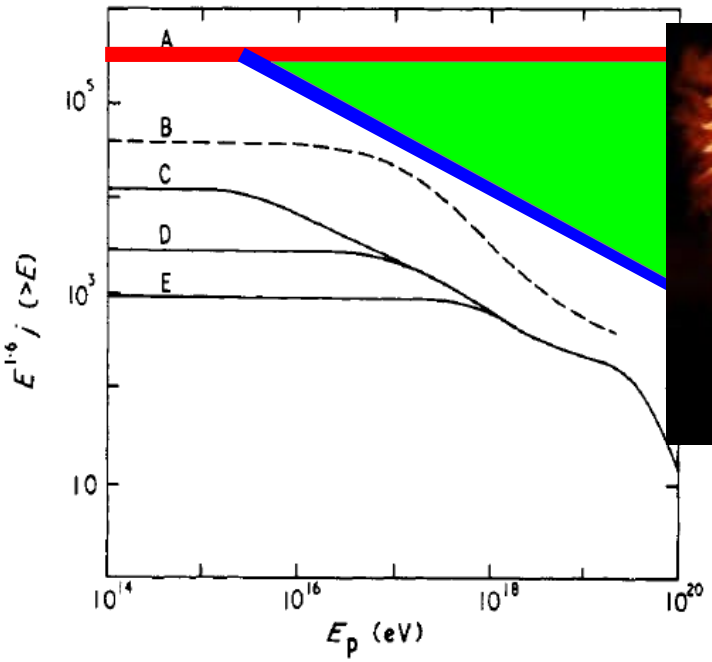

Figure 1. Primary spectra on Hillas' theory for various parameters, compared with (normalized) experimental summary. Curve A, experimental; B, $z_D = 10$; C, $z_m =$ D, $z_m = 3$ and E, $z_m = 1$. Power law evolution: $\beta = 4{\cdot}5$, exponential evolution: ... $(1+z_D)z(1+z)^{-1}$.

See later ….

Extragalactic gamma-ray background

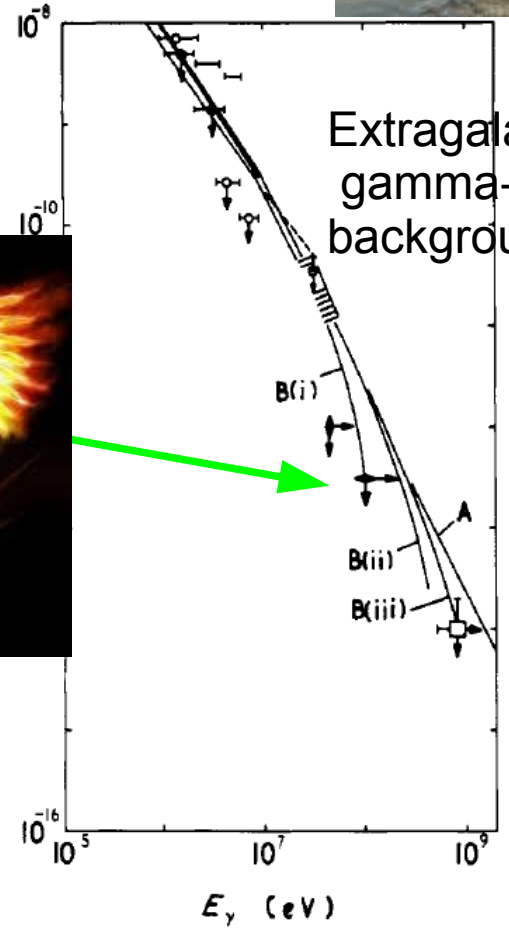

Figure 3. Gamma-ray spectrum expected from Hillas' model

Universal EGCR, zmax=15, protons > 10^{15} eV, EM cascades, source evolution
Produces CR spectral break, energy -> gamma rays, provides the normalization!

CR are extragalactic only >10^{15} eV or so REALLY?

Heresy:
Universal CR theory Brecher&Burbidge 1972
Classical proof: pion-decay gammas would violate observations of EGB !

Back-of-envelope calculation:
Galactic gamma-ray emissivity for π^o : q(>100 MeV) ~ 10^{-25} atom^{-1} s^{-1}
IGM matter density n ~ 10^{-7} atoms cm^{-3} (see next slide)
Hubble distance L ~ 10^{28} cm
Flux(>100 MeV) = $(q/4\pi)\, n\, L \sim 10^{-5}$ cm^{-2} sr^{-1} s^{-1}
Close to IGRB observed! But known to be mainly AGN.
Need to look at those numbers more closely!

But what is IGM matter density? Lower limit from normal galaxies,
But they certainly contribute at percent level to EGB even though
CR probably similar to MW.

Also CR gradients in Galaxy: but how solid are they
Small gradient has stimulated models, EGCR would solve the problem

Problem with CR secondaries?
They are Galactic certainly, but that does not exclude that primaries are extragalactic.

IGM gas from QSO UV absorption lines
Neeleman etal ApJ 818, 113 (2016)
$z<0.6$

$0.25^{+0.2}_{-.12}\ 10^8\ M_{sun}\ Mpc^{-3}$
$\rightarrow 10^{-9}$ atoms cm^{-3}

Typical column densities $10^{20}\ cm^{-2}$
cf Galactic halo so similar to EGB, Galactic high-latitudes

But from CMB, BBN: $10^{-7}\ cm^{-3}$ NB not directly observed but theory solid

'Missing baryons problem': WHIM too hot to observe easily
but at least 50% seen in clusters, etc so not critical to IGRB calculation

At any rate for $E>10^{12}$ eV CR can be EG

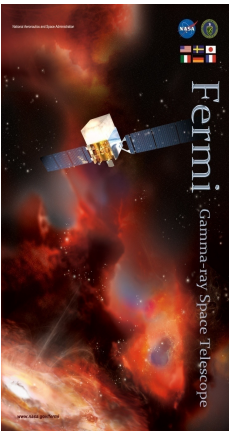

Interstellar Cosmic ray spectra derived from gamma rays

Method : Bayesian analysis (Strong et al. arXiv:1507.05006)

Gamma-ray gas emissivity *used to derive* Cosmic-ray protons via pion-decay

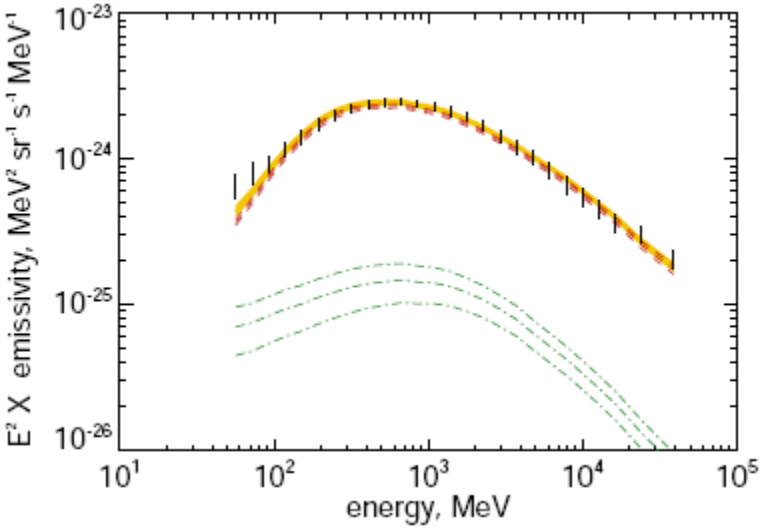

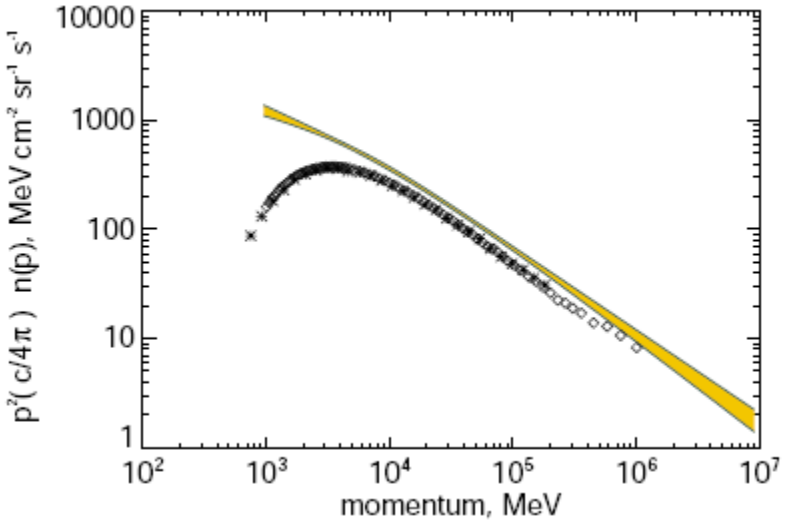

Below 10 GeV affected by solar modulation, but gamma rays probe the **interstellar** spectrum.

Emissivity of local interstellar gas – Jean-Marc Casandjian (Fermi-LAT Collab).

Power-law in momentum overall, but low-energy break
e.g. from power-law injection and interstellar propagation (diffusion = f(E))

Extragalactic gamma-ray background from Fermi-LAT
Ackermann et al 2015
IGRB = radiation not from (yet) detected sources
  Time-dependent, decreases as detections go deeper
Appropriate for comparison with non-source components
IGRB < EGB (total intergalactic photon field)

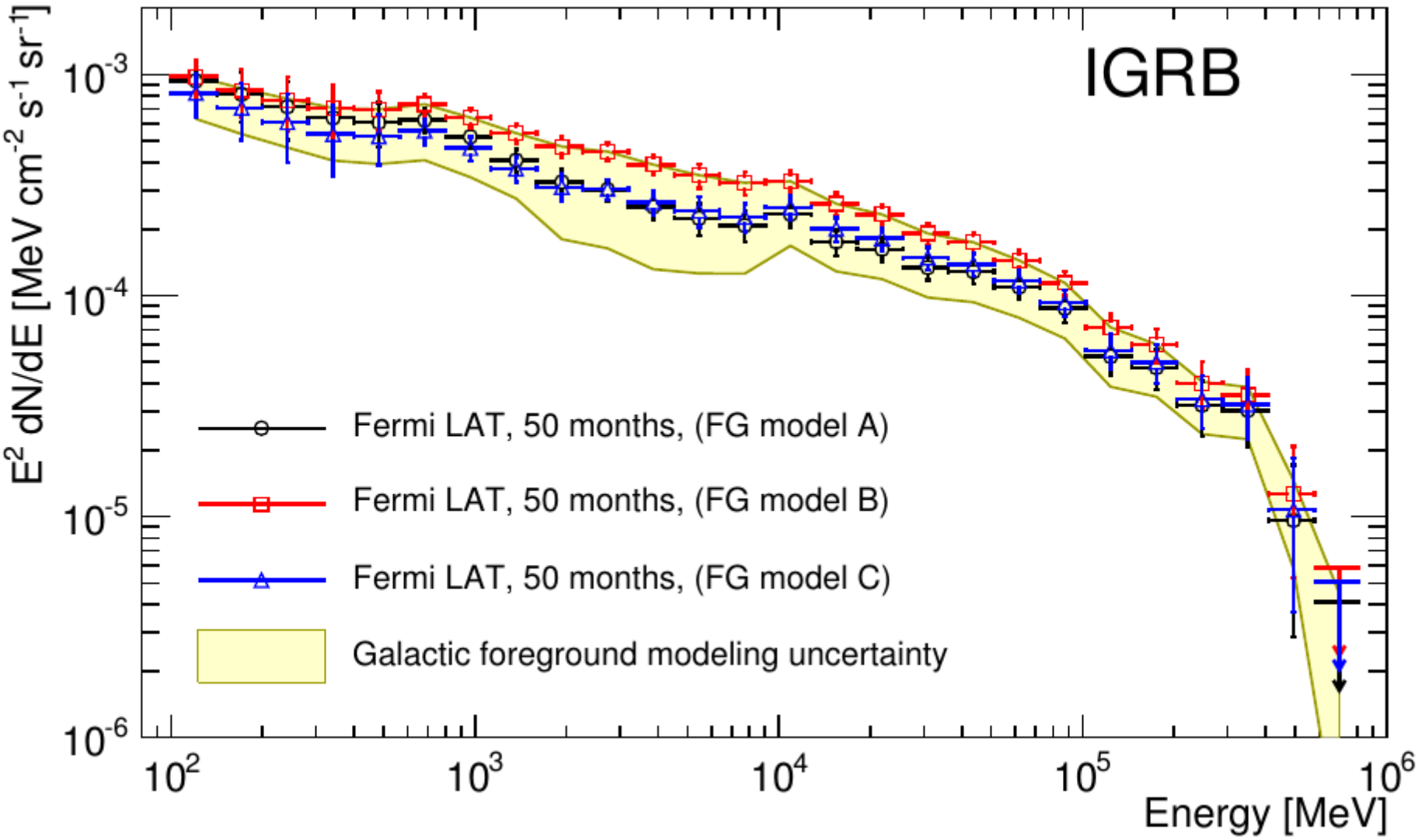

What if CR were universal?

Local gamma-ray emissivity per atom

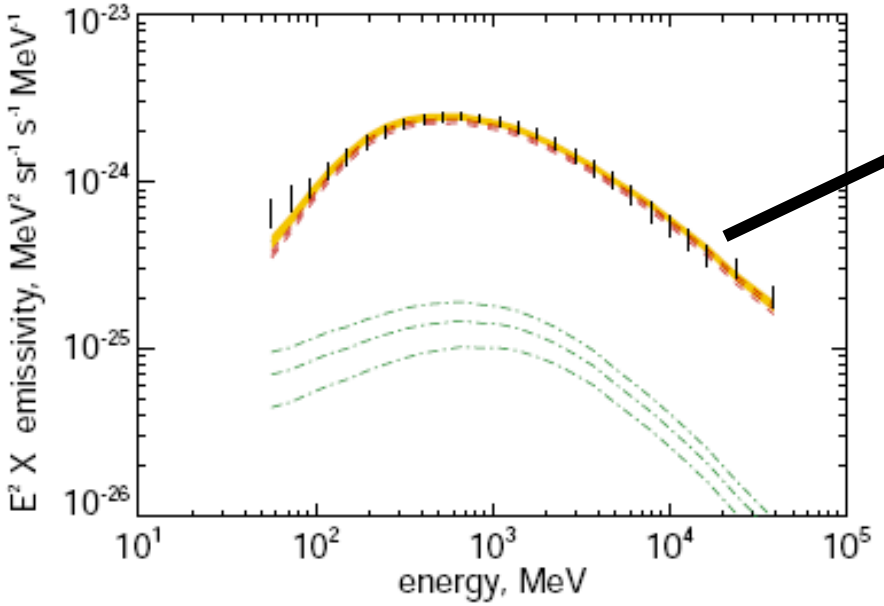

IGRB fromFermi-LAT

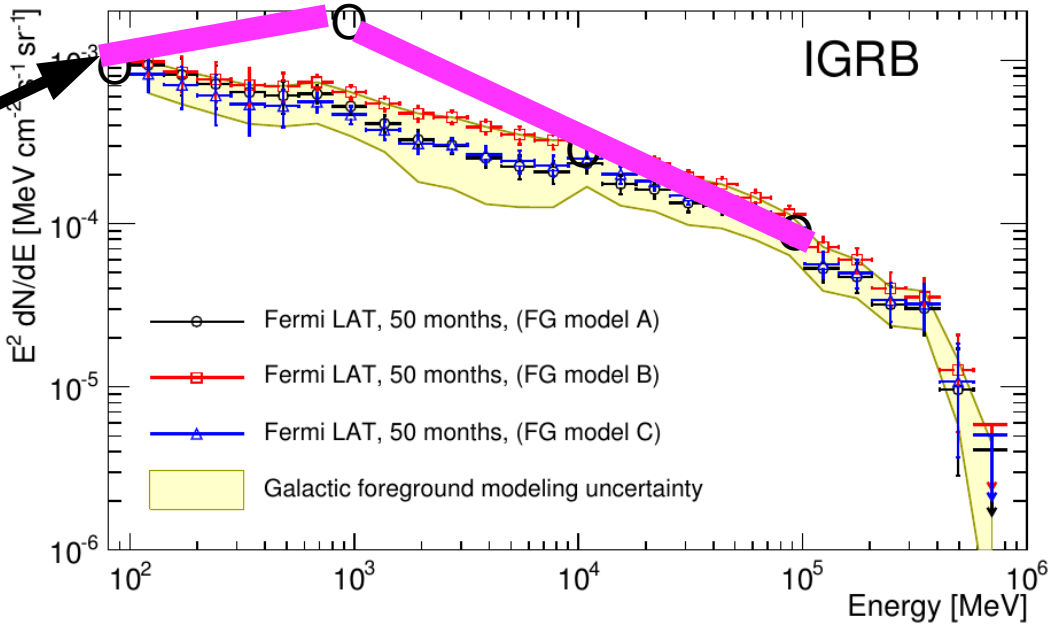

Extragalactic intensity ~ Hubble distance X gas density X emissivity
= 10^{28} cm X 10^{-7} cm^{-3} X emissivity = 10^{21} X emissivity

E MeV	E^2 X emissivity	E^2 X extragalactic intensity
10^2	1 10^{-24}	1 10^{-3}
10^3	2 10^{-24}	2 10^{-3}
10^4	4 10^{-25}	4 10^{-4}
10^5	1 10^{-25}	1 10^{-4}

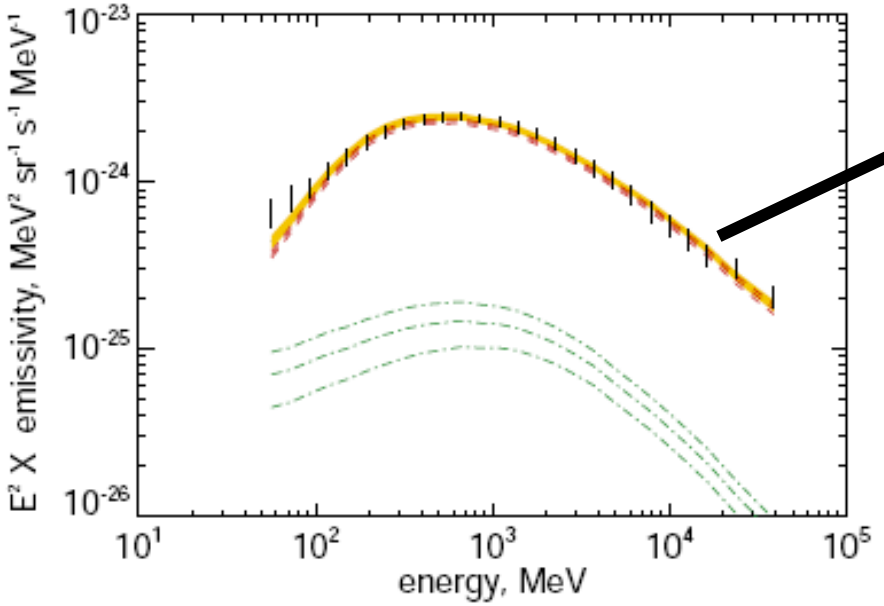

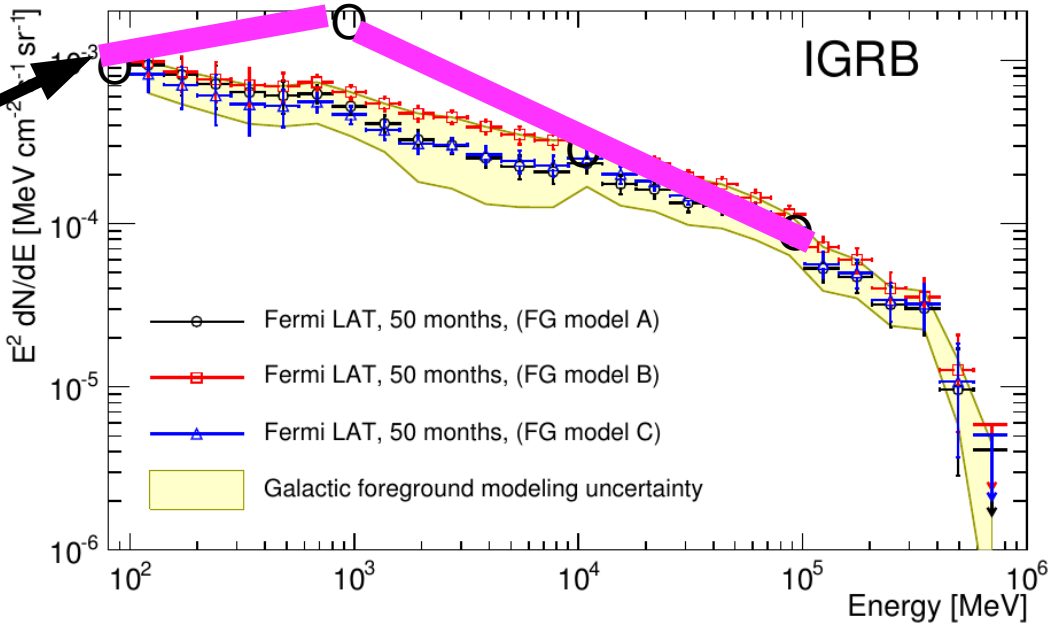

But IGRB thought to be mainly AGN etc (>80%) so EGCR must be much less than GCR
EGCR/GCR = 5 - 10% still allowed below 1 TeV

Beyond 1 TeV no IGRB measurements (now; any prospects?) so anything goes!!

THE ASTROPHYSICAL JOURNAL, 174:253–291, 1972 June 1

EXTRAGALACTIC COSMIC RAYS

K. BRECHER AND G. R. BURBIDGE
Department of Physics, University of California, San Diego
Received 1971 September 27; revised 1971 December 28

ABSTRACT

A detailed analysis is given of the possibility that a large part of the primary cosmic-ray flux is of extragalactic origin. Following the introduction, § II contains a critical discussion of problems en-

Both gamma-ray and cosmological information have improved! 44 years on:
Intergalactic gas density and gamma-ray background much lower
Constraints on EGCR much stronger but still margin for speculation.

Thus the limits of the background γ-ray flux only rule out extragalactic cosmic-ray schemes in cosmological models in which mass at a number density of 10^{-5} cm^{-3} exists in the form of diffuse gas in contact with the cosmic rays, or in models in which it is supposed that there was rapid evolution of sources in the past. There is certainly no evidence that gas at a density 10^{-5} cm^{-3} is present (Burbidge 1971), and the evidence for rapid

CR Escape from normal galaxies,
luminosity times Hubble time

Using MW luminosity paper Strong et al. ApJL 722, L58 (2010) :

Cosmic-ray proton luminosity of MW Galaxy = 10^{41} erg s^{-1}
Space density of normal galaxies = 10^{-2} per Mpc^{-3}
→ 10^{-5} eV cm^{-3}

Guaranteed minimum EGCR density!

Energy-dependent escape steepens the Galactic spectrum
But the universe has no boundary so nucleon calorimeter and reflects the injection spectrum! e.g. 2.3

Aublin & Parizot: A&A 452, 19 (2006)

Holistic model: all CR have same sources!
Escape from normal galaxies.

Global CR index 2.23

EGCR(10^{19} eV)/GCR(10^{9} eV) = 2.4 10^{27}
→ GCR/EGCR(1 GeV) = 10^{-5}

Consistent with above estimate.

Cosmic-ray energy spectrum and composition up to the ankle — the case for a second Galactic component

S. Thoudam[1,2,⋆], J.P. Rachen[1], A. van Vliet[1], A. Achterberg[1], S. Buitink[3], H. Falcke[1,4,5], J.R. Hörandel[1,4]

arXiv:1605.03111

Cosmic-ray energy spectrum and composition up to the ankle — the case for a second Galactic component

S. Thoudam[1,2,⋆], J.P. Rachen[1], A. van Vliet[1], A. Achterberg[1], S. Buitink[3], H. Falcke[1,4,5], J.R. Hörandel[1,4]

arXiv:1605.03111

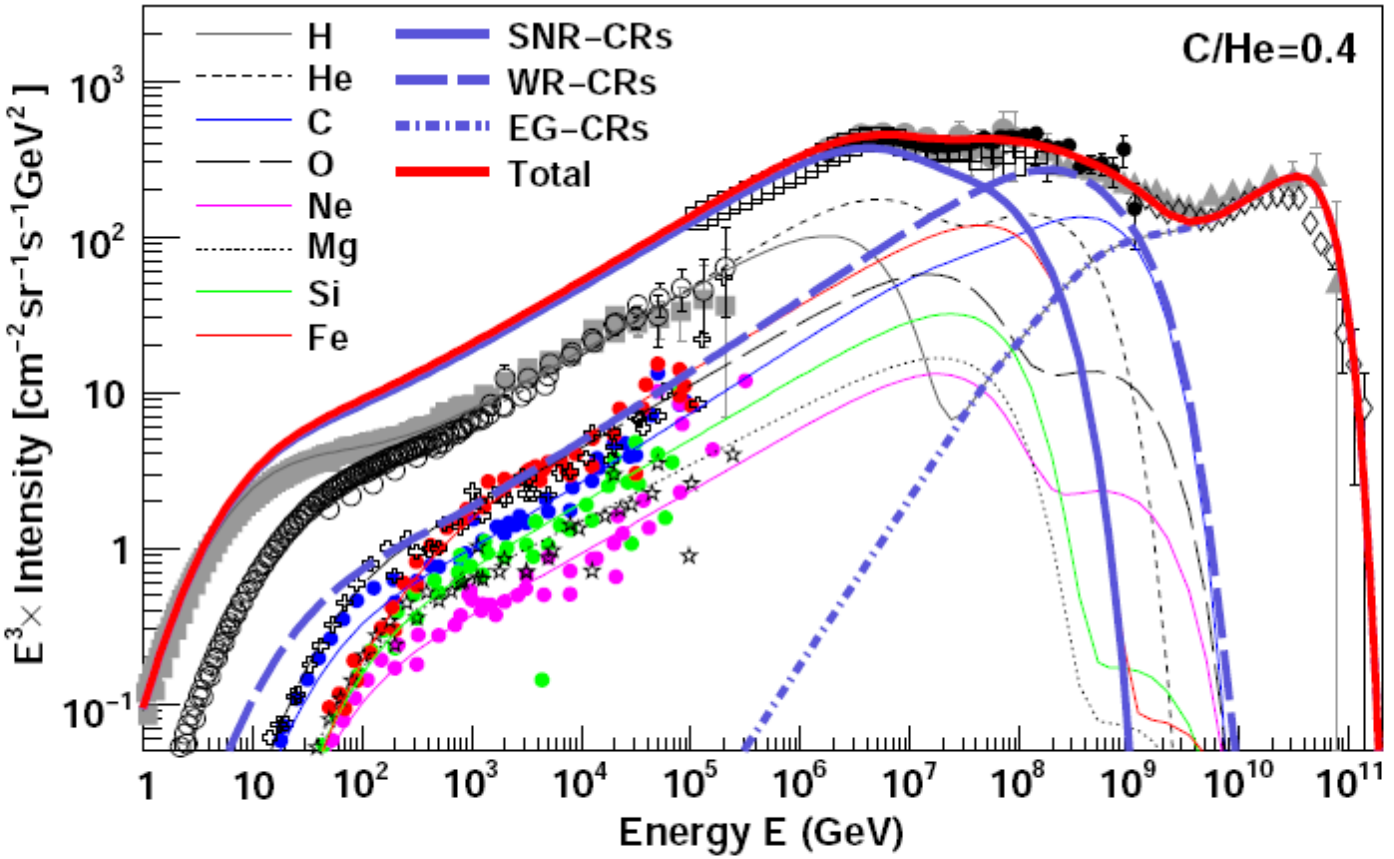

Fig. 6. Model prediction for the all-particle spectrum using the Wolf-Rayet stars model. *Top*: C/He = 0.1. *Bottom*: C/He = 0.4. The thick solid blue line represents the total SNR-CRs, the thick dashed line represents WR-CRs, the thick dotted-dashed line represents EG-CRs, and the thick solid red line represents the total all-particle spectrum. The thin lines represent total spectra for the individual elements. For the SNR-CRs, an exponential energy cut-off for protons at $E_c = 4.1 \times 10^6$ GeV is assumed. See

Cosmic-ray energy spectrum and composition up to the ankle — the case for a second Galactic component

S. Thoudam[1,2,⋆], J.P. Rachen[1], A. van Vliet[1], A. Achterberg[1], S. Buitink[3], H. Falcke[1,4,5], J.R. Hörandel[1,4]

arXiv:1605.03111

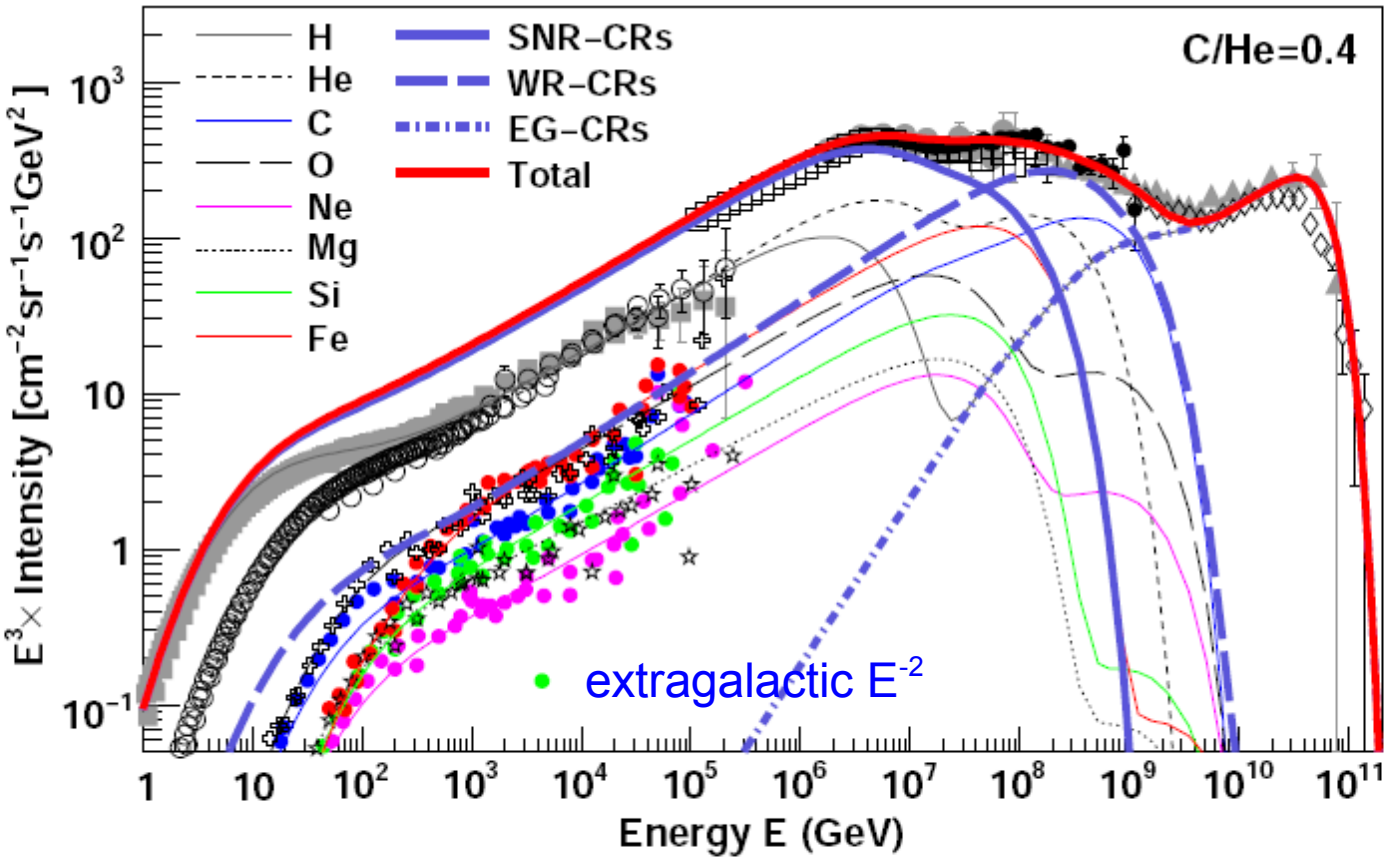

Fig. 6. Model prediction for the all-particle spectrum using the Wolf-Rayet stars model. *Top*: C/He = 0.1. *Bottom*: C/He = 0.4. The thick solid blue line represents the total SNR-CRs, the thick dashed line represents WR-CRs, the thick dotted-dashed line represents EG-CRs, and the thick solid red line represents the total all-particle spectrum. The thin lines represent total spectra for the individual elements. For the SNR-CRs, an exponential energy cut-off for protons at $E_c = 4.1 \times 10^6$ GeV is assumed. See

WHY extragalactic E^{-2} ?

Cosmic-ray energy spectrum and composition up to the ankle — the case for a second Galactic component

S. Thoudam[1,2,⋆], J.P. Rachen[1], A. van Vliet[1], A. Achterberg[1], S. Buitink[3], H. Falcke[1,4,5], J.R. Hörandel[1,4]

arXiv:1605.03111

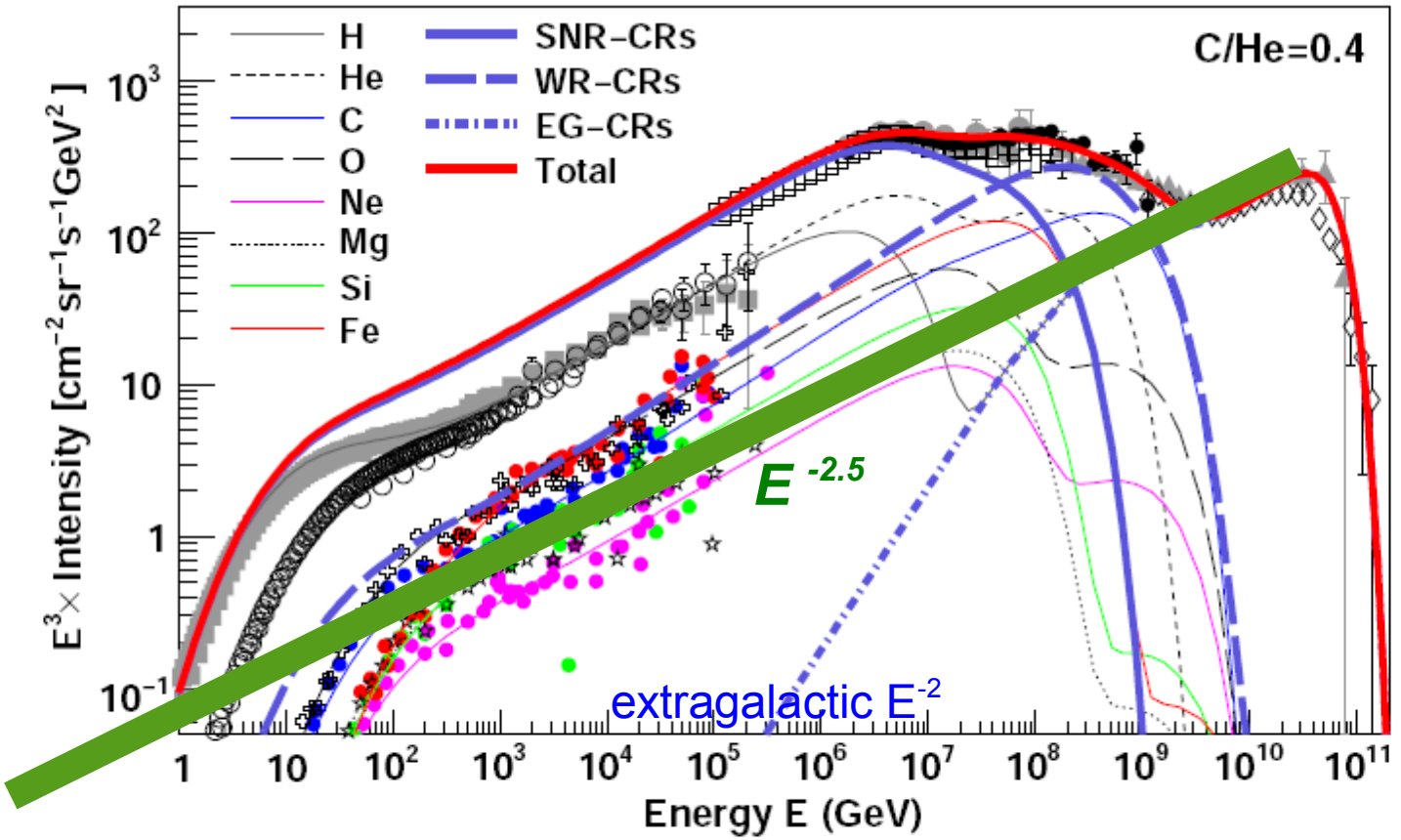

Fig. 6. Model prediction for the all-particle spectrum using the Wolf-Rayet stars model. *Top*: C/He = 0.1. *Bottom*: C/He = 0.4. The thick solid blue line represents the total SNR-CRs, the thick dashed line represents WR-CRs, the thick dotted-dashed line represents EG-CRs, and the thick solid red line represents the total all-particle spectrum. The thin lines represent total spectra for the individual elements. For the SNR-CRs, an exponential energy cut-off for protons at $E_c = 4.1 \times 10^6$ GeV is assumed. See

WHY not e.g. extragalactic $E^{-2.5}$? then significant EG component down to GeV
EGCR/GCR = 1% at 10 GeV is OK for pion-decay background

Cosmic-ray energy spectrum and composition up to the ankle — the case for a second Galactic component

S. Thoudam[1,2,⋆], J.P. Rachen[1], A. van Vliet[1], A. Achterberg[1], S. Buitink[3], H. Falcke[1,4,5], J.R. Hörandel[1,4]

arXiv:1605.03111

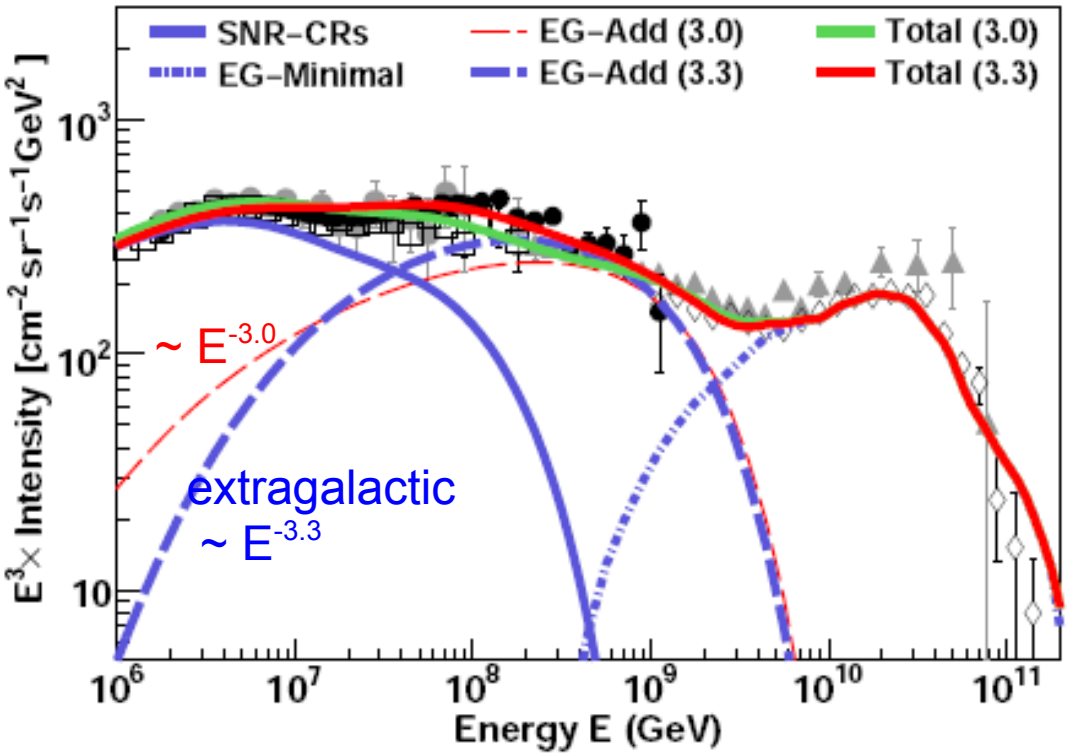

Fig. 13. All-particle energy spectrum for an additional component of EG-CR protons extended down to low energies and modulated by Galactic wind. The numbers within the parentheses denote the injection index for the additional extra-galactic component. For the SNR-CRs, an exponential cut-off energy for protons at 4.1×10^6 GeV is assumed. See text for other details.

Only to 10^{15} eV

Cosmic-ray energy spectrum and composition up to the ankle — the case for a second Galactic component

S. Thoudam[1,2,⋆], J.P. Rachen[1], A. van Vliet[1], A. Achterberg[1], S. Buitink[3], H. Falcke[1,4,5], J.R. Hörandel[1,4]

arXiv:1605.03111

An additional problem for EG-CRs with an overall spectrum steeper than $E^{-2.7}$ is that, if one assumes that they fill the extra-galactic space homogeneously with energies from $\sim$1 GeV to 10^9 GeV, it contains more energy than the gravitational binding energy released in the universe during structure formation (Rachen 2016). Using realistically low efficiencies for this energy – which is, besides the lower overall nuclear binding energy released in fusion by all primordial baryonic matter going into stars, the only fundamental energy budget present in the late universe – to be converted into cosmic rays, one can conclude that spectral indices as discussed here for a dominant extra-galactic component below the second knee cannot easily be reconciled with this energy budget, no matter which kind of sources one proposes. Mainly on the basis of this argument, together with the difficulties of a sufficient spectral modification at low energies discussed above, we consider a dominantly extra-galactic explanation of cosmic rays below 10^8 GeV as implausible.

The jury is still out (or ought to be)

A complete model of the CR spectrum and composition across the Galactic to Extragalactic transition

Noemie Globus
School of Physics & Astronomy, Tel Aviv University, Tel Aviv 69978, Israel

Denis Allard and Etienne Parizot
Laboratoire Astroparticule et Cosmologie, Université Paris Diderot/CNRS, 10 rue A. Domon et L. Duquet, 75205 Paris Cedex 13, France

We present a complete phenomenological model accounting for the evolution of the cosmic-ray spectrum and composition with energy, based on the available data over the entire spectrum. We show that there is no need to postulate any additional component, other than one single Galactic component depending on rigidity alone, and one extragalactic component, whose characteristics

PRD 92, 021302, 2015 arXiv:1505.01377

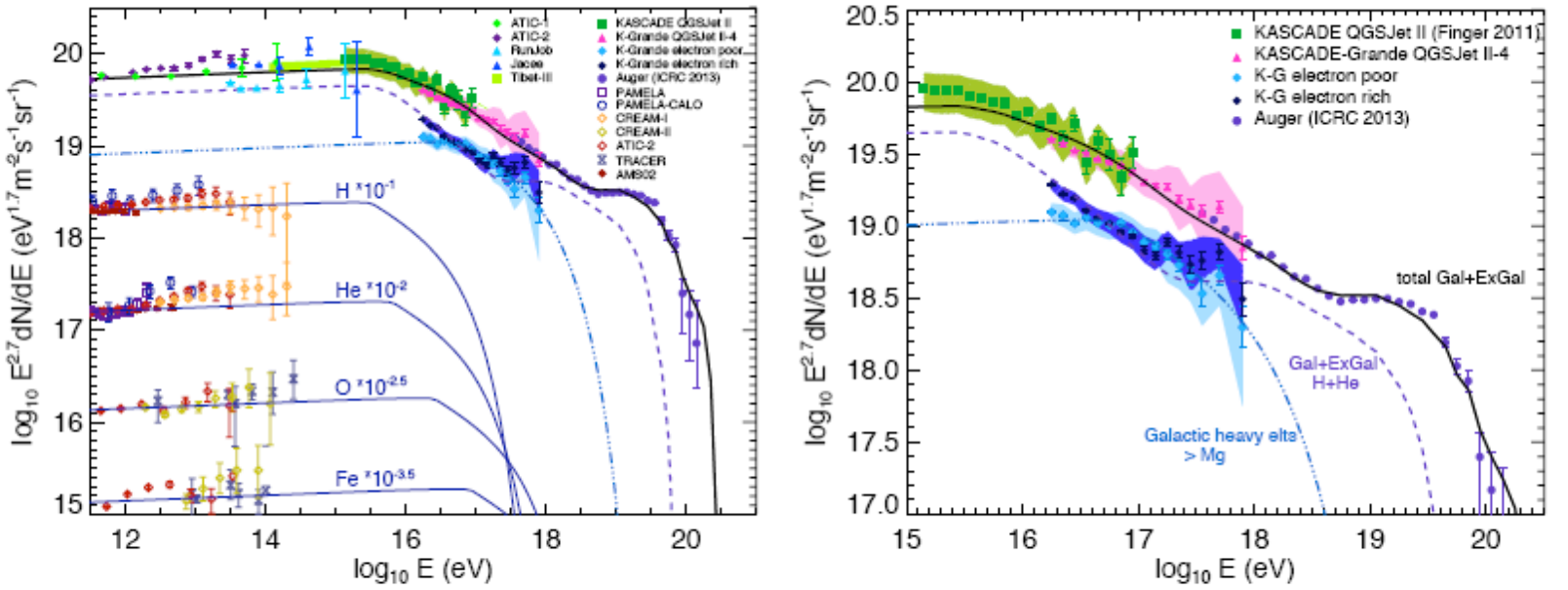

FIG. 2. Comparison between the spectrum of our global CR model and the available data, detailed in the upper right corners. The individual spectra of H, He, O and Fe are shown for the GCR component (left, with the indicated rescaling). In addition, the "heavy" and "light" components determined by KASCADE-Grande are shown with dashed and dotted-dashed line (see text). Right: close up view, showing the sum of the H and He fluxes (dashed) and the elements heavier than Mg (dotted-dashed).

Cascade photons as test of protons in UHECR

V. Berezinsky,[1,2] A. Gazizov,[1] and O. Kalashev[3]

[1] *INFN, Laboratori Nazionali del Gran Sasso, Assergi (AQ), 67010, Italy*
[2] *INFN, Gran Sasso Science Institute, viale F.Crispi 7, 67100 L'Aquila, Italy*
[3] *Institute for Nuclear Research of the Russian Academy of Sciences, Moscow 117312, Russia*[*]

(Dated: August 30, 2016)

An isotropic component of high energy γ-ray spectrum measured by Fermi LAT constrains the proton component of UHECR. The strongest restriction comes from the highest, $(580-820)$ GeV, energy bin. One more constraint on the proton component is provided by the IceCube upper bound on ultrahigh energy cosmogenic neutrino flux. We study the influence of these restrictions on the source properties, such as evolution and distribution of sources, their energy spectrum and admixture of nuclei. We also study the sensitivity of restrictions to various Fermi LAT galactic foreground models (model B being less restrictive), to the choice of extragalactic background light model and to overall normalization of the energy spectrum. We claim that the γ-ray-cascade constraints are stronger than the neutrino ones, and that however many proton models are viable. The basic parameters of such models are relatively large γ_g and not very large $z_{\rm max}$. The allowance for He^4 admixture also relaxes the restrictions. However we foresee that future CTA measurements of γ-ray spectrum at $E_\gamma \simeq (600-800)$ GeV, as well as resolving of more individual γ-ray sources, may rule out the proton-dominated cosmic ray models.

arXiv:1606.09293

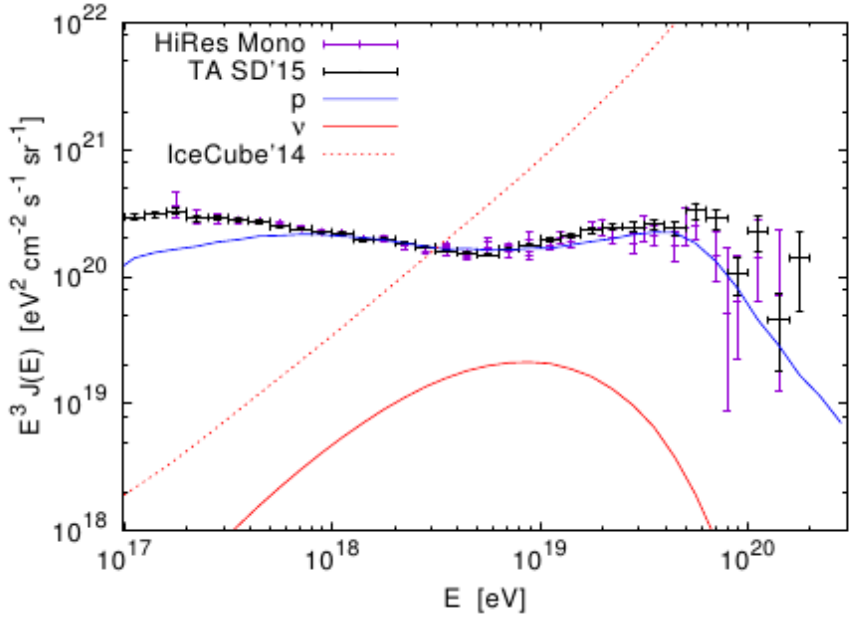

(a) UHECR and secondary ν

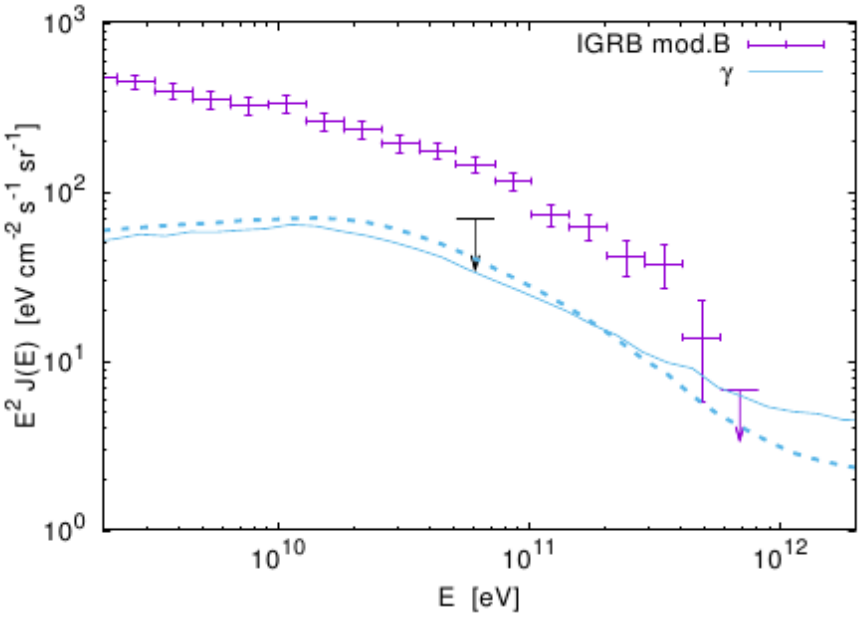

(b) secondary γ

FIG. 1: Energy spectra of protons and neutrinos (left panel) and of cascade photons (right panel) from sources emitting protons with $\gamma_g = 2.6$, $m = 1$ and $z_{\max} = 5$ normalized on TA spectrum [41]. Also, the Fermi IGRB measurements are shown for galactic foreground model B, as well as secondary ν-spectrum along with IceCube neutrino 'differential flux' upper limit [18]. The Fermi LAT constraint of Eq. (13) is shown by the black arrow. EBL models of Ref. [36] (solid lines) and [35] (dashed line) were used in calculations. Only γ-ray spectrum is shown for EBL model [35] since p- and ν-spectra calculated using different EBL models are practically indistinguishable.

Berezinsky et al. arXiv:1606.09293

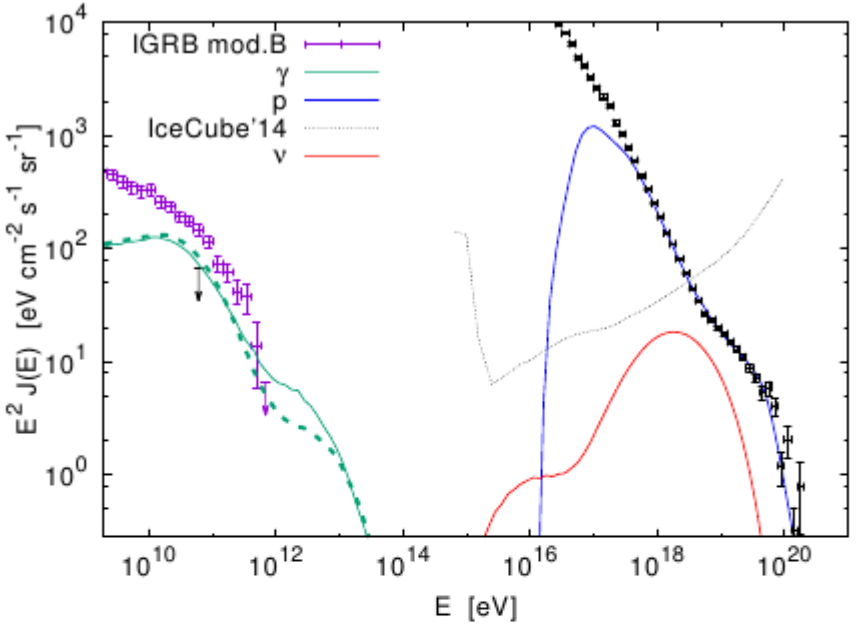

FIG. 2: Energy spectrum of cosmic rays and secondary ν's and γ's from sources emitting protons with $\gamma_g = 2.4$ and evolution corresponding to star formation rate (SFR) [37] normalized on TA spectrum [41]. The Fermi LAT constraint given by Eq. (13) is shown by the black arrow. The EBL models of Refs. [36] (solid lines) and [35] (dashed line) are used in calculations. The γ-ray spectrum is shown only for EBL of model Ref. [35] since $p-$ and ν-spectra calculated using different EBL models are almost indistinguishable.

Berezinsky et al. arXiv:1606.09293

Indication of a Local "Fog" of Sub-Ankle UHECR

Ruo-Yu Liu[1], Andrew M. Taylor[2], Xiang-Yu Wang[3] and Felix A. Aharonian[1,2]
[1] *Max-Planck-Institut für Kernphysik, Saupfercheckweg 1, 69117 Heidelberg, Germany*
[2] *Dublin Institute for Advanced Studies, 31 Fitzwilliam Place, Dublin 2, Ireland and*
[3] *School of Astronomy and Space Science, Nanjing University, Nanjing 210093, China*

During their propagation through intergalactic space, ultrahigh energy cosmic rays (UHECRs) interact with the background radiation fields. These interactions give rise to energetic electron/positron pairs and photons which in turn feed electromagnetic cascades, contributing to the isotropic gamma-ray background (IGRB). The gamma-ray flux level generated in this way highly depends upon the UHECR propagation distance, as well as the evolution of their sources with redshift. Recently, the *Fermi*-LAT collaboration reported that the majority of the total extragalactic gamma-ray flux originates from extragalactic point sources. This posits a stringent upper limit on the IGRB generated via UHECR propagation, and subsequently constrains their abundance in the distant Universe. Focusing on the contribution of UHECR at energies below the ankle within a narrow energy band ($(1-4)\times10^{18}$ eV), we calculate the diffuse gamma-ray flux generated through UHECR propagation, normalizing the total cosmic ray energy budget in this band to that measured. We find that in order to not over-produce the new IGRB limit, a local "fog" of UHECR produced by nearby sources may exist, with a possible non-negligible contribution from our Galaxy. Following the assumption that a given fraction of the observed IGRB at 820 GeV originates from UHECR, we obtain a constraint on the maximum distance for the majority of their sources. With other unresolved source populations still contaminating the new IGRB limit, and UHECR above the ankle invariably contributing also to this background, the results presented here are rather conservative.

arXiv: 1603.03223 6 Sept 2016

EM cascades from 10^{18} eV extragalactic CR protons

evolution | no evolution | local to 120 Mpc

EGCR

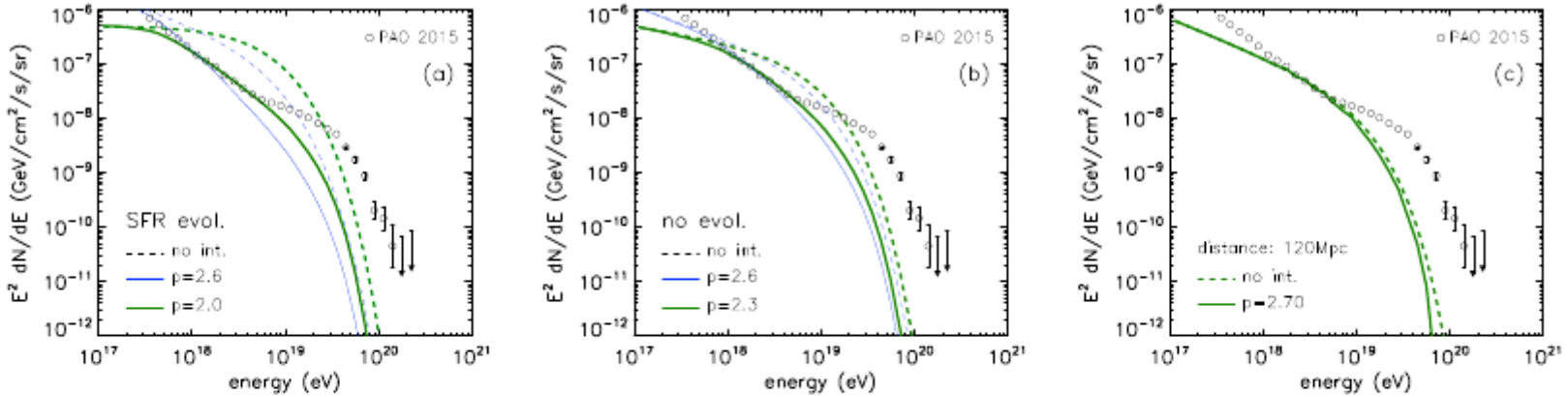

Gamma ray background

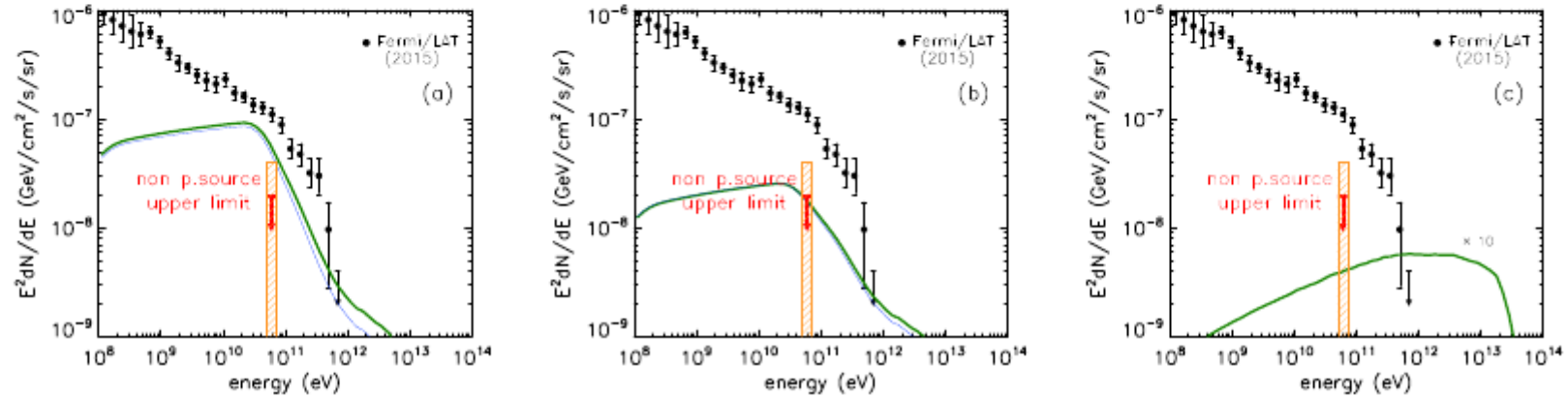

Over Fermi limit | OK? | OK

Fermi IGRB limit considering unresolved source populations (sources~80%)
Severe limit on EGCR! those we see are local, not universal? Anisotropy?

Liu et al. arXiv: 1603.03223

FIG. 1. Fitting to UHECR spectrum below the ankle and the corresponding diffuse gamma-ray flux initiated by CR propagation with different source distributions (**left**: (a) SFR evolution; **middle**: (b) no evolution; **right**: (c) sources located at 120 Mpc). In the upper panels, the green solid lines represent the best-fit UHECR fluxes for each source distribution considered, while the dashed lines represent the unattenuated flux. The thin blue lines show the results for a soft injection spectrum of $p = 2.6$, normalized to the data at 1 EeV. Hollow circles show the PAO[5] data. The adopted values of the power-law index p and the local energy production rate are provided within the figure. The lower panels show the corresponding diffuse gamma-ray emission resulting from the cascade initiated by UHE protons, with thick lines and thin lines are respectively for best-fit case and $p = 2.6$ case. The black filled circles show the IGRB measured by Fermi/LAT([3]). The IGRB upper limit for the non-point-source component (or the truly diffuse component) are shown as a red bar with an arrow. The orange hatched region represents the uncertainty of the limit due to the uncertainties in the obtained source count distribution (i.e., dN/dS). The cascade flux in the right panel is multiplied by 10.

Cosmogenic photons strongly constrain UHECR source models

Arjen van Vliet[1,⋆]

[1] *Department of Astrophysics/IMAPP, Radboud University, P.O. Box 9010, 6500 GL Nijmegen, The Netherlands.*

Abstract. With the newest version of our Monte Carlo code for ultra-high-energy cosmic ray (UHECR) propagation, CRPropa 3, the flux of neutrinos and photons due to interactions of UHECRs with extragalactic background light can be predicted. Together with the recently updated data for the isotropic diffuse gamma-ray background (IGRB) by Fermi LAT, it is now possible to severely constrain UHECR source models. The evolution of the UHECR sources especially plays an important role in the determination of the expected secondary photon spectrum. Pure proton UHECR models are already strongly constrained, primarily by the highest energy bins of Fermi LAT's IGRB, as long as their number density is not strongly peaked at recent times.

arXiv:1609.03336 12 Sept 2016

… and so it goes.... (Billy Joel)

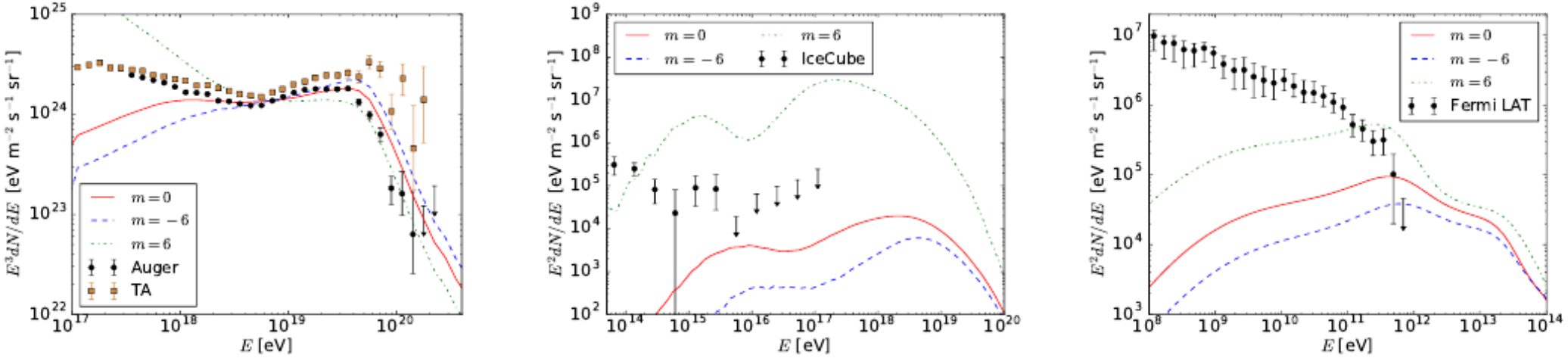

(a) Cosmic rays (b) Neutrinos (c) Photons

Figure 1. (a) Simulated cosmic ray spectra normalized to the Auger flux [3] (circles) at $E = 10^{18.85}$ eV. The spectrum measured by TA [5] (squares) is given as well. (b) Corresponding neutrino spectra compared with IceCube data [2] (circles). (c) Corresponding photon spectra compared with Fermi-LAT IGRB data [1] (circles) using Galactic foreground model A. The cosmic ray simulations were done starting a pure proton injection at $E_{\rm min} = 0.1$ EeV with an exponential cutoff at a cutoff energy of $E_{\rm cut} = 200$ EeV and an injection spectral index of $\alpha = 2.5$ using the Gilmore 2012 EBL model [15]. The simulations were done up to a maximum redshift of $z_{\rm max} = 6$ with a comoving source evolution multiplied by $(1+z)^m$ with $m = 0$ (solid lines), $m = -6$ (dashed lines) and $m = 6$ (dashed-dotted lines). See text for further details.

Van Vliet arXiv:1609.03336

Challenge: reduce IGRB with deep source detections
To actually detect the cascade diffuse gamma background!

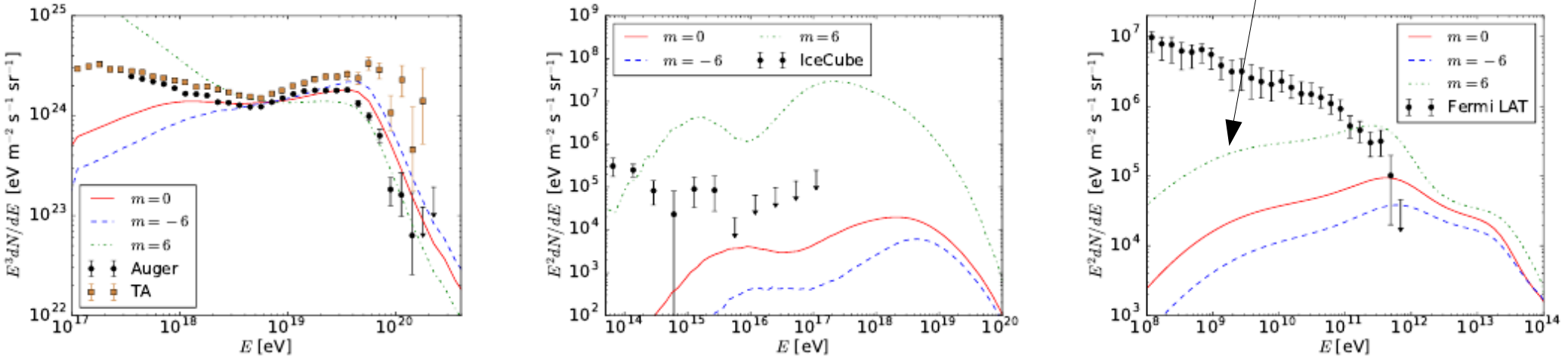

(a) Cosmic rays (b) Neutrinos (c) Photons

Figure 1. (a) Simulated cosmic ray spectra normalized to the Auger flux [3] (circles) at $E = 10^{18.85}$ eV. The spectrum measured by TA [5] (squares) is given as well. (b) Corresponding neutrino spectra compared with IceCube data [2] (circles). (c) Corresponding photon spectra compared with Fermi-LAT IGRB data [1] (circles) using Galactic foreground model A. The cosmic ray simulations were done starting a pure proton injection at $E_{\rm min} = 0.1$ EeV with an exponential cutoff at a cutoff energy of $E_{\rm cut} = 200$ EeV and an injection spectral index of $\alpha = 2.5$ using the Gilmore 2012 EBL model [15]. The simulations were done up to a maximum redshift of $z_{\rm max} = 6$ with a comoving source evolution multiplied by $(1+z)^m$ with $m = 0$ (solid lines), $m = -6$ (dashed lines) and $m = 6$ (dashed-dotted lines). See text for further details.

Van Vliet arXiv:1609.03336

COMPTEL reloaded: new initiatives in heritage MeV gamma-ray astronomy

A. W. Strong[1], W. Collmar[1], T. A. Enβlin[2], M .Reinecke[2], D. Pumpe[2], F. Guglielmetti[2]

1. MPE Garching 2. MPA Garching

ABSTRACT

The COMPTEL gamma-ray telescope on NASA's Compton Gamma Ray Observatory (CGRO) operated from 1991 to 2000. It was a double-scatter Compton instrument covering the energy range 0.75-30 MeV, both in continuum and lines. Full-sky maps and a source catalogue were the main outcome of the mission. While the Fermi-LAT instrument has now vastly enhanced our knowledge of the gamma-ray sky at higher energies, the MeV range remains devoid of new missions, so that the heritage COMPTEL data is an essential resource. Data analysis has continued at MPE Garching, with improved event processing and selections. The original skymapping method using Maximum Entropy has been adapted to current technology. A new initiative for skymapping using state-of-the-art Bayesian techniques has been started at MPA Garching; this involves Information Field Theory with the D³PO system.

INSTRUMENT

COMPTEL on CGRO (1991 - 2000)

DETECTION TECHNIQUE

The double-Compton scattering detection technique means that each photon is associated with an annulus on the sky, with known centre, radius and shape; this makes deconvolution essential for imaging. One method is Maximum Entropy (Maxent), which has been used to make all-sky images. The large instrumental background is a further challenge for any COMPTEL analysis.

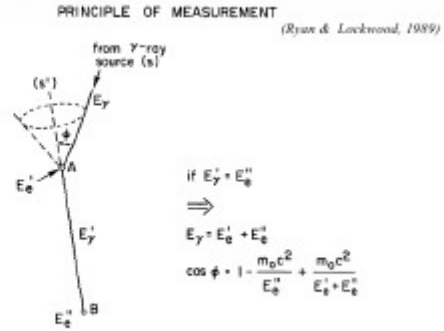

Gamma-2016 Heidelberg

Original Maxent images (A)

In the original work (Strong et al. 1998) the MEMSYS5 Bayesian 'Classic' Maxent package was used (Skilling, 1989). It employed a template for the instrumental background taken from high Galactic latitudes where the celestial signal is small. In the original work 240 COMPTEL observations were used, and the data and instrumental response were treated in the instrumental coordinate system. Because of the large computing requirements the computation was performed on 240 CPUs of a Cray supercomputer which was state-of-the-art at the time.

Classic Maxent

Entropic prior on image:

$$\Phi(S) \propto \exp(\alpha S)$$

Posterior of image:

$$\begin{aligned} \Pr(h, \alpha, \boldsymbol{D}) &= \Pr(\alpha)\, \Pr(h \mid \alpha)\, \Pr(\boldsymbol{D} \mid h) \\ &= \Pr(\alpha)\, \frac{\exp(\alpha \mathcal{S}(h) - \mathcal{L}(h))}{Z_{\mathcal{S}}(\alpha)\, Z_{\mathcal{L}}} \end{aligned}$$

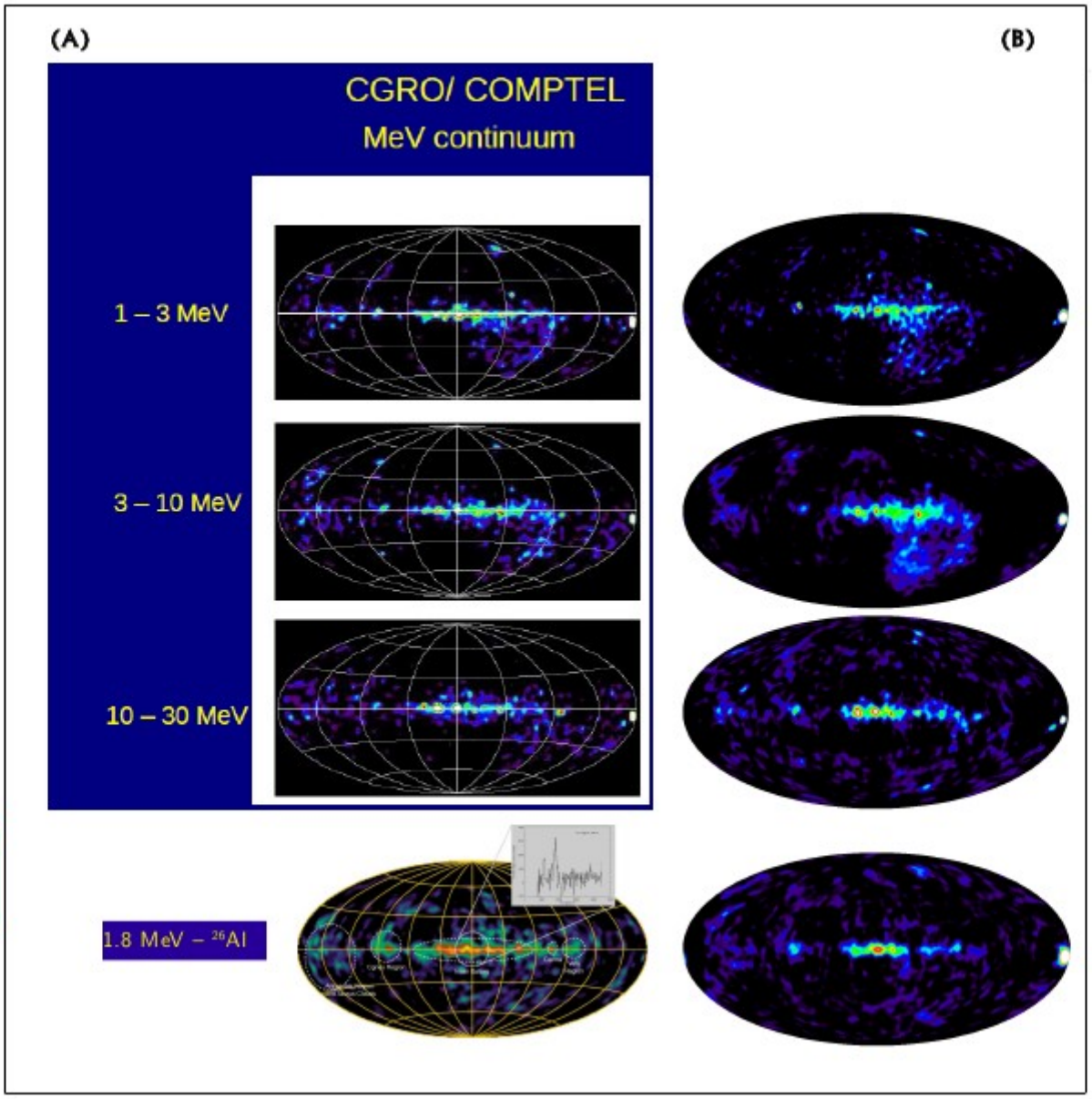

New Maxent images (B)

In view of the importance of the COMPTEL data, we have recently revisited imaging with current software and hardware technology. The original code was adapted to use the *HEALPix* sky representation for a uniform sky coverage both in data and image space instead of the original straight (l,b) system. This also allows fast convolution/correlation on the sphere, replacing the original "brute-force" method. This already gives an enormous speed gain, and running in on a multicore machine produces images in hours (compared to weeks on the original Cray implementation). A finer pixelization (0.5° instead of the original 1°) is hence possible. The *HEALPix* format enhances the value of the images and the speed allows investigation of more imaging parameters, data selection etc.

The new images are fully consistent with the original ones, with the Galactic plane clearly visible, and in addition the well-known sources including the Crab, Vela, Cyg X-1, LS5039, 3C273, 3C279, PKS0528+134 and the Galactic Centre. (Note: the excess at lower right is due to Earth atmospheric emission)

In addition we have produced a 1.8 MeV ^{26}Al line map which can be compared with the standard Maxent image (Plüschke et al. 2001).

Comparison with Fermi-LAT

Fermi-LAT energy range extends to lower energies with Pass 8, and this allows a comparison with COMPTEL.

(from A. Strong on behalf of Fermi-LAT Collaboration, talk at MeV Conference, APC Paris 2012)

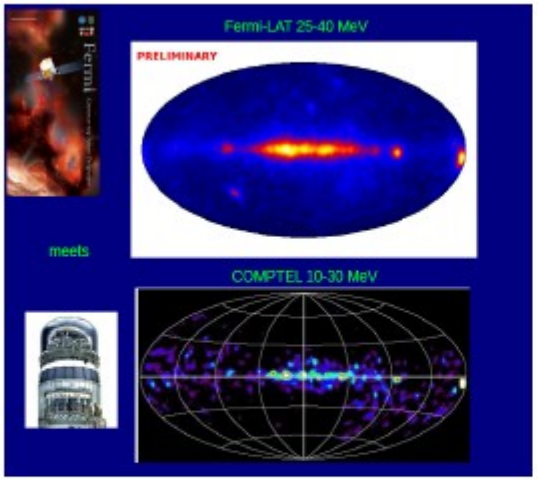

OUTLOOK

New COMPTEL photon data processing

COMPTEL data analysis continues at MPE (Collmar & Zhang 2014). The event processing and selection is also under study at MPE with improved time-of-flight calculation and other enhancements to reduce the instrumental background. More observations are also now available than for the skymaps shown above. This new data will be used to generate updated images in the near future.

Future methods

While Maxent has been very successful for image COMPTEL data, further advances in data analysis have been made in the last decade. Information Field Theory (IFT) as implemented in the NIFTY and D^{3}PO software has been applied to Fermi-LAT data (Selig et al. 2015), see talk 'Gamma-ray analysis with D^{3}PO' at this symposium. Application of this method to COMPTEL is in progress.

References

Collmar, W., Zhang S., 2014, A&A 565, A38
Plüschke, S., Diehl, R., Schönfelder, V., et al. 2001, in Exploring the Gamma-Ray Universe, ESA SP, 459, 55
Selig, M., et al., 2015, A&A 581, A126
Skilling, J. , 1989 in Maximum Entropy and Bayesian Methods, (Dordrecht: Kluwer), ISBN-0-7923-0224-9, 45
Strong, A.W. et al. 1998, Proc. 3rd INTEGRAL Workshop, arXiv:astro-ph/9811211; Astrophys. Lett. Commun. 39, 209

END

Gamma-ray sky points to radial gradients in cosmic-ray transport

Daniele Gaggero,[1,2,*] Alfredo Urbano,[1,†] Mauro Valli,[1,2,‡] and Piero Ullio[1,2,§]

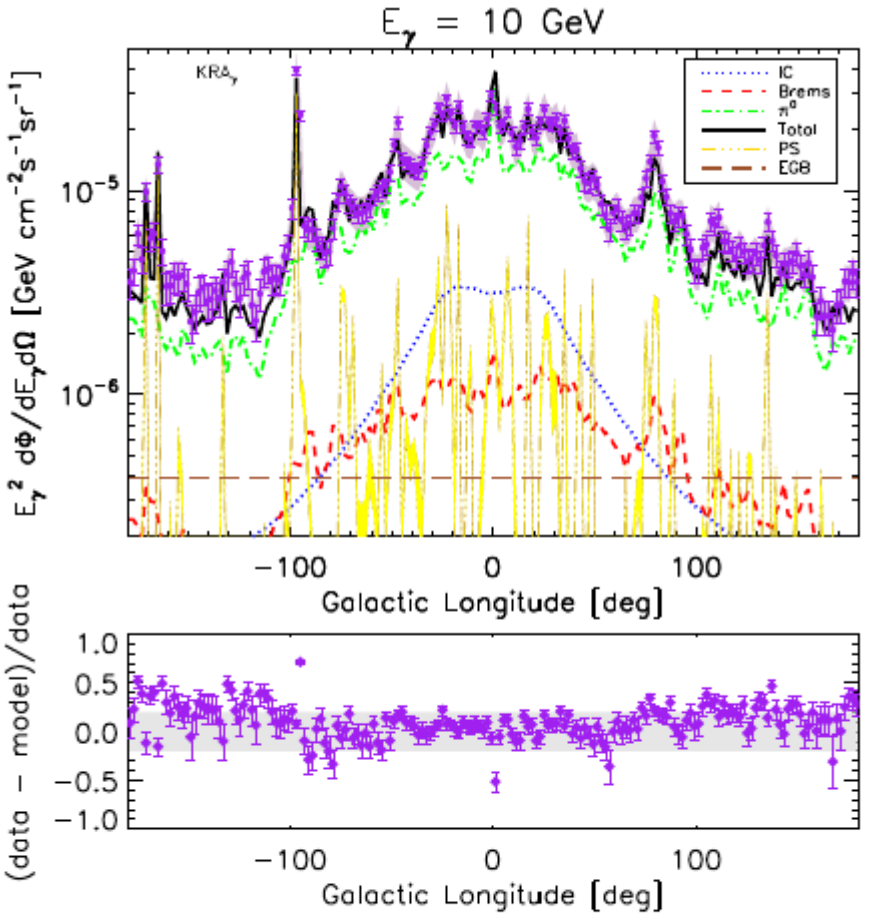

FIG. 8. *Longitudinal profile at fixed energy* $E_\gamma = 10$ *GeV. We average in latitude over the interval* $|b| < 5^\circ$.

Gamma-ray sky points to radial gradients in cosmic-ray transport

Daniele Gaggero,[1,2,*] Alfredo Urbano,[1,†] Mauro Valli,[1,2,‡] and Piero Ullio[1,2,§]

Phys. Rev. D 91, 083012 (2015)

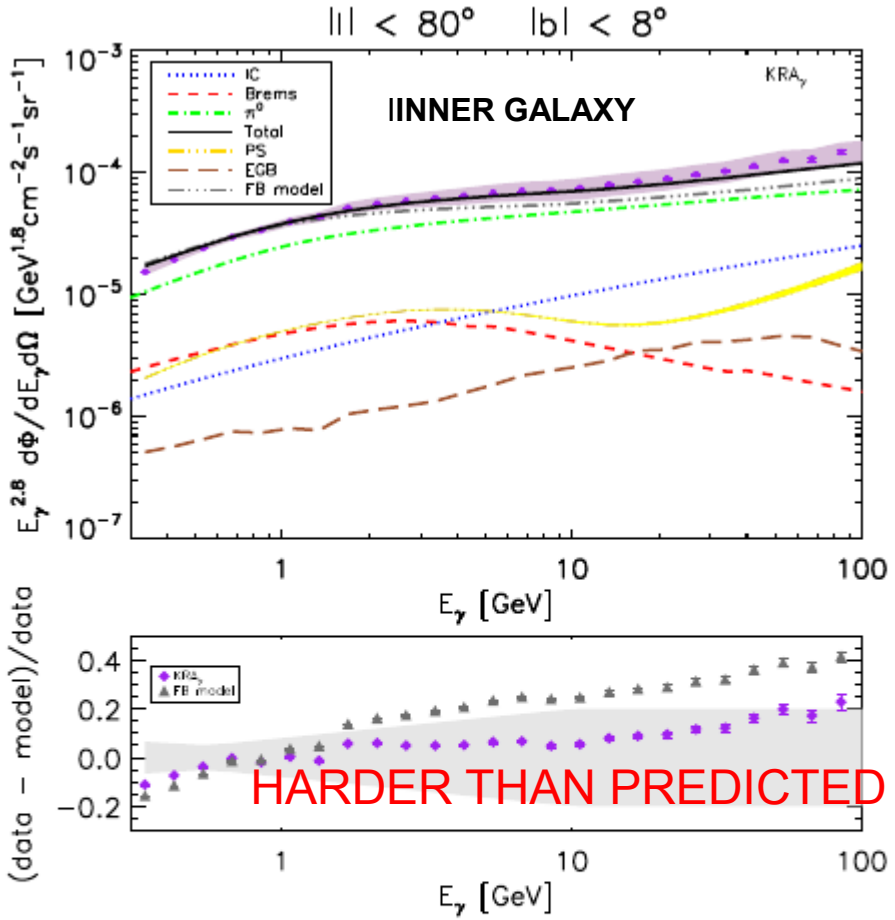

FIG. 1. *Upper panel. Comparison between the γ-ray flux computed with the CR propagation model proposed in this Letter (KRA$_\gamma$ total flux: solid black line; individual components shown) and the* Fermi-LAT *data (purple dots, including both statistic and systematic errors) in the Galactic disk. For comparison, we also show the total flux for the FB model defined in ref. [1] (double dot-dashed gray line). Lower panel. Residuals computed for the KRA$_\gamma$ and FB models.*

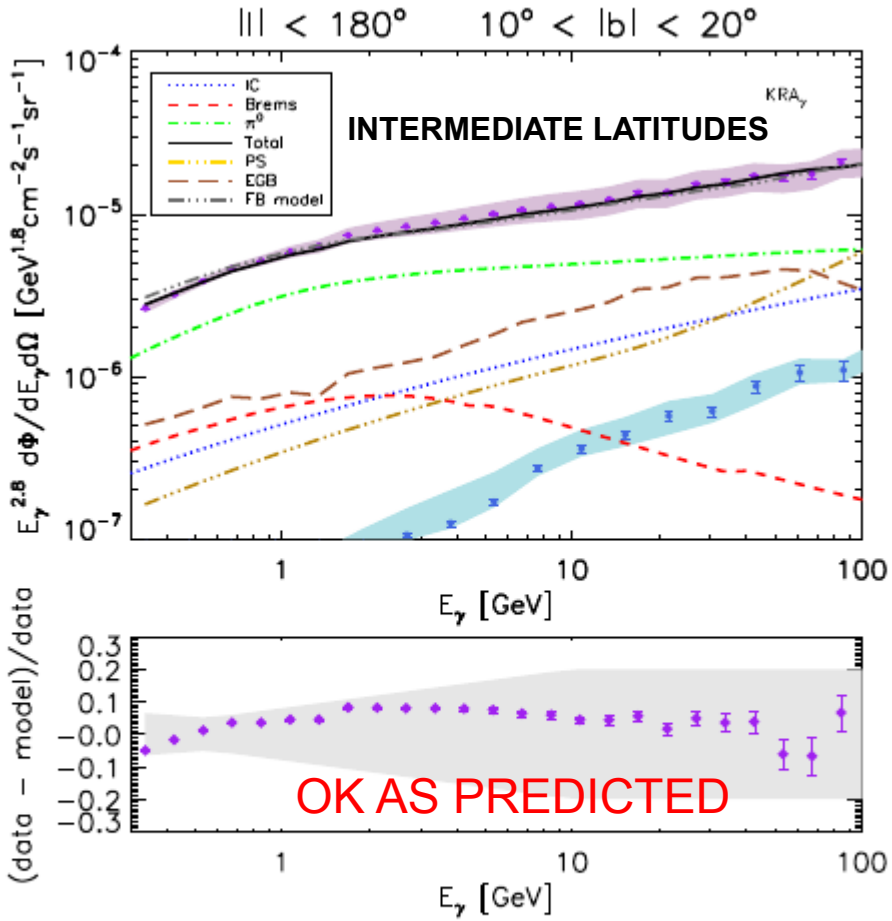

FIG. 7. *The same as in fig. [1] but considering the strip $|l| < 180°$, $10° < |b| < 20°$. The azure band represents the contribution of the Fermi bubbles according to ref. [37].*

Interstellar gamma-ray spectrum

Harder gamma-ray spectrum in Galactic plane than expected from
local cosmic-ray proton spectrum via pion-decay

Gaggero et al. 2015 invoke spatially varying momentum-dependence of diffusion coeffiicient.

But since Galactic plane spectrum is harder than local, can be just a local CR source

Then spectral index in the plane is the "normal" one!

THIS IS A BIG EFFECT AND DESERVES MORE ATTENTION!

Normal spectrum is hard, local is special (local source?)

Affects everything in CR studies!

B from harder C, compare with B, then B/C not meaningful
B comes from everywhere

C with index = 2.4 instead of 2.8

B normally index = 2.8+0.5 = 3.3 to fit data

If C index = 2.4 then B 2.9 from D(p)

But if B index = 3.3 then D(p) ~ p^0.9 !!

Should do GALPROP study

Hard spectrum of cosmic rays in the Disks of Milky Way and Large Magellanic Cloud.

A. Neronov [1], D. Malyshev [1]

1. ISDC, Astronomy Department, University of Geneva, Ch. d'Ecogia 16, 1290, Versoix, Switzerland

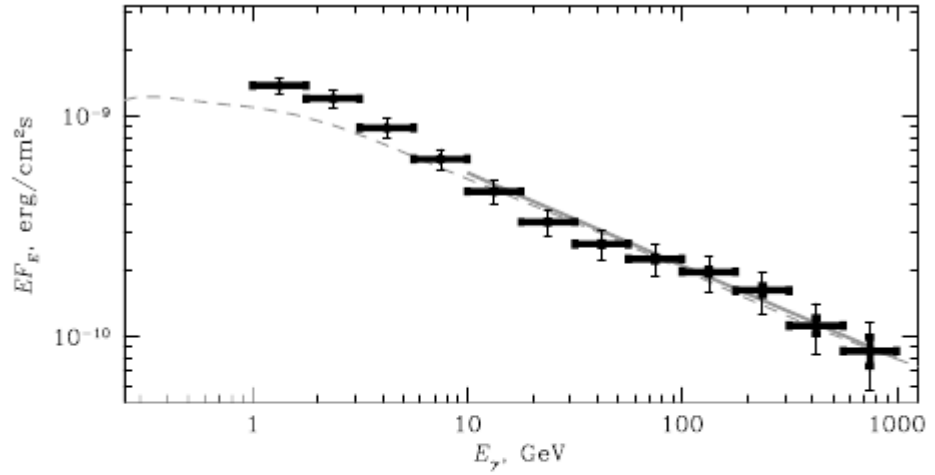

Fig. 2. Spectrum of emission from the $|l| < 90°$, $|b| < 1.5°$ part of the Galactic Plane. Thick / thin errorbars show the statistical / systematic error. Grey thick line shows the best-fit powerlaw with the slope $\Gamma_\gamma = 2.42$ in the energy range above 10 GeV. Dashed line shows the spectrum of the neutral pion decay emission produced a powerlaw proton spectrum with the slope $\Gamma_p = 2.45$.

Results. The spectrum of the pion decay γ-ray emission from the Galactic disk in the energy band 10 GeV – 1 TeV has the slope $\simeq 2.4$. There is no evidence for the variation of the slope with Galactic longitude / distance from the Galactic Centre. The slope of the spectrum of cosmic rays derived from the γ-ray data, $\simeq 2.45$, is harder than the slope of the locally observed cosmic ray proton spectrum. Pion decay emission from a powerlaw distribution of cosmic rays with the same hard slope also provides a fit to the γ-ray spectrum of the Large Magellanic Cloud.

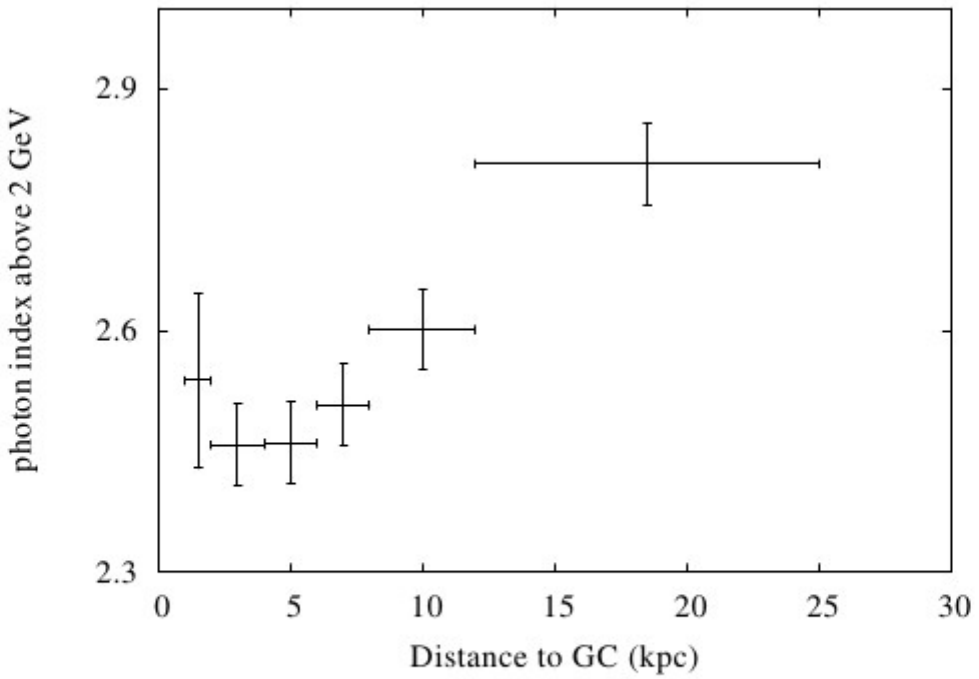

Local CR protons

FIG. 6: The distribution of the photon index of the galactic diffuse gamma ray emission associated with the gas in different rings.

Yang etal arXiv:1602.04710

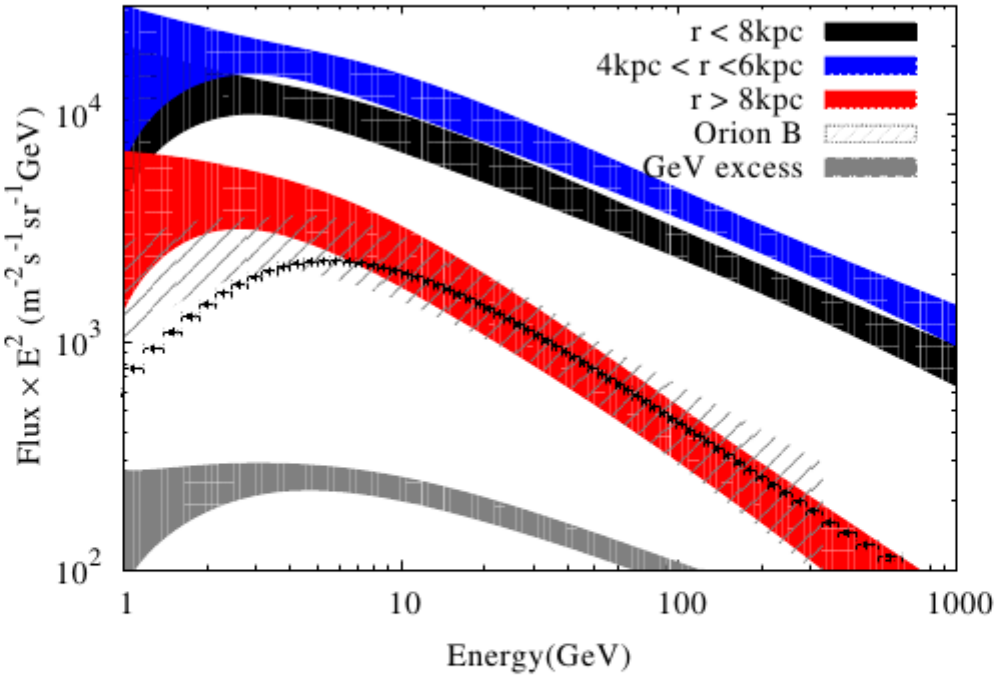

FIG. 9: The CR proton spectra in the inner ($r \leq 8$ kpc) and outer ($r \geq 8$ kpc) regions, as well as in the 4-6 kpc ring derived from γ-ray emissivities presented in Fig 7. Also are shown the proton spectra derived from the γ-ray measurements of the nearby molecular cloud Orion B [16]. and from the low-energy γ-ray component called "GeV excess". The direct measurements of the CR proton spectrum are from the AMS-02 collaboration report [17], which are shown as black squares.

Yang etal arXiv:1602.04710

Synchrotron harder spectrum in Galactic Plane
Planck XLIII (408 MHz/ 30 GHz)
WMAP Fusekland etal 2014 0.14 harder in plane
QUIET (microwave 45/90 GHz) β=2.9 in plane

PLANCK Collab. Et al 2016 A&A in press, arXiv: 1601.00546
for review of observations.

β=2.85 → electron index 2.7

Electron index
$2(\beta - 2) + 1$

2.0

3.0 ←

Locally
measured
electrons

Low latitudes = large-scale Galactic spectrum. Harder than local electrons.
Similar to proton hardening seen in gamma rays.

B/C Ratio

Stefan Schael
Gamma2016, Heidelberg

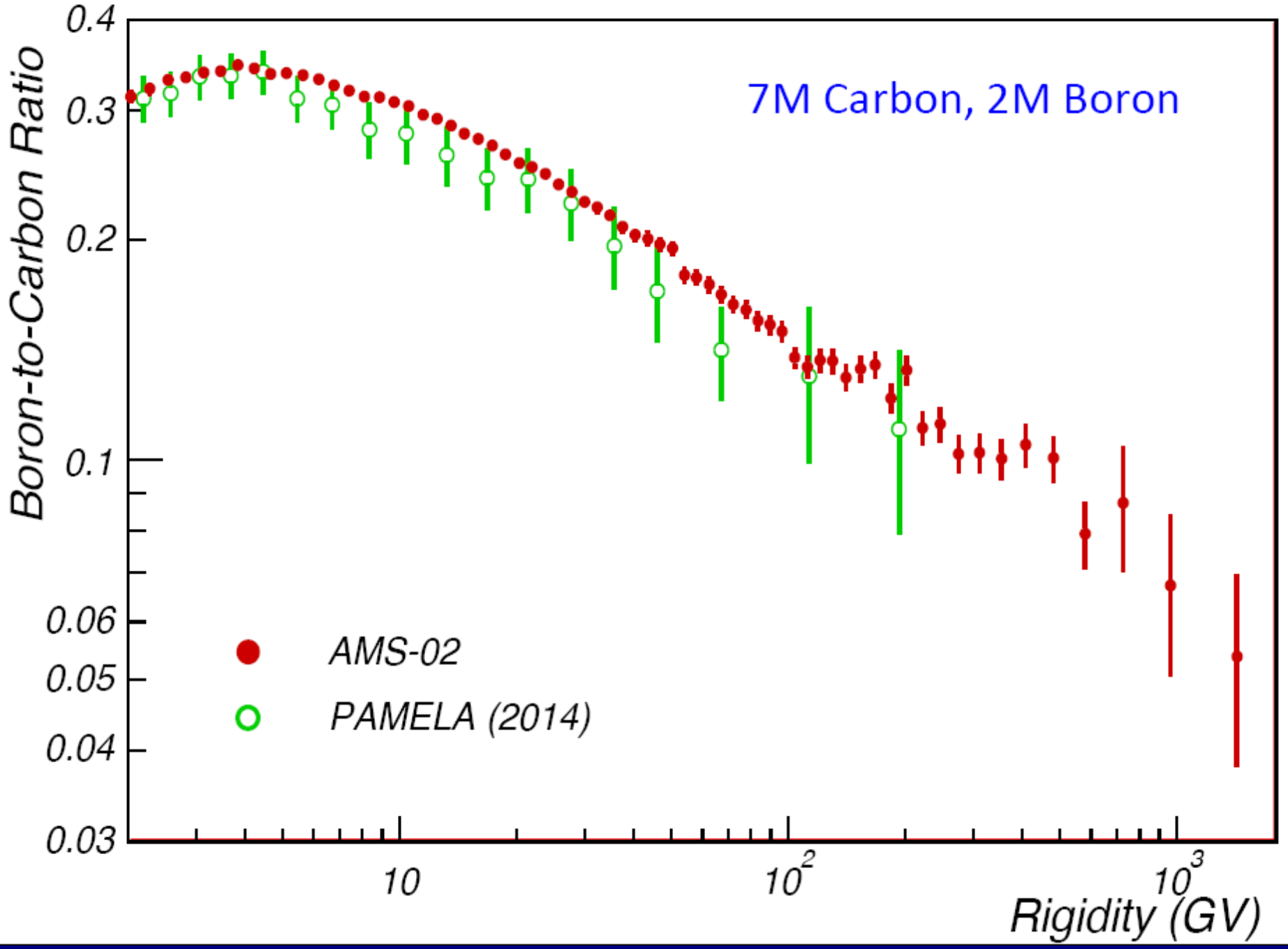

be

B/C Ratio

Stefan Schael
Gamma2016, Heidelberg

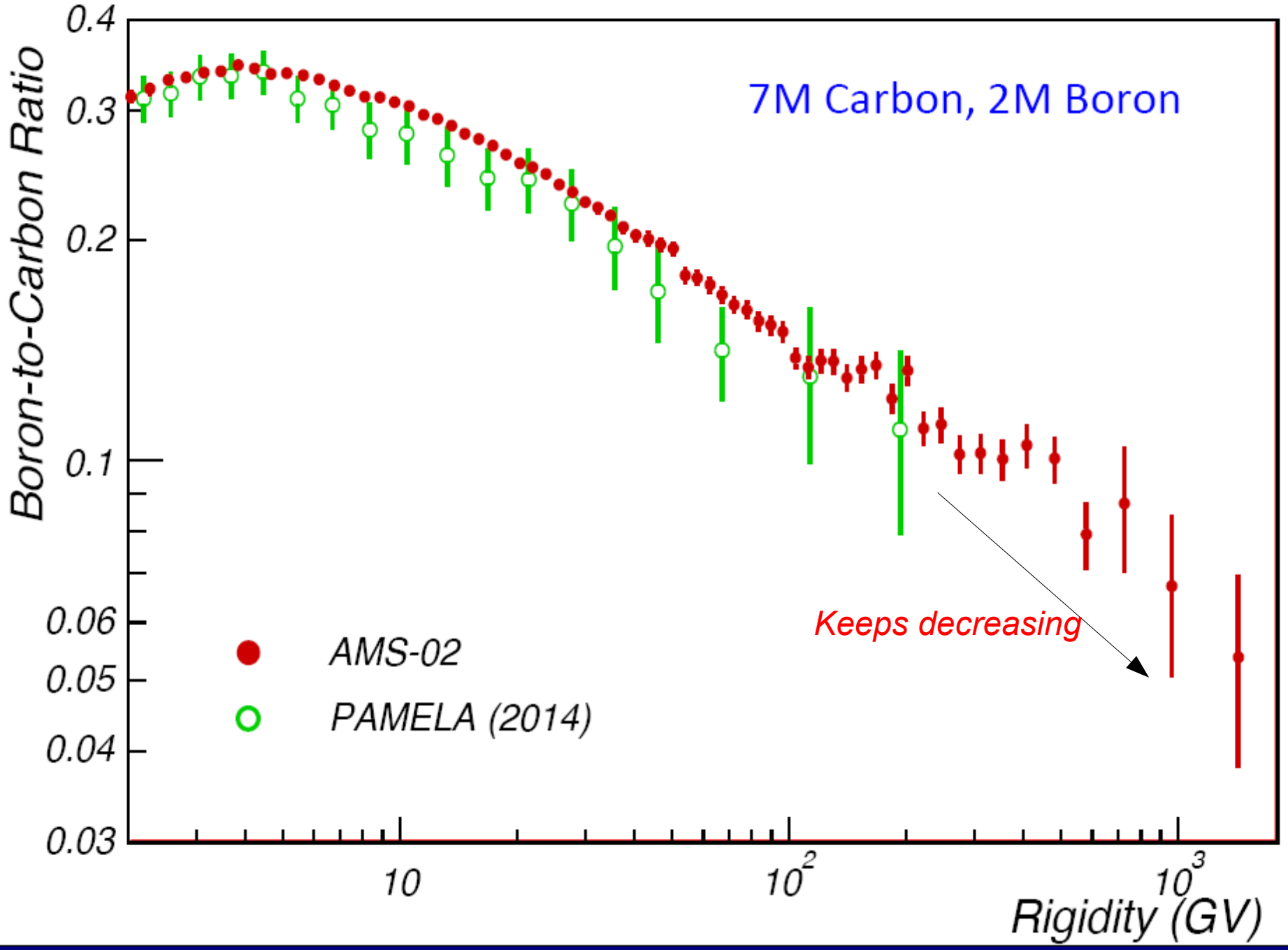

B/C Ratio converted in Kinetic Energy

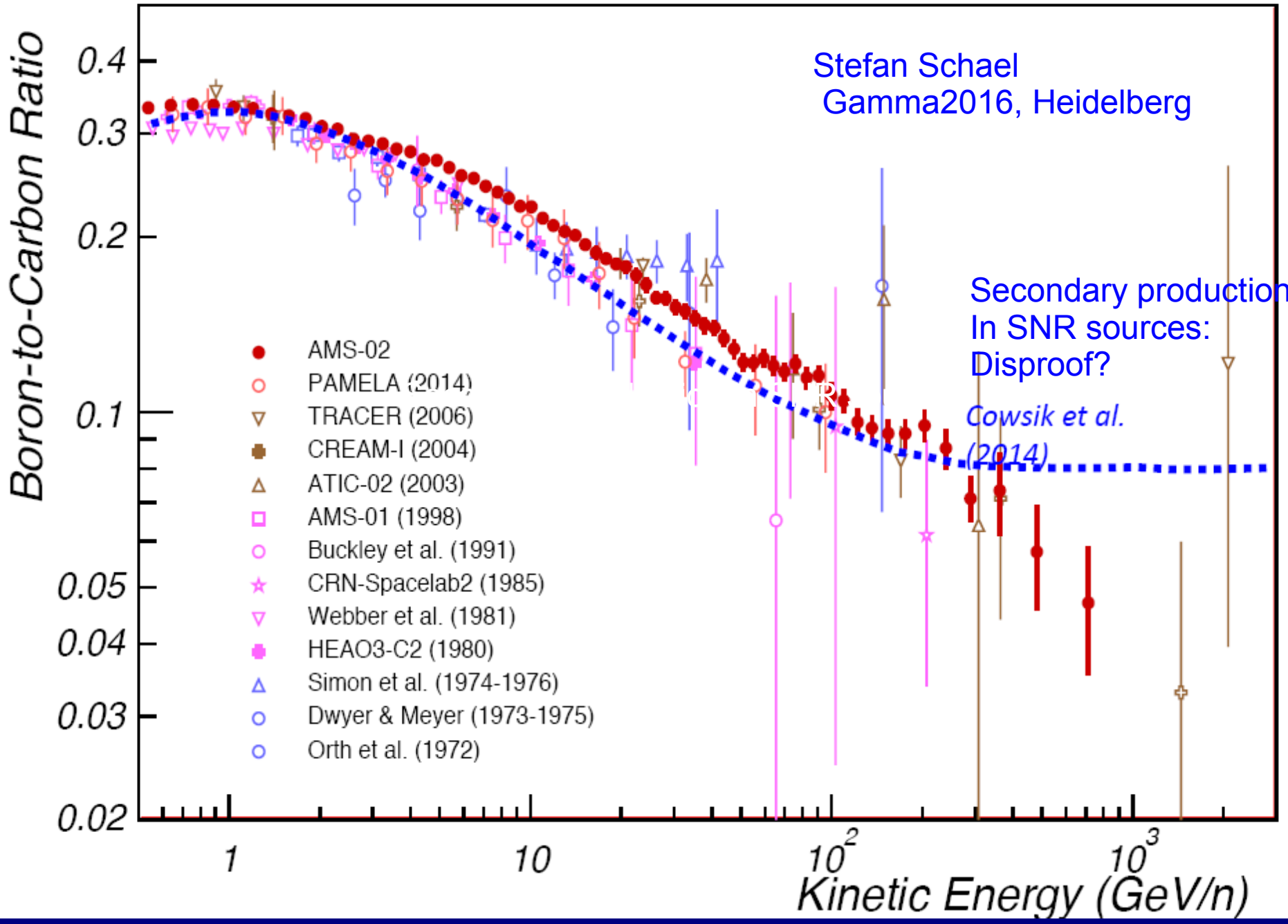

11 things which are taken as established but are not and deserve further investigation

1 The Pion Bump has been detected in SNR by Fermi-LAT
2 CR are extragalactic only >10^{15} eV or so
3 CR cannot come from the Galactic Centre only
4 The CR gradient in the Galaxy can be determined accurately
5 The spectrum of CR in the Galaxy has the same shape as the local spectrum
6 Reacceleration is a viable explanation of the B/C peak (Luke's talk)
7 Secondary production in sources is negligible (including B, positrons)
8 60Fe tells about CR age, delay (from gammas 60Fe is everwhere in ISM)
9 Positron/pbar ratio agrees with standard model (no: Lipari paper)
10 Diffuse Galactic emission is mainly interstellar not unresolved sources
11 CR are not important for galaxy evolution

Positron and pbar spectra <<<<<<<<<<<,,

Positron and pbar spectra same shape

AMS Schael

and Lipari paper and Heidelberg Gamma 2016 talk

incomplete

Flux Ratios $\bar{p}/e^+$ and p/e^+ are also energy independent in the interval 60–450 GV

Stefan Schael
Gamma2016, Heidelberg

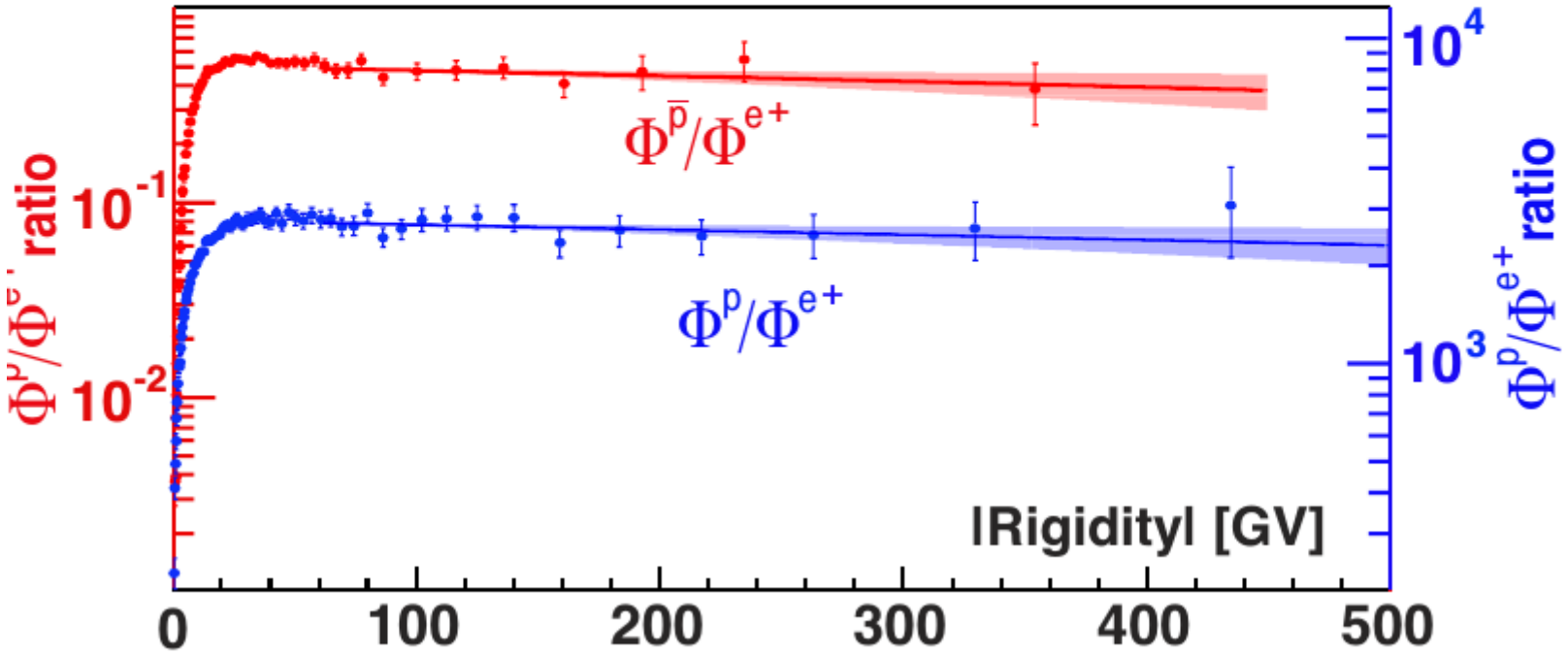

pbar and e+ production have similar spectra since hadronic interactions
But e+ are supposed to lose energy and steepen !
A mean conspiracy – a concidence? Or a challenge to standard models?

11 things which are taken as established but are not and deserve further investigation

1 The Pion Bump has been detected in SNR by Fermi-LAT
2 CR are extragalactic only >10^{15} eV or so
3 CR cannot come from the Galactic Centre only
4 The CR gradient in the Galaxy can be determined accurately
5 The spectrum of CR in the Galaxy has the same shape as the local spectrum
6 Reacceleration is a viable explanation of the B/C peak (Luke's talk)
7 Secondary production in sources is negligible (including B, positrons)
8 60Fe tells about CR age, delay (from gammas 60Fe is everwhere in ISM)
9 Positron/pbar ratio agrees with standard model (no: Lipari paper)
10 Diffuse Galactic emission is mainly interstellar not unresolved sources
11 CR are not important for galaxy evolution

The Astrophysical Journal Letters, 816:L19 (6pp), 2016 January 10 doi:10.3847/2041-8205/816/2/L19

LAUNCHING COSMIC-RAY-DRIVEN OUTFLOWS FROM THE MAGNETIZED INTERSTELLAR MEDIUM

Philipp Girichidis[1], Thorsten Naab[1], Stefanie Walch[2], Michał Hanasz[3], Mordecai-Mark Mac Low[4,5], Jeremiah P. Ostriker[6], Andrea Gatto[1], Thomas Peters[1], Richard Wünsch[7], Simon C. O. Glover[5], Ralf S. Klessen[5], Paul C. Clark[8], and Christian Baczynski[5]
[1] Max-Planck-Institut für Astrophysik, Karl-Schwarzschild-Str. 1, D-85741 Garching, Germany
[2] Physikalisches Institut, Universität zu Köln, Zülpicher Str. 77, D-50937 Köln, Germany
[3] Centre for Astronomy, Nicolaus Copernicus University, Faculty of Physics, Astronomy and Informatics, Grudziadzka 5, PL-87100 Toruń, Poland
[4] Department of Astrophysics, American Museum of Natural History, 79th Street at Central Park West, New York, NY 10024, USA
[5] Universität Heidelberg, Zentrum für Astronomie, Institut für Theoretische Astrophysik, Albert-Ueberle-Str. 2, D-69120 Heidelberg, Germany
[6] Department of Astronomy, Columbia University, 1328 Pupin Hall, 550 West 120th Street, New York, NY 10027, USA
[7] Astronomical Institute, Academy of Sciences of the Czech Republic, Bocni II 1401, 141 31 Prague, Czech Republic
[8] School of Physics & Astronomy, Cardiff University, 5 The Parade, Cardiff CF24 3AA, Wales, UK

$$\frac{\partial \rho}{\partial t} + \nabla \cdot (\rho \boldsymbol{v}) = 0$$

$$\frac{\partial \rho \boldsymbol{v}}{\partial t} + \nabla \cdot \left(\rho \boldsymbol{v}\boldsymbol{v}^{\mathrm{T}} - \frac{\boldsymbol{B}\boldsymbol{B}^{\mathrm{T}}}{4\pi} \right) + \nabla p_{\mathrm{tot}} = \rho \boldsymbol{g}$$

$$\frac{\partial e}{\partial t} + \nabla \cdot \left[(e + p_{\mathrm{tot}})\boldsymbol{v} - \frac{\boldsymbol{B}(\boldsymbol{B} \cdot \boldsymbol{v})}{4\pi} \right] = \rho \boldsymbol{v} \cdot \boldsymbol{g} + \nabla \cdot \mathsf{K} \nabla e_{\mathrm{CR}} + \dot{u}_{\mathrm{chem}} + \dot{u}_{\mathrm{inj}}$$

$$\frac{\partial \boldsymbol{B}}{\partial t} - \nabla \times (\boldsymbol{v} \times \boldsymbol{B}) = 0$$

$$\frac{\partial e_{\mathrm{CR}}}{\partial t} + \nabla \cdot (e_{\mathrm{CR}} \boldsymbol{v}) = -p_{\mathrm{CR}} \nabla \cdot \boldsymbol{v} + \nabla \cdot (\mathsf{K} \nabla e_{\mathrm{CR}}) + Q_{\mathrm{CR}}.$$

The Astrophysical Journal Letters, 816:L19 (6pp), 2016 January 10 doi:10.3847/2041-8205/816/2/L19

LAUNCHING COSMIC-RAY-DRIVEN OUTFLOWS FROM THE MAGNETIZED INTERSTELLAR MEDIUM

Philipp Girichidis[1], Thorsten Naab[1], Stefanie Walch[2], Michał Hanasz[3], Mordecai-Mark Mac Low[4,5], Jeremiah P. Ostriker[6], Andrea Gatto[1], Thomas Peters[1], Richard Wünsch[7], Simon C. O. Glover[5], Ralf S. Klessen[5], Paul C. Clark[8], and Christian Baczynski[5]
[1] Max-Planck-Institut für Astrophysik, Karl-Schwarzschild-Str. 1, D-85741 Garching, Germany
[2] Physikalisches Institut, Universität zu Köln, Zülpicher Str. 77, D-50937 Köln, Germany
[3] Centre for Astronomy, Nicolaus Copernicus University, Faculty of Physics, Astronomy and Informatics, Grudziadzka 5, PL-87100 Toruń, Poland
[4] Department of Astrophysics, American Museum of Natural History, 79th Street at Central Park West, New York, NY 10024, USA
[5] Universität Heidelberg, Zentrum für Astronomie, Institut für Theoretische Astrophysik, Albert-Ueberle-Str. 2, D-69120 Heidelberg, Germany
[6] Department of Astronomy, Columbia University, 1328 Pupin Hall, 550 West 120th Street, New York, NY 10027, USA
[7] Astronomical Institute, Academy of Sciences of the Czech Republic, Bocni II 1401, 141 31 Prague, Czech Republic
[8] School of Physics & Astronomy, Cardiff University, 5 The Parade, Cardiff CF24 3AA, Wales, UK

Modified FLASH code

$$\frac{\partial \rho}{\partial t} + \nabla \cdot (\rho \boldsymbol{v}) = 0$$

$$\frac{\partial \rho \boldsymbol{v}}{\partial t} + \nabla \cdot \left(\rho \boldsymbol{v}\boldsymbol{v}^{\mathrm{T}} - \frac{\boldsymbol{B}\boldsymbol{B}^{\mathrm{T}}}{4\pi} \right) + \nabla p_{\mathrm{tot}} = \rho \boldsymbol{g} \qquad p_{\mathrm{tot}} = p_{\mathrm{th}} + p_{\mathrm{mag}}$$

$$\frac{\partial e}{\partial t} + \nabla \cdot \left[(e + p_{\mathrm{tot}})\boldsymbol{v} - \frac{\boldsymbol{B}(\boldsymbol{B} \cdot \boldsymbol{v})}{4\pi} \right] \qquad e = \rho v^2/2 + e_{\mathrm{th}} + B^2/8\pi$$
$$= \rho \boldsymbol{v} \cdot \boldsymbol{g} + \dot{u}_{\mathrm{chem}} + \dot{u}_{\mathrm{inj}}$$

$$\frac{\partial \boldsymbol{B}}{\partial t} - \nabla \times (\boldsymbol{v} \times \boldsymbol{B}) = 0$$

The Astrophysical Journal Letters, 816:L19 (6pp), 2016 January 10 doi:10.3847/2041-8205/816/2/L19

LAUNCHING COSMIC-RAY-DRIVEN OUTFLOWS FROM THE MAGNETIZED INTERSTELLAR MEDIUM

Philipp Girichidis[1], Thorsten Naab[1], Stefanie Walch[2], Michał Hanasz[3], Mordecai-Mark Mac Low[4,5], Jeremiah P. Ostriker[6], Andrea Gatto[1], Thomas Peters[1], Richard Wünsch[7], Simon C. O. Glover[5], Ralf S. Klessen[5], Paul C. Clark[8], and Christian Baczynski[5]
[1] Max-Planck-Institut für Astrophysik, Karl-Schwarzschild-Str. 1, D-85741 Garching, Germany
[2] Physikalisches Institut, Universität zu Köln, Zülpicher Str. 77, D-50937 Köln, Germany
[3] Centre for Astronomy, Nicolaus Copernicus University, Faculty of Physics, Astronomy and Informatics, Grudziadzka 5, PL-87100 Toruń, Poland
[4] Department of Astrophysics, American Museum of Natural History, 79th Street at Central Park West, New York, NY 10024, USA
[5] Universität Heidelberg, Zentrum für Astronomie, Institut für Theoretische Astrophysik, Albert-Ueberle-Str. 2, D-69120 Heidelberg, Germany
[6] Department of Astronomy, Columbia University, 1328 Pupin Hall, 550 West 120th Street, New York, NY 10027, USA
[7] Astronomical Institute, Academy of Sciences of the Czech Republic, Bocni II 1401, 141 31 Prague, Czech Republic
[8] School of Physics & Astronomy, Cardiff University, 5 The Parade, Cardiff CF24 3AA, Wales, UK

Modified FLASH code

$$\frac{\partial \rho}{\partial t} + \nabla \cdot (\rho \boldsymbol{v}) = 0$$

$$\frac{\partial \rho \boldsymbol{v}}{\partial t} + \nabla \cdot \left(\rho \boldsymbol{v}\boldsymbol{v}^{\mathrm{T}} - \frac{\boldsymbol{B}\boldsymbol{B}^{\mathrm{T}}}{4\pi} \right) + \nabla p_{\mathrm{tot}} = \rho \boldsymbol{g}$$

$$p_{\mathrm{tot}} = p_{\mathrm{th}} + p_{\mathrm{CR}} + p_{\mathrm{mag}}$$

$$\frac{\partial e}{\partial t} + \nabla \cdot \left[(e + p_{\mathrm{tot}}) \boldsymbol{v} - \frac{\boldsymbol{B}(\boldsymbol{B} \cdot \boldsymbol{v})}{4\pi} \right] = \rho \boldsymbol{v} \cdot \boldsymbol{g} + \nabla \cdot \mathsf{K} \nabla e_{\mathrm{CR}} + \dot{u}_{\mathrm{chem}} + \dot{u}_{\mathrm{inj}}$$

$$e = \rho v^2/2 + e_{\mathrm{th}} + e_{\mathrm{CR}} + B^2/8\pi$$

$$\frac{\partial \boldsymbol{B}}{\partial t} - \nabla \times (\boldsymbol{v} \times \boldsymbol{B}) = 0$$

$$\frac{\partial e_{\mathrm{CR}}}{\partial t} + \nabla \cdot (e_{\mathrm{CR}} \boldsymbol{v}) = -p_{\mathrm{CR}} \nabla \cdot \boldsymbol{v} + \nabla \cdot (\mathsf{K} \nabla e_{\mathrm{CR}}) + Q_{\mathrm{CR}}.$$

Supernovae energy input

only thermal only cosmic rays both

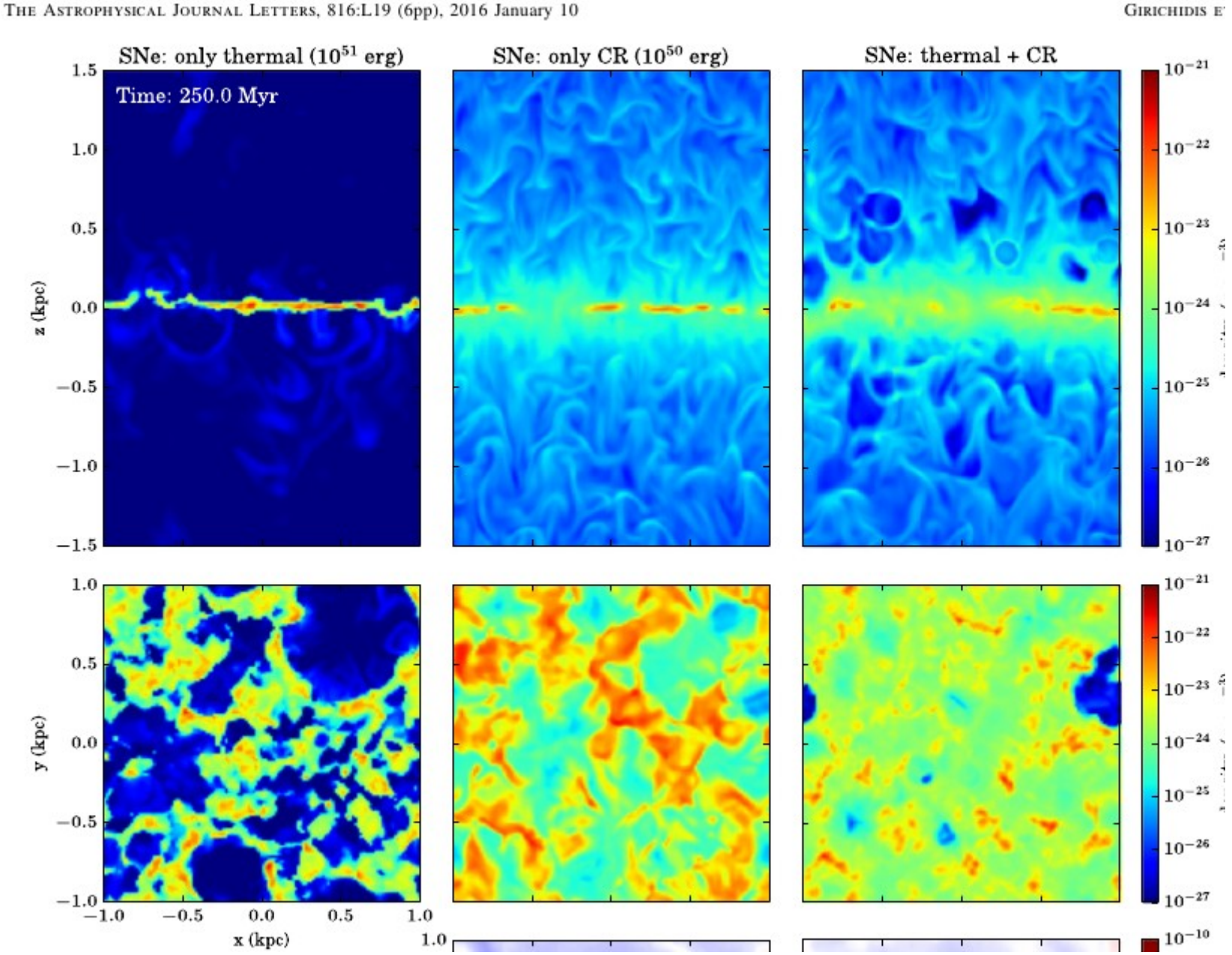

Time-dependent simulations avaiable for download

Supernovae energy input

only thermal only cosmic rays both

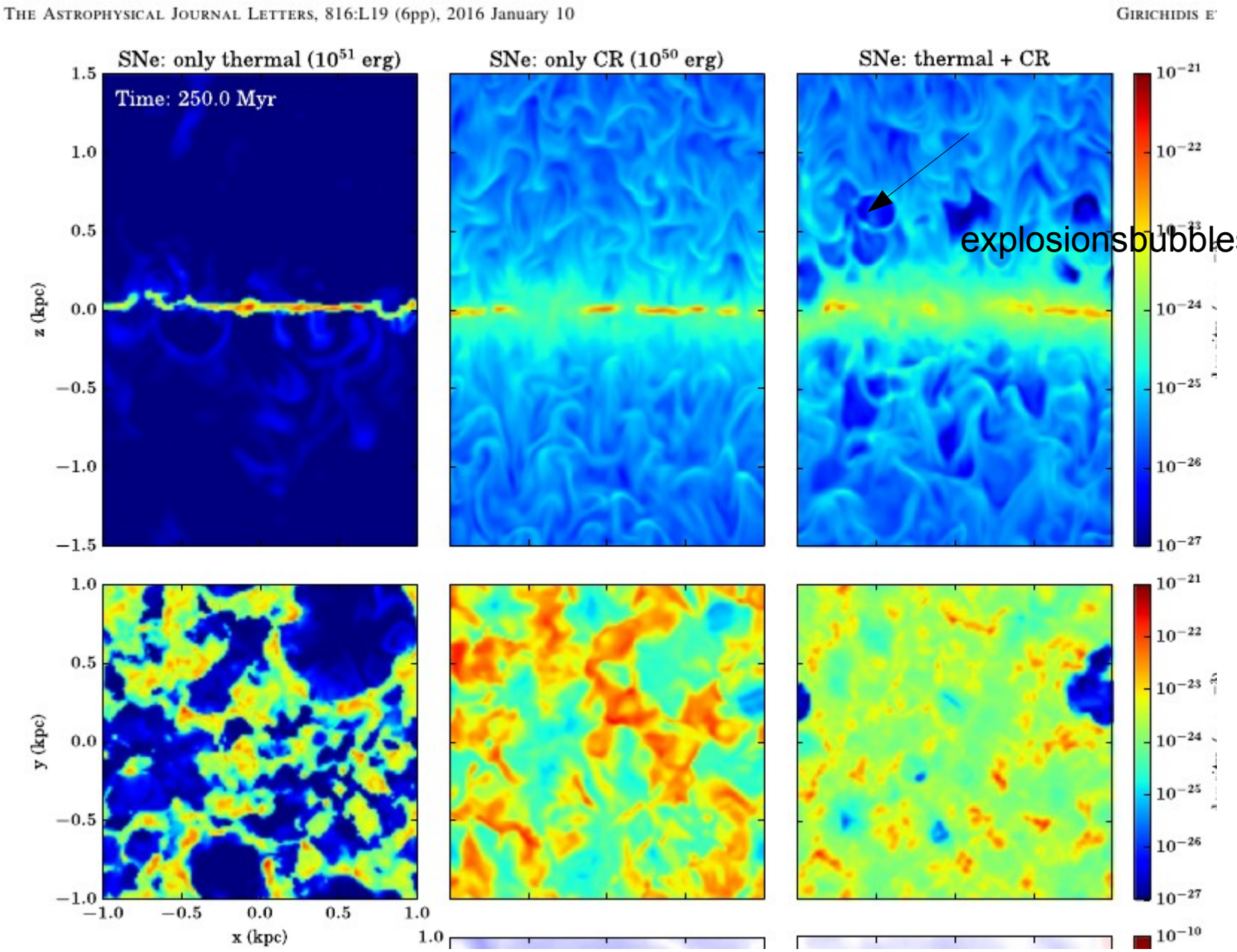

Time-dependent simulations avaiable for download

Cosmic rays increase vertical gas scale

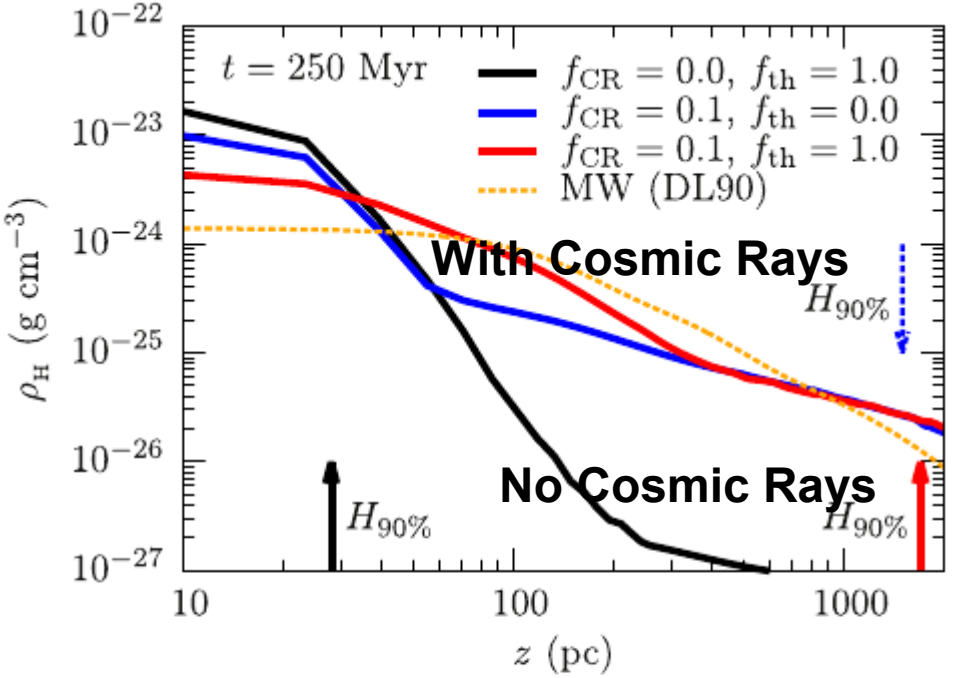

Figure 2. Vertical profiles of the total gas density for all simulations. The arrows indicate the height of 90% enclosed mass. A fit to the observed density profile of the solar neighborhood (Dickey & Lockman 1990) are shown in yellow. Thermal energy injection alone leads to a compact atomic gas distribution. Including CR feedback results in very extended distributions, which are much closer to the observed extent of the gas. The profiles indicate that CRs have their main impact at larger altitudes.

1. Including CRs thickens the galactic disk. The height of 90% enclosed total mass is found to be $\sim$1.5 kpc in the case of 10% CR energy injection per SN after 250 Myr and to increase continuously. Comparison with the vertical density distribution in the MW indicates good agreement.
2. We find that CRs quickly lead to the formation of a warm and neutral galactic atmosphere providing a mass reservoir for galactic winds and outflows. Whereas the thermal contribution of the SNe mainly shapes the disk close to the midplane, the additional CR energy shows the strongest impact above the disk and in the halo.
3. All simulations drive gas out of the midplane with little variation over time. For purely thermal SN feedback, the outflows are hot and composed of mainly ionized hydrogen with rates below the star formation rate. They are fast (up to $\sim$ a few 100 km s^{-1}) with low densities ($\rho \lesssim 10^{-27}$ g cm^{-3}). CRs alone can drive outflows with mass loading factors of order unity, which are warm (10^4 K) and mainly composed of atomic hydrogen. They are a factor of a few slower ($\sim$10–50 km s^{-1}) and 1–2 orders of magnitude denser ($\rho \sim 10^{-26}$–10^{-25} g cm^{-3}) compare to their thermally driven counterparts.

Future work in context of cosmic-ray physics:

* Test such cosmic-ray-driven wind models against cosmic-ray and gamma-ray data.
* Extend models to include energy spectrum of cosmic rays (at present just a single fluid)
* Use to make GALPROP-like approaches more physical for convection and halo structure instead of simple pre-defined forms.

B-field in Girichidis et al. Models

Dynamo-produced B-field (ab initio from seed field)
Small-scale, turbulent dynamo
Not large-scale dynamo.

MHD EQUATIONS

$$\frac{\partial \boldsymbol{V}}{\partial t} + (\boldsymbol{V}\cdot\nabla)\boldsymbol{V} = -\frac{1}{\rho}\nabla(p+p_{CR}) + \boldsymbol{g} + \frac{1}{\rho}\nabla\left(\frac{B^2}{8\pi}\right) + \frac{\boldsymbol{B}\cdot\nabla\boldsymbol{B}}{4\pi\rho}$$

$$\frac{\partial \rho}{\partial t} + \nabla\cdot(\rho\boldsymbol{V}) = 0$$

$$p = c_s^2\rho \qquad \text{(isoth.approx)}$$

$$\frac{\partial \boldsymbol{B}}{\partial t} = \nabla\times(\boldsymbol{V}\times\boldsymbol{B}) + \eta\nabla^2 B$$

Credit: Michal Hanasz

CR TRANSPORT EQUATION

Diffusion - advection approximation

(e.g. Schlickeiser & Lerche 1985, A&A, 151, 151)

$$\frac{\partial e_{\rm cr}}{\partial t} + \nabla(e_{\rm cr}\boldsymbol{V}) = -p_{\rm cr}\nabla\boldsymbol{V} + \nabla(\hat{K}\nabla e_{\rm cr}) \qquad (1)$$

$$+ \text{ CR sources (SN remnants)}$$

$$p_{\rm cr} = (\gamma_{\rm cr} - 1)e_{\rm cr} \qquad (2)$$

Anisotropic diffusion of CRs

(Giaccalone & Jokipii 1998 , Jokipii 1999, Ryu et al. 2003)

$$K_{ij} = K_\perp \delta_{ij} + (K_\parallel - K_\perp) n_i n_j, \quad n_i = B_i/B, \qquad (3)$$

$$K_\parallel = 3 \cdot 10^{28} \text{cm}^{\ 2}\text{s}^{-1}, \qquad K_\perp = (1-10)\%\,(K_\parallel)$$

Credit: Michal Hanasz